UNIVERSITAT POLITÈCNICA DE CATALUNYA

Programa de Doctorat:

AUTOMÀTICA, ROBÒTICA I VISIÓ

Tesi Doctoral

CONTRIBUTIONS TO PROGNOSTICS AND HEALTH-AWARE CONTROL OF DYNAMIC SYSTEMS

Khoury Boutrous

Directors de tesi:

Dra. Fatiha Nejjari

Dr. Vicenç Puig Cayuela

July de 2022

To my mom Rose and Vicençs.

Abstract

Maintenance is indispensable in every industry that uses machines and is inevitable regardless of the attention paid to it. The cumulative effect of its neglect or a non-optimized approach is a long or short-term shock on a company's growth. It, therefore, comes as no surprise, the overwhelming interest in the area of intelligent maintenance where comprehensive control units can detect, alert personnel, predict when a failure will occur, and manage faults to extend the life of components. Borne out of this is a new field of study, ***Prognostics and Health Management***, which emerged only about two decades ago.

This thesis contributes to this nascent field of study, and most importantly to a novel interest in the field of incorporating component prognostic information into control to manage the extent of influence degradation has on the efficient output of a plant. In sum, the thesis seeks to (1.) Contribute to component prognostics and how uncertainty can be efficiently handled and (2.) Promote the incorporation of prognostic information in a control scheme (i.e. Model Predictive Control).

For prognostics, the thesis considers two critical components, a wind turbine blade composite material and an insulated gate bipolar transistor utilizing two different types of prognostic methods, the model and data-based methods respectively. Wind turbine blades are by far the most exposed component to damage predominately due to their level of mechanical activity in the turbine operation. Forces such as gyroscopic and gravity, debris in wind, and the effect of the stochastic nature of wind contribute to a gradual damaging effect culminating in a complete blade breakdown. Given that the blade material itself is innate, mathematical degradation equations dependent on material properties to predict the extent of the material damage in the absence of sensor information is used. Therefore, with a stiffness degradation algorithm aided by a zonotopic Kalman filter, the remaining useful life of a wind turbine's blade is predicted with a model-based prognostic technique. For the data-based technique on the insulated gate bipolar transistor, a run-to-failure data set from NASA Ames was used on a novel data-based Evolving Ellipsoidal Fuzzy Information Granule modelling (EFFIG) scheme to predict the remaining useful life of the component with appropriate metrics proving its effectiveness when compared to other methods and also offers an online recursive learning advantage and explainability characteristics, a sought-after quality in practice. The issue of uncertainty quantification has been one of the main conundrums in prognostics, thus in both cases, this thesis contributes to using set-based methodologies which are known to be easy to formulate and computational friendly to quantify and propagate. Two

geometric candidates are considered, a zonotope for the model-based case (wind turbine blade) and interval sets for the data-based (Insulated gate bipolar transistor).
For health management by a suitable control scheme, two variants are proposed. First, a controller that takes a direct consideration of prognostics information via the stiffness degradation algorithm proposed as done in the model-based prognostics case and a health management scheme that considers the characteristic property of reliability of pumps in a network.
Various contributions were made in this research undertaking. For, the reliability aware control, an MPC controller is designed that ensures reliability of the Drinking Water Networks using the Bayesian theorem, specifically for the Barcelona drinking water network. Even though some papers have indeed tackled the issue of network reliability in the literature, they fail to account for uncertainties that arise from consumer demand, which cannot be ignored. This thesis thus considers the effects of uncertainty in a set-based concept aided by zonotopic sets.
It is axiomatic that in a multi-objective optimization problem such as in Model predictive control design, there is a fated trade-off between primary set goals and other peripheral requirements from controller designers. Therefore, the use of model predictive controllers for wind turbines considering health variables results in a deration of turbines of which most papers in the literature fail to appropriately consider the long-term viability of a purported constant deration for health reasons. In this thesis, a controller that relates the deration of the turbine according to the rate and extent of degradation of the blade with the conflicting health index is proposed. It basically involves scheduling the extent of deration of the wind turbine according to a predefined degradation path acquired from a run-to-failure test on a wind turbine blade using the stiffness degradation algorithm. The results prove its efficacy and practicality when tested on the high fidelity FAST.

Resumen

El manteniment és indispensable en tota indústria que utilitza màquines i és inevitable independentment de l'atenció que se li presti. L'efecte acumulat de la seva negligència o un enfocament no optimitzat és un xoc a llarg o curt termini en el creixement de l'empresa. Per tant, no sorprèn l'aclaparador interès en l'àmbit del manteniment intel·ligent on les unitats de control integrals poden detectar, alertar el personal, predir quan es produirà una fallada i gestionar les avaries per allargar la vida útil dels components.

D'això neix un nou camp d'estudi, ***Pronòstic i gestió de la salut***, que va sorgir fa només unes dues dècades.

Aquesta tesi contribueix a aquest camp d'estudi naixent i, sobretot, a un nou interès en l'àrea d'incorporar informació pronòstica dels components al control per gestionar l'abast de la influència que té la degradació en la producció eficient d'una planta. En resum, la tesi pretén (1.) Contribuir al pronòstic dels components i com es pot gestionar de manera eficient la incertesa i (2.) Promoure la incorporació d'informació pronòstica en un esquema de control (és a dir, Model Predictive Control).

Per al pronòstic, la tesi considera dos components crítics, un material compost de pales d'aerogenerador i un transistor bipolar de porta aïllada que utilitza dos tipus diferents de mètodes de pronòstic, el model i els mètodes basats en dades, respectivament. Les pales de l'aerogenerador són, amb diferència, el component més exposat a danys, principalment pel seu nivell d'activitat mecànica en el funcionament de la turbina. Forces com la giroscòpica i la gravetat, les deixalles del vent i l'efecte de la naturalesa estocàstica del vent contribueixen a un efecte danyós gradual que culmina amb una ruptura completa de la paleta. Atès que el material de la fulla en si és innat, s'utilitzen equacions de degradació matemàtiques que depenen de les propietats del material per predir l'abast del dany material en absència d'informació del sensor. Per tant, amb un algorisme de degradació de la rigidesa ajudat per un filtre de Kalman zonotòpic, la vida útil restant de la pala d'un aerogenerador es preveu amb una tècnica de pronòstic basada en models. Per a la tècnica basada en dades sobre el transistor bipolar de porta aïllada, es va utilitzar un conjunt de dades d'execució fins a la fallada de la NASA Ames en un nou esquema de modelització de gràmuls d'informació difusa elipsoïdal en evolució (EFFIG) basat en dades per predir la vida útil restant del component amb mètriques adequades que demostren la seva eficàcia en comparació amb altres mètodes i també ofereix un avantatge d'aprenentatge recursiu en línia i característiques d'explicabilitat, una qualitat buscada a la pràctica. El tema de la quantificació de la incertesa

ha estat un dels principals enigma en pronòstic, per la qual cosa, en ambdós casos, aquesta tesi contribueix a utilitzar metodologies basades en conjunts que se sap que són fàcils de formular i computacionalment fàcils de quantificar i propagar. Es consideren dos candidats geomètrics, un zonotop per al cas basat en el model (pala de la turbina eòlica) i conjunts d'intervals per al basat en dades (transistor bipolar de porta aïllada).
Per a la gestió sanitària mitjançant un esquema de control adequat, es proposen dues variants. En primer lloc, un controlador que té una consideració directa de la informació de pronòstic mitjançant l'algoritme de degradació de la rigidesa proposat tal com es fa en el cas de pronòstic basat en models i un esquema de gestió de la salut que considera la propietat característica de fiabilitat de les bombes en una xarxa.
S'han fet diverses contribucions en aquesta tasca de recerca. Per al control de fiabilitat, es dissenya un controlador MPC que garanteix la fiabilitat de les xarxes d'aigua potable mitjançant el teorema bayesià, específicament per a la xarxa d'aigua potable de Barcelona. Tot i que alguns articles han tractat el tema de la fiabilitat de la xarxa a la literatura, no tenen en compte les incerteses que sorgeixen de la demanda dels consumidors, que no es poden ignorar. Per tant, aquesta tesi considera els efectes de la incertesa en un concepte basat en conjunts ajudat per conjunts zonotòpics.

Es consideren dos candidats geomètrics, un zonotop per al cas basat en el model (pala de la turbina eòlica) i conjunts d'intervals per al basat en dades (transistor bipolar de porta aïllada).
Per a la gestió sanitària mitjançant un esquema de control adequat, es proposen dues variants. En primer lloc, un controlador que té una consideració directa de la informació de pronòstic mitjançant l'algoritme de degradació de la rigidesa proposat tal com es fa en el cas de pronòstic basat en models i un esquema de gestió de la salut que considera la propietat característica de fiabilitat de les bombes en una xarxa.
S'han fet diverses contribucions en aquesta tasca de recerca. Per al control de fiabilitat, es dissenya un controlador MPC que garanteix la fiabilitat de les xarxes d'aigua potable mitjançant el teorema bayesià, específicament per a la xarxa d'aigua potable de Barcelona. Tot i que alguns articles han tractat el tema de la fiabilitat de la xarxa a la literatura, no tenen en compte les incerteses que sorgeixen de la demanda dels consumidors, que no es poden ignorar. Per tant, aquesta tesi considera els efectes de la incertesa en un concepte basat en conjunts ajudat per conjunts zonotòpics.
És axiomàtic que en un problema d'optimització multi-objectiu, com en el disseny de control predictiu del model, hi ha una compensació predestinada entre els objectius principals establerts i altres requisits perifèrics dels dissenyadors de controladors. Per tant, l'ús de controladors predictius de models per a aerogeneradors tenint en compte les variables de salut es tradueix en una disminució de les turbines de la qual la majoria dels articles de la literatura no tenen en compte adequadament la viabilitat a llarg termini d'una suposada disminució constant per motius de salut. En aquesta tesi, es proposa un controlador que relaciona la deració de la turbina segons la velocitat i l'extensió de degradació de la pala amb l'índex de salut conflictiu. Bàsicament implica programar l'extensió de la deració de l'aerogenerador d'acord amb un camí de degradació predefinit adquirit a partir d'una prova d'execució fins a fallada en una pala d'un aerogenerador mitjançant l'algoritme de degradació de la rigidesa. Els resultats demostren la seva eficàcia i practicitat quan

es prova en el FAST d'alta fidelitat.

Acknowledgements

Above all things, I will like to thank God for the gift of wisdom and perseverance through these challenging formative years of my life on this path not taken.
This thesis was carried out at the Research Center for Supervision, Safety and Automatic Control (CS2AC) at Universitat Politècnica de Catalunya (UPC) with financial support from the Spanish State Research Agency (AEI) and the European Regional Development Fund (ERFD) through the project SaCoAV (ref. MINECO PID2020-114244RB-I00), by the European Regional Development Fund of the European Union in the framework of the ERDF Operational Program of Catalonia 2014-2020 (ref. 001-P-001643 Looming Factory) and by the DGR of Generalitat de Catalunya (SAC group ref. 2017/SGR/482. The opportunity and support is greatly appreciated.
A big gratitude to my advisors and Ph.D. supervisors: Prof. Fatiha Nejjari and Prof. Vicenç Puig for their dedication during these years. Especially for their resolute support even through less opportune circumstances of a pandemic, their attention and dedication to my cause were unwavering. Thank you for giving me the opportunity to study under you, your insightful inputs and sagacious advice, indeed meant more than pedagogy to me. Without you, this thesis would not see the light of day. A special appreciation to Prof. Vicenç Puig for the guidance and support all through my graduate education. I especially appreciate the valuable time offered to me even during off days.
The life of a Ph.D. student is an arduous one, but thanks to my wonderful colleagues at the SAC lab, a conducive environment for work was cultivated that kept me going, I carry with me profound memories. Notably and in no particular order, my sincere appreciation to Débora Alves, Carlos Trapiello, Sergio Samada and Iury Bessa. Your words of encouragement and advice meant the world to me, thank you, and wish you all well in future endeavors. I wish to also extend a special thank you to Dr. Iury Bessa, for the valuable collaboration and advice occasioned me during the final year of my Ph.D. Thanks to Maria Begona, Maria Rosa Cunil and Isabel for their administrative support and ever willingness to help whenever it was needed.
Last but not least my profound gratitude to my family, especially my mom, all those sleepless nights, selfless sacrifices and prayers have finally paid off, I have reached the pinnacle of it all. Special gratitude to my dad whom I lost early in my life, my vivid memory of you was your insistence I take my education very seriously, I have not disappointed you.

Contents

List of Figures

List of Tables

Acronyms

AFTC	Active Fault Tolerance Control
AI	Artificial Intelligence
AM	Asset Management
BN	Bayesian Network
BRM	Blade Root Moment
CI	Critical Infrastructure
CMS	Condition Monitoring Systems
CNN	Convolutional Neural Network
CPM	Controller Performance Monitoring
DAG	Directed Acyclic Graph
DWN	Drinking Water Network
EFFIG	Evolving Ellipsoidal Fuzzy Information Granule
eMPC	Economic Model Predictive Control
EOL	End of Life
FAST	Fatigue Aerodynamics Structures Turbulence
FD	Fault Diagnosis
FDI	Fault Detection and Isolation
FTC	Fault Tolerant Control
HAC	Health Aware Control
HAMPC	Health Aware Model Predictive Control
HMI	Human Machine Interface
IEA	International Energy Agency
IFAC	International Federation of Automatic Control
IoT	Internet of Things
IPC	Individual Pitch Control
LCoE	Levelized Cost of Energy
LIDAR	Light Detection and Ranging
LPV	Linear Parameter Varying
LQR	Linear Quadratic Regulator
LSTM	Long Short-Term Memory

MPC	Model Predictive Control
NPV	Net Present Value
NREL	National Renewable Energy Laboratories
PORFC	Parametric Online Rain Flow Counting
OM	Operation and Maintenance
PFTC	Passive Fault Tolerance Control
PHM	Prognostics and Health Management
PID	Proportional Integrative Derivative
PoF	Physics of Failure.
RFC	Rainflow Counting
RUL	Remaining Useful Life
RMS	Root Mean Square
SCADA	Supervisory Control and Data Acquisition
SHM	System Health Monitoring
SoC	State of Charge
UUT	Unit Under Test

Chapter 1

Introduction

1.1 Introduction and Motivation

Maintenance in every industry is undoubtedly one of the most crucial aspects of industrial operations to protect and preserve companies' assets. However, considering all its essence, a lack of insightful approach may only lead to counterproductive consequences, such as unintended cost and unnecessary downtime. Hence, it is only prudent to consider inventive ways of maintenance that do not only regard the mere preservation of assets but factors in other relative important elements such as minimization of its associated cost and most importantly, a complete information and control over all constituents and variables of maintenance in what is termed as a System Health Monitoring (SHM) procedure, a part of the much-touted digital transformation drive. According to (Ofsthun, 2002), a System Health Monitoring (SHM) module once implemented in a monitored system, must have the real-time capabilities of diagnosing the root cause of an anomaly from a normal machinery operation (i.e fault, cyberattacks), supply relatable data on the abnormalities, prognosticate when needed based on the available data and recommend prescriptive solutions including recently, managing the resulting deterioration before a critical failure state (Compare et al., 2020) .

This digitalization of maintenance is essential to a modern Asset Management (AM) regime. Indeed according to the ISO 55 000, it is standard for advanced AM systems to explicitly introduce risk management during an asset's life cycle, especially in the era of industry 4.0. The advent of advanced and increasingly reliable sensors have aided in this cause with the ability to collect meaningful large amounts of relevant real-time data for different levels of maintenance purposes (Pech et al., 2021).

The precursor to failure in a component is a gradual or abrupt degradation that is initiated when a fault occurs, in a dormant state or when active. For degradation initiated by a fault, it is important to detect this deviation via fault diagnosis procedures which abound in literature for e.g. in reviews on the subject such as (Gertler, 1998);(Isermann, 2011);(Patton et al., 1989), to isolate fault sources, collect data that could be used to evaluate the Remaining Useful Life (RUL) values of a Unit Under Test (UUT). The field of FDI is a much more matured field compared to prognos-

tics, primarily due to the fact that FDI is based on interpretation and decisions based on real-time data whilst prognostics has the challenge of predicting a future behaviour based on present and assumed future variables (Onori et al., 2012).

Prognostics, a Condition-Based Maintenance (CBM) module, has recently been a part of a new revolution in maintenance. Its end goal is to afford practitioners the opportunity to not only use data for instantaneous maintenance purposes, but also forecast behaviours based on available data. The use of such information offers exciting applications such as appropriately planned maintenance and control designs that manage degradation before maintenance can be undertaken (Cieslak and Gucik-Derigny, 2018) or optimally delay degradation to meet mission targets (Karimi Pour et al., 2021). But forecasting is an uncertain undertaking, which is at present the main conundrum in prognostics as discussed at length in (Sankararaman and Goebel, 2013). The effort in uncertainty description must henceforth outweigh the point-wise predictions as produced in most papers.

From the aforementioned relevance of deploying these modern maintenance schemes, it is quite clear its importance in industries where the cost of operation is relevant in staying competitive. A prime example is in the energy sector. With many competing options, such as fossil fuel plants that offer relatively cheaper and more mature technologies, clean energies are essentially viable investments primarily due to government subsidies. Therefore, there is a push for sustainable models of operation to ensure a more global clean energy mix. It is for this reason that savings gained through effective CBM methods cannot be overlooked. Thus in wind turbines, there have been works on a number of it's components in the field of fault detection (Gong and Qiao, 2015);(Ren et al., 2019), prognostics (Xiong et al., 2018); (Rezamand et al., 2020) and health related control (Odgaard et al., 2015b);(Badihi et al., 2015) for all categories of failure modes, which is categorized and discussed in (Aisha Sa'ad, 2022) as a catastrophic failure, critical failures, and minor failure, primarily dependent on the affected component. Therefore, there has been a plethora of works in the literature on certain critical components of the wind turbine with good results, most featured been the gearbox (Chen, 2010) (Kia et al., 2009), bearings Gong et al. (2010), pitch system (Schulte et al., 2012) and electrical system (Karimi et al., 2008; Campos-Gaona et al., 2013; Parker et al., 2013; Bernal-Perez et al., 2013; Freire et al., 2013; Vedreño Santos et al., 2014). The blades are by far the most exposed component to factors of degradation and are ranked the second most failure-prone component in the plant (Beauson et al., 2022). This is especially prevalent of late due to the increasing size of turbines for an increased rating of turbines (Sanchez et al., 2015). Fatigue and thus degradation of a wind turbine's rotor blade is on a microscopic level, which subsequently requires fatigue models for predicting degradation's trend to failure. For example, the popular Palmgren-Miner's rule (Miner, 1945) has been used to good effect in many works (Gray and Watson, 2010), (Horn and Leira, 2019) as well linear crack propagation models such as (Lampman, 2009); (Gray and Watson, 2010).

The level of safeguarding in Critical Infrastructure (CI) such as sewage systems and Drinking Water Network(DWN) must comparatively be stringent as much as possible due the dire consequences when unaccounted failure occurs. Maintenance in such systems most follow a strict

organised protocol to ensure a high level of availability. Most of these CIs are networked systems, that is, failure in a component can have a cascading effect on other components and hence the network as a whole. Thus the interacting relationship through the network needs investigation before concise prognostics can take place, extrapolating aging behaviour of individual components as well the overall system. There are papers that have sought to solve this problem, fundamentally posing the problem based on dynamical interactions from a component, sub-component and system level such as in (Onori et al., 2012); (Lakehal and Laouacheria, 2017). To better manage the level of failure in these systems, it is only right to solve the problem from a controller design perspective which is dependent on these dynamical interaction. That is to consider degradation dependent models in control designs or identify degradation variables, such that variables can be manipulated to contain faults or extended failure time before an organized maintenance procedure takes place. Fundamentally, the dynamical relationships between components allows to ensure availability of service through compensation from unaffected components in the network.

1.2 Thesis Objectives

The objectives of this thesis are as follows:

- To investigate on a suitable degradation algorithm for the degradation of an innate plant's component such as a wind turbine blade.
- To propose a methodology to predict the RUL of a wind turbine's blade using algorithm from objective 1, including an appropriate uncertainty quantification specifically, a set-based one.
- To design a health aware controller using information from objective 2 that ensures extension of components' life in a practical manner as against other methods in the literature.
- To propose a novel data-based prognostics scheme which is simple but yet promotes explainability and investigate on an accompanying suitable set-based uncertainty quantification.
- To propose the design of a controller that preserves the health of an interconnected network of components, considering known individual prognostic information.

1.3 Outline of the Thesis

This thesis manuscript is organized in seven chapters. **Chapter 2** presents the background theory and bibliographical review of prognostics and health management in general. **Chapter 3** Presents some introductory information for itself and subsequent chapters in wind turbine modelling and zonotopes. It then proceeds to propose a set based prognostics methodology for wind turbine's blades. **Chapter 4** proposes a health ware control drawing inspiration from **Chapter 3**. **Chapter 5** proposes a data-based prognostics scheme for IGBTs using an EEFIG methodology. **Chapter 6**

proposes a reliability-aware control of a DWN considering the overall as well as individual reliability of pumps in the network using MPC. Finally, the conclusions are outlined in **Chapter 7** with suggested future works.

The outline of the thesis is detailed below:

- **Chapter 2:** This chapter presents a detailed summary from the literature about the concept of degradation leading to maintenance and ending with how maintenance can be managed from a controller point of view. In all, a historical background of maintenance is given, showing the trend over the years to the current condition-based maintenance schemes from which is the modern scheme of prescriptive maintenance employed in **chapters 4 & 6** of the thesis. The chapter elaborates on condition-based maintenance schemes of fault detection and isolation and also prognostics, primarily it's types, the model-based, data-based and hybrid, with relevant reference on each case. A bibliographical review of uncertainty quantification and propagation is also given in this chapter. The chapter ends with a review on how maintenance is considered in controller designs.

- **Chapter 3:** The wind turbine modelling is detailed in this chapter as well as some mathematical preliminaries on zonotopes and reachability analysis for subsequent chapters. Stiffness degradation algorithm with its application to a wind turbine blade's composite material is explained mathematically, discretized and appended to the nonlinear wind turbine model which is then represented in an LPV form. A zonotopic Kalman filter is used to quantify various uncertainties as a zonotope which is then propagated to determine the RULs with associated uncertainty for wind turbine's blades.

- **chapter 4:** In this chapter, the stiffness degradation is utilized once again but for its incorporation into a controller, an MPC. A wind turbine blade is run to failure considering stress from a flapwise root moment. The path to failure is then segmented in chosen stages of degradation from the algorithm, each with predefined weights. All this information is included in a health-ware controller design.

- **Chapter 5:** This chapter deals with the data based prognostics of an IGBT. Using data sets from NASA AMES, the RUL of an IGBT is determined through a novel method using EEFIG. The chapter then introduces an extension where the issue of uncertainty for data-based prognostics based on set-based theory is introduced using set-based membership and interval arithmetic.

- **Chapter 6:** Considering the reliability of pumps in a network, the cumulative reliability via a Bayesian theorem is evaluated. This information of the overall network's reliability with individual reliabilities in a dynamic mathematical form is included in a DWN model which is used in the design of a Reliability-aware MPC for DWNs.

- **Chapter 7:** The main contributions and conclusions of the thesis are outlined as well some ideas for future works and research directions proposed.

Chapter 2

Bibliography Review

A bibliographical review of the important areas of interest that motivates the contributions of this thesis is presented in this chapter. A review of the classification of the concept of component degradation, culminating in various associated branches of study: *Fault diagnosis, Reliability, and Prognostics* is presented. Consequently, how the problem of uncertainty related to prognostics is handled in the literature is also presented. The chapter ends with the diverse schemes of incorporating health management in control theory from the literature.

2.1 Degradation Of System Components

Degradation of components is an inevitable part of any system´s lifetime when subjected to certain endogenous and/or exogenous factors no matter the extent of precautionary measures taken to curb it. Such variables which (Zagórowska et al., 2020) terms as influencing factors, like temperature, friction, etc. interact with the component's composite material causing deficiencies in suitable fabrication properties that affect their optimal functionalities.
As (Kang et al., 2020) rightly puts it "The second law of thermodynamics implies that any animate or inanimate system degrade and inevitably stops functioning". Degradation is defined by (Gorjian et al., 2010b) as a reduction in performance, reliability, and lifespan of assets. Even though this definition and others from (Peng et al., 2017);(Nikulin et al., 2010) capture an expansive view of degradation, it fails to establish the temporal nature of degradation and also the fact that degradation is more or less a material level deterioration, thus a definition by (Zagórowska et al., 2020) as the detrimental change in *physical condition*, with *time*, use, or external cause is considered the most appropriate.
It is thus imperative to understand this phenomenon, employing countermeasures, that would seek to manage their extent of influence in machine processes. This is important to minimize plant downtime, increasing profit, and ensuring that mission targets are met (Madhav, 2016), especially in modern plant processes where unplanned offline scenarios may be detrimental to the everyday life of modern societies, for example in Critical Infrastructure (CI) such as Drinking Water Networks (DWN). This has been considered and researched in works such as in (P. Weber, 2012);

(Puig and Ocampo-Martínez., 2015). Other considerations in the literature with respect to CI are the ones developed in (Gono et al., 2012);(Liang et al., 2018) for power networks and (Nagy-Kiss et al., 2015); (C. Ocampo-Martinez and Ingimundarson., 2006) in sewage systems. It is also worth noting that the majority of these CIs are interconnected systems. The interconnection between different components and their subsequent dynamic interactions makes them susceptible to the propagation of faults due to degradation between components, emanating from a single degraded component. Placement of sensors on every component in the network is of course not economically prudent, thus works such as in (Nejjari et al., 2015); (Casillas et al., 2015) provide optimal sensor placement procedures that help in detecting influencing factors such as water pressure for leak detection.

Unplanned running costs as a consequence of failure due to degradation may also render certain technologies with slim profit margins not worth investing in if degradation of its constituent components triggers frequent unexpected failures. This is evident in industries where diverse competing technologies exist. For instance, in the field of energy, there is a dilemma for clean energy technologies to minimize the Levelized Cost of Energy (LCoE) to stay competitive in an era of subsidy cuts from governments, hence factoring in the impact of degradation in cost analyses becomes a must. Indeed, this motivated the inclusion of degradation as a factor in a projected Net Present Value (NPV) assessment of projects, as done by (Kharait et al., 2017), considering a study on the viability of a Photo Voltaic (PV) project with a degradation model considered. Also in (Urbano et al., 2021), risk analyses were conducted on the back of uncertainties in equipment degradation for renewable energy investments by considering component degradation's effect on economic variables. A study into battery degradation in smart homes was also conducted by (Toosi et al., 2022), the authors were able to establish the importance of decreasing the carbon footprint of domestic households with an understanding of battery degradation. (Javidsharifi et al., 2022), also concluded by performing a reduced unscented transformation (RUT) test, that a substantial decrease in operational cost is achievable considering battery degradation in smart homes. One may argue for the case of investments in improving material properties to produce resilient components, but as alluded in (Li et al., 2020), today's consumer behavior is one that requires components with high-performance indices that also factor in cost-effectiveness. R&D investments in material science increase price.

There are no clear standards in the literature concerning degradation, but existing reviews attempt to formalise it differently from the perspective of its branches, namely: *Fault diagnosis (Isermann, 2011), Maintenance (Kang et al., 2020); (Peng et al., 2010), Prognostics (Liao and Kóttig, 2004);(Jardine et al., 2006), Component reliability (Weber et al., 2012); (Gorjian et al., 2010a)* and *Degradation's application in control (Zagórowska et al., 2020)*. However broadly speaking, degradation can be considered an event observable or sudden. The evolution of an observable degradation as shown in Fig.2.1, involves initially an upstate where degradation is assumed to be absent. Subsequently, at t_0, substantial degradation d_0 is assumed to have occurred such that it is observable and mostly represented by plant variables or a function of them. From this point onwards, the progression of degradation can be observed, whose impact on the plant's functionality invariably depends on

its level of progress. The gradual/accelerated (i.e. due to external factors) process of degradation thus occurs between $t_0 \leq t \leq t_f$, where d is considered manageable, in essence by decreasing $\dot{d} = f(d(t), t)$ through Engineering Asset Management (EAM) schemes either online or offline. At t_f, the material property is thought of as deteriorated to such an extent d_f, that further degradation becomes evident from noticeable variability from a considered norm in the plant's operation. The ultimate price of degradation is thus a failure and hence a fault occurrence i.e $d > d_f$ when components are installed.

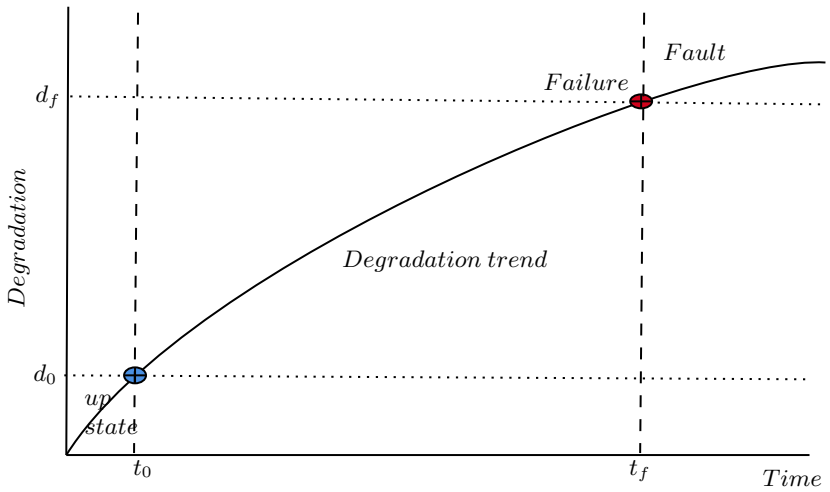

Figure 2.1: Trend of degradation in relation to system's behaviour. from (Zagórowska et al., 2020)

Faults basically occur when degradation triggers an abnormal state. As defined by (Isermann, 2011), "A fault is an unpermitted deviation of at least one characteristic property (feature) of the system from the acceptable, usual, standard condition." and "A failure is a permanent interruption of a system's ability to perform a required function under specified operating conditions". Thus the knowledge of these deviations in features must necessarily be observable as explained with Fig.2.1 to detect a fault that could be incipient or abrupt. For example, degradation such as in condensing boilers as done in (Baldi et al., 2017), affects the behaviour of the plant, such that they can be quantified by deviation in water mass flow rate to ultimately detect an anomaly in a system property of the boiler efficiency which is regarded as synonymous to a fault in a diagnosis procedure. In some cases, this knowledge of feature, parameter, or variable deviations is unknown until a detrimental change in behaviour at a future time affects the material properties to levels that are conspicuous in the plant's behaviour, thus a failure event occurrence. For example, cracks occur on wind turbine's blades due to interactions between stochastic wind disturbance and the blade's material. They primarily commence immediately after installation, but these progressive cracks do not affect the behaviour of the wind turbine until they reach disruptive levels, such that if precautionary actions are not taken, the turbine ceases to function. The behaviour of this type of degradation is acquired through accelerated tests under controlled environments to attain material property constants that modify with time and with influencing factors' effects. Some exam-

ples are in lubricants (reaction rate experiment) (Pfaendtner and Broadbelt, 2008), wind turbine's blade (blade crash testing) (Yang et al., 2013), insulation (Use-rate acceleration tests) (Johnston et al., 1979);(Meeker et al., 2003) etc.

It must, however, be noted that degradation does not merely occur when components are active, but could occur in events such as deterioration due to manufacturing defects, storage (e.g. rust), intrinsic material deficiencies, etc. The conventional measures against degradation involved undertaking frequent inspections and scheduled maintenance by operators such as regular oiling of machine moving parts to avoid wear and tear, a passive approach of maintenance which involved taking action only when a failure occurs. The definition of maintenance as standardized in (Gouriveau et al., 2016a) is a "Combination of all technical, administrative and managerial actions during the life cycle of an item intended to retain it in, or restore it to, a state in which it can perform the required function". There has been immense progress in the area of maintenance as shown in Fig.2.2. The first generation of maintenance, the corrective maintenance involved a passive approach of allowing a failure to occur before maintenance is effected. Since the time of failure is uncertain, this approach does not allow for rapid system restoration, thus system availability is low (Luo et al., 2003). This is exacerbated in circumstances where the plants are not "*easy to access*", for example with offshore wind turbines or off-shore oil rigs, where even one repair requires substantial man-hours and financing. Also, since the plant's health is left to chance with no prior knowledge before maintenance, the complexity of health restoration is greater in this approach, since there is no mechanism to isolate and understand the behaviour of a particular fault mode or the root cause of a failure. In an era of intricate machinery, this may require an overhaul of a plant, instead of a targeted approach to maintenance. Thus, this approach is definitely not practical at this moment in time and is indeed archaic. The second generation of maintenance called the preventive maintenance approach involves "maintenance carried out at predetermined intervals or according to a prescribed criterion and intended to reduce the probability of failure or the degradation of the operation of an item" (Gouriveau et al., 2016a). It considers either a "condition-based maintenance" or a "predetermined maintenance" where scheduled maintenance is prescribed no matter the current health of the system, usually based on reliability prediction based on manufacturer's recommendations or historical data. Even though this may lead to good availability compared to corrective maintenance (Luo et al., 2003), it leads to "over care" (Gouriveau et al., 2016a) and "wasted maintenance" (Kim et al., 2017) and hence is not the most financially prudent option. It only becomes useful when all the components are deemed to fail at the same time (Kim et al., 2017). The probability of such an event is very unlikely. As such, in 1979, the maintenance cost of industries in the USA was upwards of $200 billion, increasing by $10 - 15\%$ year on. Therefore, the introduction of a new type of maintenance became necessary, thus the emergence of the condition-based approach.

Condition-based maintenance is defined as "a preventive maintenance based on performance and/or parameter monitoring and the subsequent actions" (Gouriveau et al., 2016a). This involves the real-time analysis of a health variable (temperature, vibration etc.) of a system such that decisions can be undertaken considering an understandable behaviour's anomaly. Under

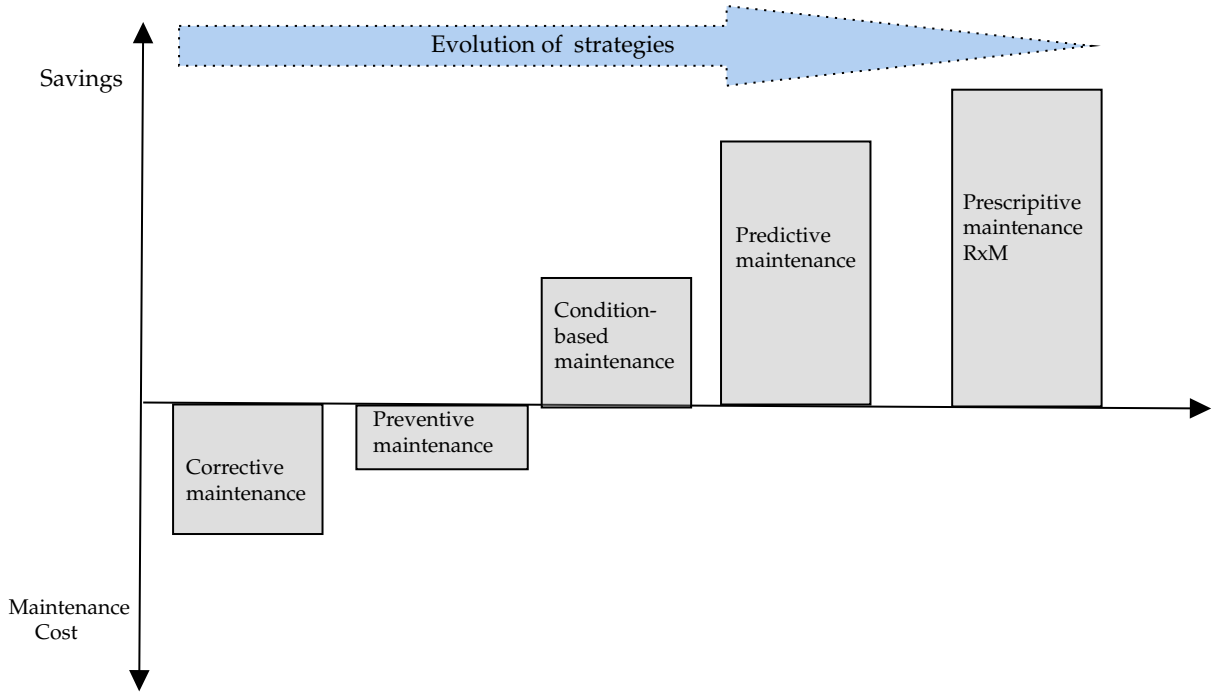

Figure 2.2: Evolution of maintenance strategies.

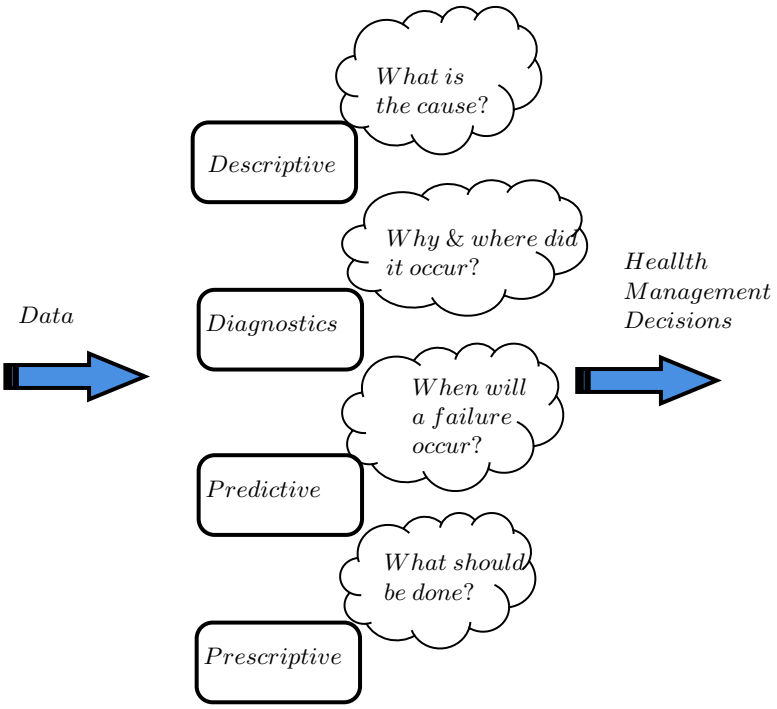

Figure 2.3: Modern maintenance proposal.

this, a diagnostic or predictive maintenance (prognostic) approach can take place. With the observed variables from the plant's operation, the remaining useful life (RUL) of a component can be

forecasted with knowledge of the degradation behaviour for a comprehensive decision on maintenance.
With the emergence of industry 4.0, IoT technologies enable communication of sensor data in real-time with cloud technology, making optimal decentralized decisions on machine health, therefore presenting a suitable platform for the complexities a modern condition-based maintenance approach poses. Many works, e.g. (Elattar et al., 2016a);(Baur et al., 2020) in the literature seek to distinguish "condition-based maintenance" as a third kind of maintenance from preventive maintenance, but from the accepted definition of preventive maintenance, it certainly, does not only involve the time scheduling of maintenance but also proactive measures. Thus, it is accepted in this thesis as a branch of preventive maintenance.
A new type of maintenance, prescriptive maintenance, enables the introduction of decisions with respect to an available RUL from the predictive sub-level so as to extend the RUL of associated components. This can be achieved by a health management decision system with an appropriate degradation considered in a cost function that manipulates influencing factors of degradation or gives optimal cost-effective decisions with respect to operational conditions. The topology of various decisions of maintenance when there is degradation is as shown in Fig.2.4. Even though most maintenance methodologies in industry end with predictive maintenance, a holistic approach as shown in Fig.2.3, should be considered. Degradation-based software should be able to identify a fault, know why and where it occurred, know components' RULs and finally propose solutions or take actions locally against it. In an optimal framework, variables such as the availability and cost associated with:

- Maintenance operators.
- Logistical resources e.g transport, inventory, etc.
- Environmental and operational conditions.
- Cost associated with managing degradation before repair or failure.

should be considered to make optimal decisions such as:

- Determining the optimal time to attend to maintenance.
- Set a maintenance order.
- Create a purchase order to replenish inventory.
- Managing degradation locally (e.g Fault-tolerant, Health-Aware controllers).

This thesis is focused on the *predictive* and *prescriptive* maintenance approaches. Henceforth, the classification of degradation from two schools of thought is considered. In the area of prognostics and diagnostics, degradation is popularly classified as:

- model-based- Knowledge of the physics of degradation.

- Data-based- Relationship of degradation derived from system's data.
- Hybrid-based- Combination of model and data-based techniques.

From (Zagórowska et al., 2020), the concept of degradation is formalised with respect to controller design. The authors classify it based on its interaction with model variables and vice versa. They categorize it into two primary groups with respect to the degradation effect on model behaviour. Considering a dynamic model and outputs $y(t) \in \mathbb{R}^y$ devoid of degradation,

$$\dot{x} = f(x(t), u(t), t), \tag{2.1a}$$

$$y(t) = g(x(t), u(t)). \tag{2.1b}$$

such that $x \in \mathbb{R}^n$ and $u \in \mathbb{R}^m$ are vectors of system states and inputs, respectively. $f(.) : \mathbb{R}_+ \times \mathbb{R}^n \times \mathbb{R}^m \mapsto \mathbb{R}^n$ is the flow map and $g(.) : \mathbb{R}^n \times \mathbb{R}^m \mapsto \mathbb{R}^y$ the output function.
Then the above dynamic model is described as a *Degradation independent model*. Degradation affecting the behaviour of the system is thus termed as a *Degradation dependent model*, where there is a possibility of observability of degradation. Hence, this can be represented as:

$$\dot{x_d} = f(x_d(t), u_d(t), h_d(t), t), \tag{2.2a}$$

$$y_d(t) = g(x_d(t), u_d(t), h_d(t), t). \tag{2.2b}$$

Therefore for the degradation of the system affecting the model variables (u_d, x_d), the system behaviour degenerates from its normal behaviour. Indeed, (Frank et al., 2000) argues that it is only appropriate if possible, to consider (2.2) in all modeling undertakings, stating that models without consideration for degradation are only a partial representation. For the effects of the system variables on degradation, two classes of models are suggested. A factor-free model and a factor-based model. The factor-free model is basically a time function of degradation that does not depend on influencing factors such as the plant and exogenous variables, whereas factor-based models depend on these variables. This could be appropriate degradation path models that inherently involve time functional models involving material properties of the UUT. They are, therefore, mathematically represented as

$$h_d(t) = h(d(t), t) \longrightarrow \text{(Factor-free degradation model)}, \tag{2.3a}$$

$$h_d(t) = h(d(t, w(t), u(t), y(t)) \longrightarrow \text{(Factor-based degradation model)}. \tag{2.3b}$$

Each model from, (2.2) can be used with models from (2.3) to capture degradation behaviours. As evident, these descriptions are controller design-friendly.

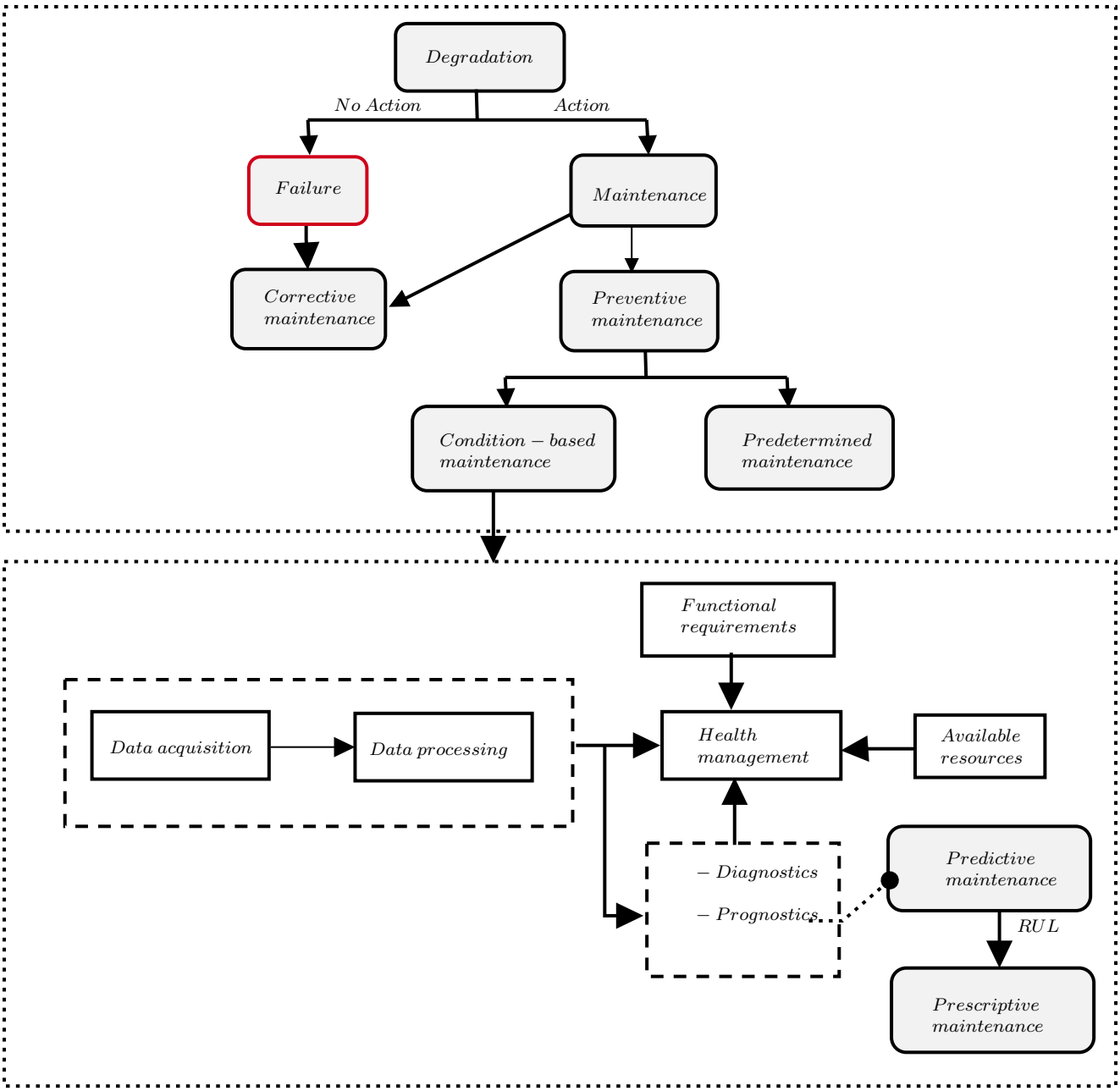

Figure 2.4: Topology of maintenance strategies updated from (Madhav, 2016)

2.2 Prognostics and Health Management

(Lee et al., 2014) describes prognostics and health management (PHM) as a condition-based maintenance scheme that involves the detection of incipient faults, monitoring current health conditions, and predicting remaining useful life.

After a conspicuous degradation event is detected, as shown in Fig.2.6, a prediction of the time before failure can be deduced, hence prognostication, for various maintenance schemes to be employed. As stated in the prequel, that may not always be the case as some degradation processes may not be observable, in which case a time-dependent factor-free or factor-based degradation model can be used to monitor the degradation in time to an End of Life (EOL). But regardless of the type of degradation, there must be a concrete prior knowledge of the behaviour of the drift of degradation to the EOL, to make good predictions enabling improved system safety, increased system reliability, improved system availability, avoidance of unnecessary maintenance, and decreased system life-cycle cost (Sun et al., 2012). Caution must, however, be taken when performing this exercise, as invalid predictions may be tantamount to wasted maintenance as in predetermined maintenance or may conversely lead to a corrective maintenance scenario where actions are taken when the failure has already occurred i.e when there is a substantial negative forecast error. Thus, inasmuch as it is a desirable tool to have, it is a very delicate endeavor that requires a high level of attention to detail. As a matter of fact, prognostics is only a *calculated* (informed) "guess" of a future event, thus it is important to consider attentively all factors prior to the forecast to arrive at a well-informed conclusion, as well as to account for future conditions which are uncertain. Unfortunately, most works do not even quantify uncertainty when performing prognostics.

There is a plethora of definitions of prognostics (Bayington et al., 2002); (Vachtsevanos and Roemer, 2016); (Wu and J., 2007); (Zio and Di Maio, 2010) mostly biased towards their area of applications in the literature. However, the accepted standardized definition of prognostics is the "estimation of time to failure and risk for one or more existing and future failure modes" (ISO-13381-1, 2004). From this definition, there must first be a quantification of this time of failure primarily dependent on the system under study. This could be the state of charge (SoH) in the case of batteries or RUL quantified in terms of blade material deterioration in wind turbine's blades etc. Consequently, this quantified time of failure must have characteristic variables readily available through sensor measurements whose behaviour signifies a degradation course of the UUT to failure. These variables are termed failure precursor parameters are events or series of events that signify an impending failure. This could be the collector-emitter voltage for RUL predictions in semi-conductors (Samie et al., 2015);(Patil et al., 2009), vibration signals for bearing (Hong L., 2014);(Heng et al., 2009) or charge-discharge cycles for batteries (Zheng et al., 2015).

For illustrative purposes, we assume an observed degradation for the prediction of a RUL as shown in Fig.2.6 from (Gouriveau et al., 2016a). RUL is the time interval between a forecast time tc; ($tc > tD$) after detection of a degradation at tD to a prescribed failure threshold at tf. This threshold most often than not is minimized from its true value to prevent negative forecast errors

that may arise due to inevitable uncertainties in modellings. Thus the RUL is:

$$RUL = tf - tc \tag{2.4}$$

RUL is a forecast, therefore as stated earlier, it is cogent to have an accompanying uncertainty description, as shown on the right side of figure 2.6. Health management can also be represented in terms of the reliability of a component or system in the area of reliability engineering. Reliability is defined as the ability of an item to perform a required function, under given environmental and operational conditions and for a stated period of time (ISO8402). That is to say, given an imperfect perception of the reliability state of a system and/or component, an estimate of future failure can be evaluated for a system or its component availability assessment in a probabilistic manner. Thus, a probabilistic reliability function for an unrepairable component can be described as:

$$R(t) = 1 - F(t) = p_r(T > t), for, t > 0 \tag{2.5}$$

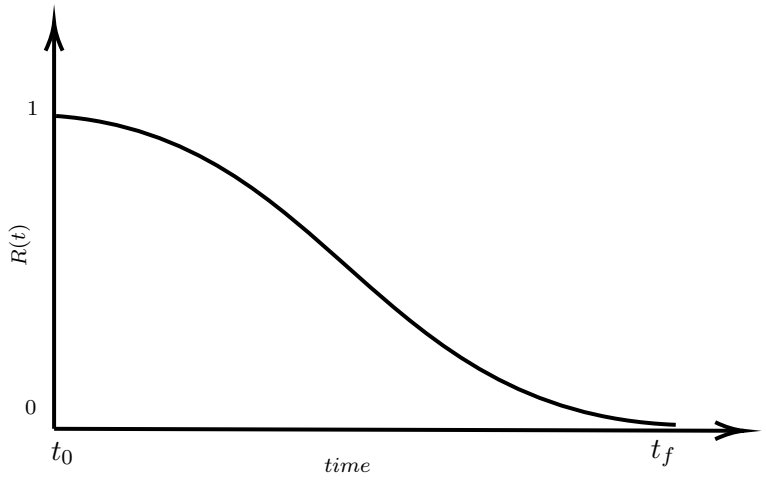

Figure 2.5: Reliability or survival function of an unrepairable component.

where F(t) is the lifetime distribution function and R(t), the reliability function. Repairability is used in the context here to associate (2.5) to components that are assumed not repairable after failure. The distributions used in the literature are the exponential distribution (Khelassi et al., 2011); (Theilliol et al., 2015), normal distribution (Yang, 2004), log-normal distribution, Birnbaum-Saunders distribution (Birnbaum and Saunders, 1969), inverse Gaussian distribution, Weibull distribution (Mudholkar and Srivastava, 1993); (Jiang and Murthy, 1999) as well as binomial, geometric and Poisson (Nelson, 1982) distributions for discrete-time domain applications. The authors in (Compare et al., 2017) discuss how to integrate the two fields of reliability engineering and prognostics, mainly by considering how metrics of prognostics can be incorporated in reliability modelling such as the $\alpha - \lambda$ prognostic metric. A good review of all areas of interest in reliability engineering can be found in (Marvin Rausand, 2004).

To promote the inclusion of health management in everyday industrial activities a step-by-step module as shown in Fig.3.7 is proposed, which has been standardized (ISO-13381-1, 2004) into seven modules

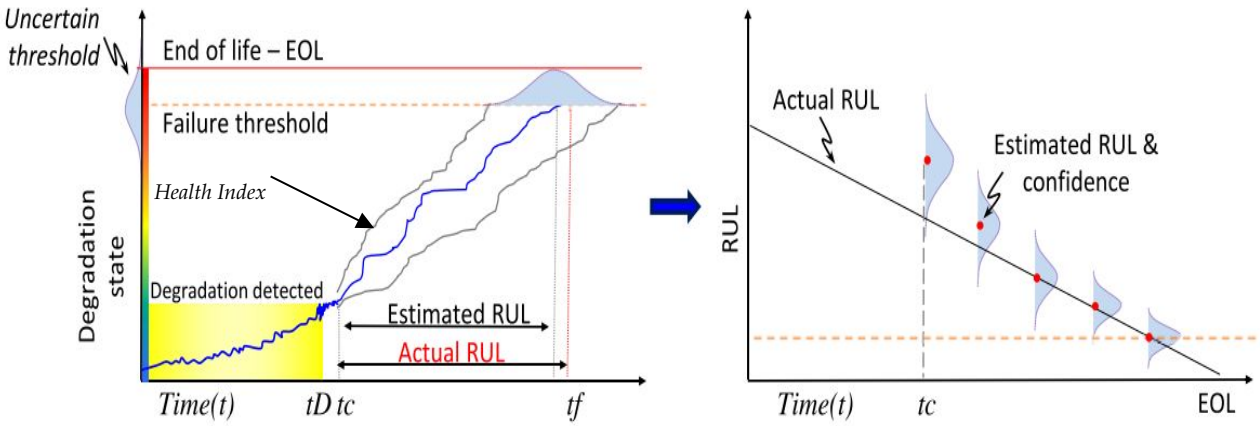

Figure 2.6: Illustration of a prognostic process. From (Gouriveau et al., 2016a)

namely:

1. *Data acquisition*: In this module, a critical component is identified from a dependability and risk management analysis such as fault trees(Fan et al., 2012), failure mode, effects and criticality analysis (FMECA)(Chen et al., 2011b), experience feedback etc. Thereafter, a physical parameter is identified as representative of degradation whose data is acquired from an appropriate sensor.

2. *Data processing*: Data from the sensors may sometimes, be corrupted with noise or not make useful sense to an algorithm or operator. Therefore meaningful features are extracted from the data called health indicators, which are indicative of a degradation initiation, a fault, or an evolution of a degradation.

3. *Detection*: This real-time module should have the capability of alerting an anomaly based on the nature of the health indicator compared to healthy conditions. Usually a fault detection and isolation unit. This could be model-based involving the use of Kalman filters (Donders, 2002); (Karami et al., 2010); (Sheibat-Othman et al., 2013); parity equations (Ozdemir et al., 2011); (Blesa et al., 2011b) observers (Schulte et al., 2012); (Odgaard et al., 2009); (Casau et al., 2012); (Chen et al., 2011a) etc. It may also involve data-based techniques that uses statistical (Zimroz et al., 2012); (Vapnik, 2012); (Niknam et al., 2013); (Li and Frogley, 2013) time (Futter,

1995); (Miller, 1999), frequency domain (Shuting et al., 2006); (Liu et al., 2012) analysis or lately an artificial intelligence approach (Duda and Stork., 2012);(Choi et al., 2021).

4. *Diagnostics*: This is an identification and isolation module that seeks to identify the cause, localize the source of probable failure and determine its magnitude.

5. *Prognosis*: With information from the previous modules, the future time to failure (RUL) at the present specified time is deduced.

6. *Decision analysis*: Optimal maintenance/control actions are recommended in this module with respect to the available RUL estimates to ensure mission accomplishments or management before repair or scheduled actions.

7. *Presentation*: A human-machine interface (HMI) must be available for understanding with probable explainability of the algorithm of the PHM algorithm. It should be easy to understand and devoid of mathematical complexities (Gouriveau et al., 2016a).

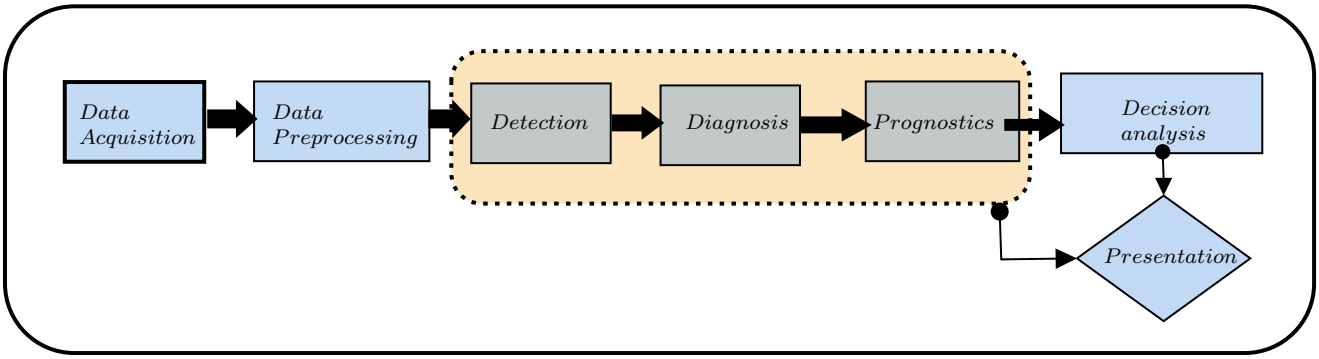

Figure 2.7: Standardized module for industrial prognostics

Prognostics can be classified into a physics-based, a data-based or a combination of both as shown in Fig.2.8.

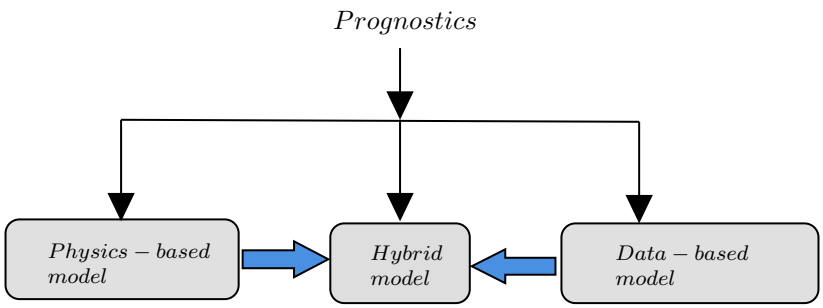

Figure 2.8: Taxonomy of prognostic approaches

2.2.1 Model-based prognostics

Model-based or physics-based prognostics are methods of prognostics that utilize mathematical models of degradation to predict a RUL either in a deterministic or stochastic form.
It involves an integration of sensory data with high fidelity models that permits in-situ identification of degradation of a healthy state of a system (Daigle et al., 2012). Therefore a complete model of a system must not only have the normal behaviour of the plant but also the time progressive failure behaviour (Daigle and Goebel, 2011).
Usually the erroneous impression created is that this type of prognostics is completely unrelated to data. That is far from the truth, as it must be noted that most good models are built on good domain knowledge of the system as well as rich and relevant model data for useful model parameters which may be updated and adaptable online.

Indeed, models can even be solely formulated on the basis of good behavioural data. Some derived physics-based models such as the Paris law (Paris and Erdogan, 1963) has been used to great effect for the prediction of crack growth on materials, dependent on the material properties of these components. This has been applied in various applications such as (Behzad et al., 2017) and (Pugno et al., 2006). Some other widely known examples are the Palmgren-Miner rule, a popularly accepted cumulative damage model in industry as well as the stiffness degradation algorithm, used in (Yuan et al., 2022) on cross-ply laminate materials.
A good implementation of a model-based approach must be on a micro and macro level as suggested by (Robinson, 2018), that is to say, there must be a physic of failure (PoF) model of how critical components affect the system as a whole and PoF models of individual critical components.
(Daigle and Goebel, 2011) provides the necessary steps for the implementation of model-based prognostics as shown in Fig.3.7. Firstly, there must be a developed physical understanding of the physical behaviour of the system. Then identify the influencing factors from the plant that contributes to degradation or failure, such that they serve as inputs to a progressive degradation model after the initiation of degradation. These variables or parameters can be estimated via estimators such as Kalman filters (Ompusunggu et al., 2016); (Al-Mohamad et al., 2021) or its various

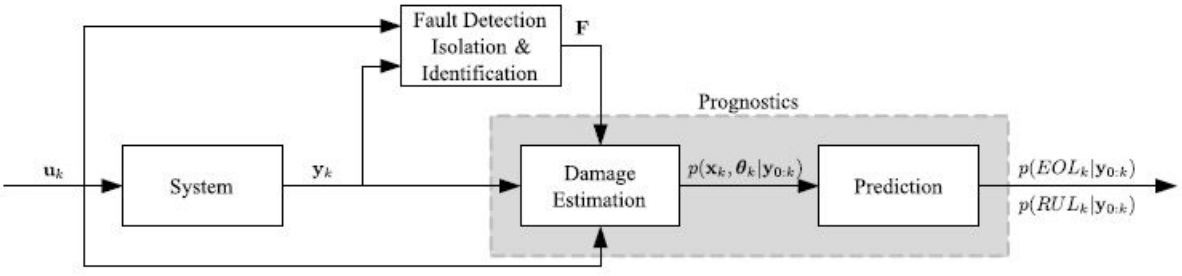

Figure 2.9: model-based prognostics architecture

variants such Extended Kalman filter (Loesch Vianna et al., 2015), unscented Kalman filter (Fan et al., 2012) ; (Sangwan et al., 2018) or particle filters (Jensen and Foster, 2019); (Wang et al., 2021); (Daroogheh et al., 2014) etc. Finally, a dynamic damage function such as the Paris law ((Paris and Erdogan, 1963)) takes as inputs estimated system's states for propagation to an EOL at each stipulated propagation time for a RUL value. Emphasis must be placed on the reduction of uncertainties in the estimation phase. As incurred prediction errors, only add to a more uncertain RUL estimation. The model-based method has the advantage of incorporating the physical understanding of the monitored system, broadening the scope of investigation, even though the process of development and validation may be tedious and is based on the assumption of a complete knowledge of the physical behaviour of the UUT (Madhav, 2016).

2.2.2 Data-based prognostics

With the availability of sufficient in-situ data, characteristics that represents the evolution of degradation are used to train models that estimate current states and also predict future states towards a EOL. In place of physics-informed models, mathematical models with parametric weights are used based on training data (An et al., 2013). The majority of prognostics algorithms are based on this method, primarily because it offers relatively easier implementation since it does not require a tedious understanding of the operational principles of the system (Elattar et al., 2016b). However, the data-based method is known to have less accuracy compared to its physics and hybrid-based counterparts. The use of AI especially deep learning models produces better accuracy, but they produce models that are essentially "black box" in nature, which is a lack of explainability of the intricacy of how results are obtained to encourage its deployment in industry. Lately, there has been an emergence of interest in refined data-based methods that offers explainability, the so-called explainability AI concept. (Kraus and Feuerriegel, 2019) proposed a structured-effect neural network, that outperforms other approaches in the literature but most importantly offers interpretability of the sources of degradation using variational Bayesian inferences. Also for the prediction of RUL for a turbofan engine fan, (Hong et al., 2020) employs Shapley additive explanation (SHAP) techniques for interpretability purposes using a deep neural network technique that combines 1D CNN, LSTM, and Bi-LSTM. Some reviews on the area of data-based prognostics in the literature are (Schwabacher and Goebel, 2007); (Elattar et al., 2018).

2.2.3 Hybrid prognostics

Hybrid prognostics combines the two fields of data and physics-based methods to predict RULs. It offers a trade-off between precision, applicability, and complexity, i.e the pros and cons of data and model-based prognostics (Medjaher and Zerhouni, 2013). There are primarily two classes of hybrid prognostics, a series approach, and a fusion approach. The series approach is used when there is an established physical model such that unobservable variables of the physics-based model are estimated via a data-based model (Baraldi et al., 2013); (Dong and Jin, 2014); (Dalal

et al., 2011). Alternatively, the fusion approach involves a parallel architecture where both models functions in tandem to augment each other for varied purposes (Cheng and Pecht, 2009); (Mangili, 2013). For example, a new research area has arisen in the area of physics-based or informed deep learning where physical models are used to augment deep learning algorithms that ensure better results and offer some form of explainability. This has been employed in prognostics undertakings such as in (Chao et al., 2022); (Gong et al., 2021) for fleet prognostics using physics-informed recurrent neural network and (Sara et al., 2022) for battery state of health. (Zhou et al., 2022) gives a good review on the merits of considering such models.

2.3 Uncertainty Identification and Quantification

Even though it is common for some articles on prognostics to only yield deterministic remaining useful life (RUL) values, it is emphatically clear that prognostics in engineering is an uncertain endeavor since it involves a prediction of a future event based on current conditions and assumed future measurements. Thus, it is only prudent to present these point-wise estimations with accompanying confidence intervals that afford a good interpretation of a reliable RUL prediction in real-life situations. Therefore, the answer to a posed RUL question should be an ”about” not an ”is”. It could not have been reiterated more by (Sankararaman and Goebel, 2013) that ”it is not even meaningful to make such predictions without computing the uncertainty associated with RUL”. Recently though, there has been a conscious effort to make the management of uncertainty in prognostics a standard procedure, with efforts on different proposed methods of identifying uncertainties, representing them, and using resource-efficient propagation methods. It is important to highlight early works such as (Sankararaman and Goebel, 2013); (Dewey et al., 2019) that sought to review the subject, emphasising the importance of uncertainty description in prognostics and equally from (Saxena et al., 2017) that goes ahead to propose the inclusion of uncertainty description in some generic prognostic metrics such as the prediction horizon (PH) and $\alpha - \lambda$ performance metrics, offering a method of comparing different quantification methods. Uncertainty in most articles in the literature seeks to formalise the types of uncertainties as epistemic uncertainty, which accounts for uncertainty in modelling, and aleatoric uncertainty which involves exogenous uncertainty sources such as sensor noise and environmental disturbances. But (Sankararaman and Goebel, 2013) contend this notion for application to condition-based monitoring, rather prescribing for an uncertainty classification involving: (i) Present uncertainty, that is uncertainty pertaining to the estimation of states before prognostics are undertaken, (ii) Future uncertainty, that describes unaccounted conditions during prognostication, (iii) Uncertainty modelling that represents the discrepancy between measured response and the true response and (iv) Prediction method uncertainty, which involves the uncertainty that arises even with the final quantification process of the RUL's uncertainty. The second classification offers a more comprehensive description that encompasses different possible uncertainty sources. Thus offering a good foundation to capture all uncertainties.

However, some authors (Gu et al., 2007); (Celaya et al., 2011) consider the use of sensitivity analy-

sis to take into account only the dominantly influential input uncertainty sources on the output in the quest to save computational cost. This may, however, result in under-representation in some cases when propagation times are long, such that the least uncertainty has a major cumulative effect.

Essentially, uncertainty management involves a transformation of input PDF to an eventual RUL output PDF (Orchard et al., 2008) such that in the literature, uncertainty quantification more often assumes a Gaussian distribution. However, this assertion is far from the truth as even with a simple prognostics model, the eventual probability distribution of RUL does not yield Gaussian distributions. Thus, such an assumption is strong and should be avoided (Sankararaman and Goebel, 2014). Indeed for this reason, for condition-based monitoring, Bayesian interpretation has become the go-to methodology. It is therefore not surprising that the particle filter has become the most featured prognostics estimator in most articles that consider prognostics uncertainty(see for e.g. (Cadini et al., 2018);(Haque et al., 2018)) as it offers suitable uncertainty representation suited for nonlinear dynamics and non-Gaussian uncertainty descriptions. The Bayesian theory has also been applied in the area of artificial intelligence (AI) in an attempt to quantify uncertainties which must be said is a difficult endeavor. However, in (Wu and Ma, 2019),(Li et al., 2020), and (Cornelius et al., 2020), different variants of Bayesian-inspired deep learning algorithms are suggested. For example in (Huang et al., 2021), a hybrid Bayesian deep learning-based prognostics approach is proposed that combines an LSTM-autoencoder with a Bayesian Neural Network (BNN) for uncertainty quantification. Other approaches such as the Confidence Prediction Neural Network, Radial Basis Function Neural Nets (RBFNN), and Probabilistic Neural Nets have also been proposed to handle uncertainty. But as stated in (Orchard et al., 2008), these approaches remain unproven as they are formulated on limited parameters and with unimodal distribution assumptions. For a system-level quantification, (Amssaouet et al., 2019) consider the use of inoperability input-output modelling for uncertainty description that handles component interactions structure, allowing for uncertainty description under component interaction. This was done considering the particles in particle filtering as representative of each system component's health. For the propagation step, it is commonplace to use Monte Carlo\ Quasi-Monte Carlo sampling, but this results in a high computational cost. In light of this, some works consider other resource-efficient methods to tackle this issue. In (Robinson et al., 2017), a concept borrowed from reliability engineering termed the inverse First Order Reliability Method (inverse FORM), is used for propagation. This offers less computational expense as only probable uncertainty sources associated with a reliability index are forecasted. The concept of stochastic response surface method (SRSM) has also been employed in (Robinson et al., 2017), where the basic function selected is polynomial. Computational costs are vastly reduced. According to the authors, similar results are obtained from just 27 simulations compared to 100,000 simulations for a Monte Carlo simulation. The method of non-intrusive polynomial chaos approach has also shown its merit as proposed by (Duong and Raghavan, 2017).

2.4 Integration of Prognostics with Control Techniques

According to Zagórowska et al. (2020), control approaches that consider the tolerance or mitigation of degradation can be classified into two main groups: (i) *Control systems aware of degradation* and (ii) *Control systems mitigating degradation*. In the first group, controllers are designed with the ability to compensate for the degradation of a controlled system with prior knowledge of the process. For example, the authors in Zagórowska et al. (2020) consider faults as a consequence of component degradation, thus classifying fault tolerant controllers as control systems aware of degradation, where there is a prerequisite for a knowledge of the fault process Isermann (2011). However, the latter involves control frameworks that seek to mitigate the extent of degradation over a component's lifetime by manipulating system variables and parameters delaying the time of failure. All these types of control methodology fall under the branch of prescriptive maintenance.

2.4.1 Control systems aware of degradation

In this control process, there must be available a degree of knowledge of degradation in other to take action against it. This process is in the field of control performance monitoring (CPM) where deterioration from different constituents of a control system is observed and actions are taken to accommodate or compensate for it. For example, this could be when a fault had already occurred in the case of fault tolerant control or other applications where compensation is initiated when the degraded behavior of the system deviates from a considered norm. Thus, from considered related fields to CPM as suggested by (Ding and Li, 2021), a Control system aware of degradation can be categorized with respect to (i) FDI (ii) Fault tolerant control (FTC) (iii) Controller optimization. In the sequel, FTC and FDI are discussed.

Fault Tolerant Control

Fault, as described in (Zhang and Jiang, 2008), can be seen as discrete events which affect a system by changing specific structural and/or parametric properties, leading to a system producing erroneous results and transitively leading to the system's failure (Shyama and Pillai, 2019). Faults in control systems are categorized into three forms.

- **Sensor fault**, f_s : Faults associated directly with the system measurements.
- **Actuator fault**, f_a : Fault that causes changes in actuator action.
- **Process fault**, f_p : Malfunction within the system process.

Occurrence of faults $f = [f_s, f_a, f_p]$ in a closed-loop network has the ability to change system behaviour from intended operating conditions which can be realised from its inclusion into the generic control model (2.6). Considering only additive faults, a model with faults, f can be represented as

$$\dot{x} = Ax + B(u + f_a) + E_d d + E_p f_p \tag{2.6a}$$

$$y = Cx + D(u + f_a) + G_d d + f_s + D_p f_p \tag{2.6b}$$

where u and d are control input and disturbance respectively. *FTC* should be able to maintain an acceptable level of performance with a tolerable level of degradation (Ocampo-Martinez and Puig, 2009). *FTC* are generally categorised as passive and active. Passive Fault Tolerance Control (*PFTC*) involves an off-line fixed structure, which is not subject to change no matter the properties of the fault. Schemes such as H_∞ and sliding mode are used in (A.Vargas-Martínez and R.Morales-Menendez, 2010) and (Alwi and Edwards, 2008) respectively as *PFTC* with promising results. On the other hand, Active Fault Tolerance Control *(AFTC)* relies on fault information from the detection level to initiate the reconfiguration of control actions ensuring control stability and acceptable performance (Ocampo-Martinez and Puig, 2009). An active *Fault Tolerant Control* (*FTC*) scheme should be able to detect and isolate faults and possibly estimate their magnitudes (fault diagnosis), from the FDI level, and adapt accordingly to faulty situations through control actions such that necessary operating conditions are satisfied even in the event of faults (Zhang and Jiang, 2008). The design of FDI should enable rapid and efficient detection and isolation from the inception of these faults to avoid further deterioration of the system's health. Resources abound in the area of model and model-free detection schemes in literature that gives a comprehensive review of various fault detection and isolation schemes over the years, the reader is referred to (Isermann, 2011);(Yassine et al., 2019). An example of an early prominent research is presented in (Isermann, 2011) that demonstrates a detection mechanism with emphasis on non-measurable quantities in models such as process parameters and process state variables. Results from this paper were particularly different from technologies at the time, which were dependent on fault detection based on upward and downward transgression of limits as well as trends that are monitorable to detect faults. The author in (Isermann, 2011) goes ahead to apply parameter monitoring and cross-correlation tools with applications to an electrical-driven centrifugal pump, and leaks in pipes respectively, concluding for instance the need for a low-order model to ensure high precision in parameter estimation. In (Yassine et al., 2019), data collected from system output were used to make inferences on deviation from a standard norm of operation, by comparing data from faulty scenarios to data from normal operations using statistical tools.

Trendy research tools such as machine learning using Artificial Neural Networks*(ANN)*, Support Vector Machines *(SVM)* among others to detect faults (Zhang et al., 2019) have not surprisingly attracted the interest of late. (Zhang et al., 2019) provides good documentation of these methods as applied to fault detection in bearings, going further by introducing the application of deep learning in fault detection, making a case for its adoption due to better algorithms, which have improved speed, convergence and generalisation, combined with an increased amount of datasets and modern hardware to match. However, this approaches lack necessary explainability which is important in FDI. In *DWNs*, the method of Principal Component Analysis (*PCA*) has been applied in (Gertler et al., 2010) with mixed results. This is mainly due to the difficulty of spatial separation of faults from normal data. This arises as a result of the presence of disturbances that are co-linear with faults limiting the reduction in dimensionality, whereas Veldman - de Roo et al.

(2015) utilises an observer-based residual generators to effectively detect leaks in pipes. Fault detection in pumps has also been studied in Kallesøe et al. (2004). *FDI* serves as the precursor for fault-tolerant mechanisms, after a fault has been duly detected and possibly diagnosed, *FTC* is applied.

As a further illustration, consider that an automated system is subject to control actions u, these control variables, $u \subseteq \mathbb{U}$ are designed based on a control law such that certain control objectives $\mathbb{O}$ are satisfied with an associated performance index $\mathbb{J}$. The system is controlled in a manner such that the evolution of the dynamic states $x \subseteq X$ and control actions u respect strict or relaxed constraints $\mathbb{C}$. $\mathbb{C}$ can be described in an affine, linear or nonlinear equality and inequality form depending on the system dynamics and process requirements. Constraint $\mathbb{C}$ therefore has a specific structure $\mathbb{S}$ and parameters θ, hence the control problem can be presented by the tuple $\langle\ \mathbb{O}, \mathbb{C}(\mathbb{S}, \theta), \mathbb{U}\ \rangle$. Considering that in real life, systems are prone to parametric variation and uncertainties, the control structure can be reformulated considering "real" parameters $\theta \in \Theta$, where Θ is a set of possible parameters as a result of variation from normal operations (Blanke et al., 2000). The problem thus becomes $\langle\ \mathbb{O}, \mathbb{C}(\mathbb{S}, \Theta), \mathbb{U}\ \rangle$ which can employ robust or adaptive control laws for desirable solutions.

Assuming nominal conditions with structure and parameter as ($\mathbb{S}^*$,θ^*), under normal operation, there should be a control action u^* restricted by $\mathbb{U} \times X$ (i.e u^* as a function of state variable) as a solution for the problem $\langle\ \mathbb{O}, \mathbb{C}(\mathbb{S}^*, \theta^*), \mathbb{U}\ \rangle$. Therefore a fault can be thought of as occurred when $(\mathbb{S}, \theta) \neq (\mathbb{S}^*, \theta^*)$.

For a case of fault, let the properties of the constraints be $(\hat{\mathbb{S}}, \hat{\theta})$ to form the real constraints $\mathbb{C}(\hat{\mathbb{S}}, \hat{\theta})$ under faulty conditions, a fault-tolerant control (*FTC*) should have the ability to accommodate a deviation from the nominal constraints but still find a feasible solution for a problem $\langle\ \mathbb{O}, (\hat{\mathbb{S}}, \hat{\theta}), \mathbb{U}\ \rangle$ with an acceptable degree of degradation. $(\hat{\mathbb{S}}, \hat{\theta})$ is estimated beforehand at the *FDI* level, this process leads to what is called *fault accommodation*. When there is no solution for the problem during fault accommodation due to the extent of the fault, the tolerance level of the actuator, a restructuring of $\langle\ \mathbb{O}, \mathbb{C}(\mathbb{S}, \Theta), \mathbb{U}\ \rangle$ is required. Henceforth, there is the introduction of a new feasible pair of constraint elements, $(\Sigma, \lambda) \in (\bar{\mathbb{S}}, \Theta)$, where $\bar{\mathbb{S}}$ comprises of different restructuring of the system which keeps the system's functionality. Therefore considering that (Σ, λ) do not result in faulty conditions, the setup must have a solution for $\langle\ \mathbb{O}, \mathbb{C}(\Sigma, \lambda), \mathbb{U}\ \rangle$, usually done with aid of redundant elements in the system. This type of *FTC* is an *AFTC* known as *reconfiguration*. Estimation can be done from the FDI to improve the possibility of a solution but is not really a prerequisite (Blanke et al., 2000).

Controller optimization

With information about the degraded state, the degradation is optimized to manage degradation or failure. The predominant controller used in this instance is an optimization-based or adaptive controller. In (Zaccaria et al., 2019) an adaptive control for the compensation of degraded perfor-

mance from a micro-gas turbine is proposed. With results from a diagnostic sub-level, showing deviation from the unhealthy operation, an MPC control is designed for compensation. Also in (Hua, 2021), reinforcement learning approaches of Q-learning and natural actor-critic methods were applied to input/output recovery and performance index-based approaches for robustness and performance optimization of feedback control systems containing degraded components. This was tested on a brushless direct current motor test rig. With a load-sharing control scheme through real-time optimization via modifier adaptation, (Milosavljevic et al., 2016) proposed compensation of degraded parallel gas compressors depending on the magnitude of a plant-model mismatch.

2.4.2 Control system mitigating degradation

This basically involves the control management of innate degradation-related model variables or integrated degradation models that are dependent on a system's controllable variables, predominantly using optimization-based controllers. It involves the manipulation of these variables arriving at a trade-off between satisfying primary control objectives and the mitigation of degradation, usually to prolong a degraded state to fulfill mission targets.
The incorporated model may involve the use of characteristic quantities such as reliability of components or SoC (State of Charge) of batteries that invariably are dynamic functions of controllable states such that a supervision layer can be set up to manage degradation via the selection of optimal operational set-points. Considering the constraints on a race track, (Pour et al., 2021) employs a health-aware control that considers the RUL of batteries of an autonomous vehicle, essentially it's SoC, optimizing it's performance to meet mission goals. For reliability-oriented applications, control allocation of an aircraft based on actuators' reliability was done in Khelassi et al. (2011) using an LQR control. The results show improved actuator health and thus overall system reliability. Similarly, in Chamseddine et al. (2014), control allocation was used based on an MIT-based reliability rule for an over-actuated octocopter helicopter testbed to maximize global reliability. In the area of DWN, Salazar et al. (2017) and Pour et al. (2018) used the interconnections between the system components to model the cumulative reliability of the system, using different statistical methods (Bayesian and Markov chains). Using an MPC, the health of the actuators was included as an objective criterion, such that through load sharing, the rate of decrease of the network's reliability was minimized at the expense of primary control goals. Also, certain variables of health are appended to plant models, thus factor-based models can be directly included in control designs. for example, in the area of wind turbines, many works include variables of health such as tower-fore aft, slip angle, etc in control designs, especially an optimization-based one, promoting component health against power extracted. Also by the prediction of component deterioration through fatigue estimation techniques, another school of thought employs directly this information into control schemes. This approach has the advantage of giving operators direct information on approximated degradation which could help operators optimize operations to maximize profit. For example, in (Barradas-Berglind et al., 2015), an MPC strategy that incorporates online fatigue estimation has been studied. The authors consider an online estimation of drive train shaft dam-

age through Preiscach hysteresis which is then incorporated into a data-based MPC; consequently tested on the nonlinear OpenFAST model showing promising results. Authors in (Sanchez et al., 2015), instead present an offline approach to fatigue estimation of wind turbine's blades, establishing a relationship between the remaining useful life (RUL) and the stress history with the help of the widely known Palmgren-Miner's damage accumulation rule, aimed at maximizing the RUL of the blades, but the authors only consider a simple case of an assumed constant wind thus neglecting the cyclic nature of stress. To include the cyclic behaviour of stress, (Löw et al., 2020) henceforth considers an external inclusion of a cycle counting technique, the rainflow counting in a process termed as Parametric Online Rainflow-counting (PORFC). But most of these techniques mentioned only considers a fixed penalization of the damage criterion, thus presenting solutions that have a notion of a perpetual deration of the turbine which is not economically viable. (Beganovic et al., 2018) thus employs the Palmgren-Miner's damage accumulation rule to model a damage function over a wind turbine's lifetime and then considers an ensemble of LQR controllers, each tuned differently per a predefined selection of weights such that an online switching mechanism is proposed on the controller at different damage points mitigating damage at a marginal cost of reduced power production. Crack mitigation in aircraft applications has also been studied by (Ray and Caplin, 2000);(Ray et al., 2000). The propagation of the cracks was modelled considering the effect of the plant's variables.

Chapter 3

Set Based Prognostics for Wind Turbine Blade

The content of this chapter is based on the following works:

- (Khoury et al., 2022e) Khoury, B., Puig, V., and Nejjari, F. (2022e). A set-based prognostics approach for wind turbine blade health monitoring. *IFAC-PapersOnLine*, 55, 402–407. doi: 10.1016/j.ifacol.2022.07.162.
- (Khoury et al., 2020b) Khoury, B., Puig, V., and Nejjari, F. (2020b). Model-based prognosis approach using a zonotopic kalman filter with application to a wind turbine. In *Proceedings of the 5th European Conference of the Prognostics and Health Management Society (PHME 2020))*, volume 5, 9. doi: p.1258:1-1258:9.ISBN978-1-936263-32-5.

Productive operation of wind turbines requires structural installations at most often unforgiving environmental conditions which invariably leads to a high rate of component damage. Due to the inevitability of these occurrences, the knowledge of the life expectancy of these components subject to adverse conditions is of importance for the effective planning of maintenance and operation to minimize the Levelized Cost of Energy (LCoE); increasing profits and accelerating wind energy's contribution to a more environmentally sustainable energy mix. Prediction of the life expectancy of components at a specific time in a plant's operation involves an efficient design of prognostic tools to establish whether operational goals can be fulfilled, whilst also considering the possibility of including online decision-making frameworks such as fault-mitigation, operational replanning, and other prescriptive policies (Sankararaman and Goebel, 2014).
Uncertainty in prognostics is inevitable since it involves an assumed knowledge of future operating conditions and also presents the prediction of states and/or parameters that are uncertain. Quantification of uncertainty in prognostics according to (Sankararaman and Goebel, 2014) can basically be posed as an uncertainty propagation problem, which can either be online or offline. (Sikorska et al., 2011) acknowledges the fact that the main bottleneck of online implementation is the computational burden that most methodologies present. In lieu of this, it is imperative to propose prognostics algorithms that are practical for easy deployment. In this chapter, to overcome

computational complexities that may arise in prognostics methodologies, a set-based prognostics of a wind turbine blade is proposed and the problem is posed as a reachability analysis problem. Reachability analysis has been extensively studied and used in diverse applications such as robust control, state-based prediction in autonomous systems, computation of region of attraction for stability, and fault detection purposes, among others. For linear dynamics, since convexity is preserved in set propagation when convex sets are used, appropriate convex sets are considered in reachability analysis. Moreover, manipulations of convex sets under mathematical operators such as linear transformation, Minkowski sum, and convex hull are also easily possible and practically implementable. The choice of the type of set however mainly depends on the computational demands of convex operands under these operators. For example, a Minkowski sum of a polytope can be a computationally demanding operation as compared to a zonotope, which is closed under linear maps and Minkowski sums for the same bounding representation. Henceforth, zonotopic sets are chosen primarily because it offers simplicity in computation of sets and flexibility in operation compared to other geometric representations e.g ellipsoids, interval sets, etc. During the estimation step, for lesser computational burden, an LPV zonotopic Kalman filter is formulated taking into account a damage-appended wind turbine model in an LPV format such that at each propagation time, with the estimated state (degradation) and its uncertainty, propagation of positive invariant zonotopic sets can be undertaken.
This chapter also introduces the nonlinear wind turbine and its blade for chapter 4 and mathematical preliminaries for chapter 6.

3.1 Non-Linear Wind Turbine

The closest mathematical representation to the complete functionality of a wind turbine, the high fidelity OpenFAST (Jonkman and Buhl, 2005) is a 24-degree-of-freedom model, thus undesirable for control design purposes (Georg, 2015). Therefore two reduced models by (Bianchi et al., 2007) and (Odgaard et al., 2015a), which capture most key dynamics of the plant are considered in this thesis. Above a certain sweeping wind speed, wind turbines capture useful kinetic energy via the blades to influence the velocity of the rotor, hence prompting the conversion of kinetic wind flows into useful electricity via internal mechanical energy. The wind turbine can therefore be categorized as an interaction between the aerodynamic, flexible drive train, power generator, and the pitch actuator sub-models.

3.1.1 Mechanical model

It is assumed that the rotor trust force F_T that acts on the tower not only causes a displacement in the tower but the blade tip. A single-shaft model which consisting of two rigid bodies linked by a flexible shaft is also considered for the drive-train. On either side of the shaft are the mechanical components represented as rigid bodies. Hence by means of Lagrangian dynamics, given a vector

of generalized coordinates:

$$\mathbf{q} = (\mathbf{y_T}, \mathbf{y_B}, \theta_\mathbf{r}, \theta_\mathbf{g})$$

and a vector of external forces:

$$\mathbf{Q} = (\mathbf{F_T}, \mathbf{F_T}, \mathbf{T_a}, \mathbf{T_g})$$

the mechanical model can be described from the equation of motion, with mass matrix **M**, damping matrix **C**, and stiffness matrix **K** as:

$$M\ddot{q} + C\dot{q} + Kq = Q\left(\dot{q}, q, t, u\right). \tag{3.1}$$

Considering that the blade tip displacement involves the tower as well, $\therefore\ y_{B_T} = y_T + y_B$. A Lagrange's equation with kinetic energy, E_K, dissipating energy E_d and potential energy E_p is given as:

$$\frac{d}{dt}\left(\frac{\partial E_K}{\partial \dot{q}_i}\right) + \frac{\partial E_p}{\partial q_i} + \frac{\partial P_D}{\partial \dot{q}_i} = f_i \tag{3.2}$$

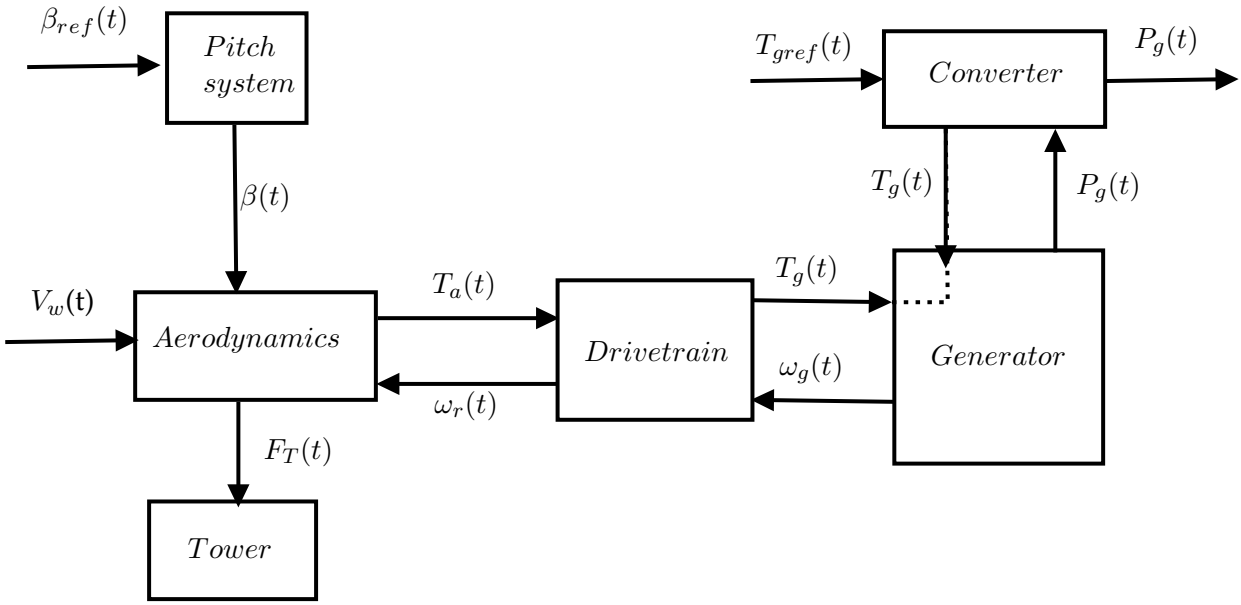

Figure 3.1: Interactions between sub-models of the wind turbine.

With the respective energies given as:

$$E_K = \frac{1}{2}m_T\dot{y}_T^2 + \frac{1}{2}Nm_B\dot{y}_{B_T}^2 + \frac{1}{2}J_r\dot{\theta_r}^2 + \frac{1}{2}J_g\dot{\theta_g}^2 \tag{3.3a}$$

$$E_p = \frac{1}{2}k_T y_T^2 + \frac{1}{2}Nk_B y_b^2 + \frac{1}{2}k_s\left(\theta_r - \frac{1}{n_g}\theta_g\right)^2 \tag{3.3b}$$

$$P_D = \frac{1}{2}d_T\dot{y}_T^2 + \frac{1}{2}Nd_B\dot{y}_B^2 + \frac{1}{2}d_s\left(\dot{\theta_r} - \frac{1}{n_g}\dot{\theta_g}\right)^2. \tag{3.3c}$$

Resulting in a four-degree-of-freedom mechanical model considering (3.2) as:

$$\left(m_T + Nm_B\right)\ddot{y}_T + Nm_B\ddot{y}_B + d_T\dot{y}_T + k_T y_T = F_T \tag{3.4a}$$

$$Nm_B\ddot{y}_T + Nm_B\ddot{y}_B + Nd_B\dot{y}_B + NK_B y_B = F_T \tag{3.4b}$$

$$J_r\ddot{\theta}_r + d_s\left(w_r - \frac{1}{n_g}w_g\right) + K_s\left(\theta_r - \frac{1}{n_g}\theta_g\right) = T_a \tag{3.4c}$$

$$d_s\left(w_r - \frac{1}{n_g}w_g\right) + K_s\left(\theta_r - \frac{1}{n_g}\theta_g\right) - J_g\ddot{\theta}_g = T_g \tag{3.4d}$$

The equations are rearranged in matrix form as in (3.1):

$$\mathbf{M} = \begin{bmatrix} m_T + Nm_B & Nm_B & 0 & 0 \\ Nm_B & Nm_B & 0 & 0 \\ 0 & 0 & J_r & 0 \\ 0 & 0 & 0 & J_g \end{bmatrix}, \tag{3.5a}$$

$$\mathbf{C} = \begin{bmatrix} d_T & 0 & 0 & 0 \\ 0 & Nd_B & 0 & 0 \\ 0 & 0 & d_s & \frac{-d_s}{n_g} \\ 0 & 0 & \frac{-d_s}{n_g} & \frac{-d_s}{n_g^2} \end{bmatrix}, \tag{3.5b}$$

$$\mathbf{K} = \begin{bmatrix} K_T & 0 & 0 & 0 \\ 0 & NK_B & 0 & 0 \\ 0 & 0 & K_s & \frac{-K_s}{n_g} \\ 0 & 0 & \frac{-K_s}{n_g} & \frac{K_s}{n_g^2} \end{bmatrix}. \tag{3.5c}$$

.

3.1.2 Pitch and generator dynamics

Pitch-controlled wind turbines control the power extracted from the wind by ensuring maximum extraction at below-rated speeds and prevent Wind-turbine damage when wind speeds are considered high by alternating the blade's surface for wind attack via the blade pitch angle. A first-order

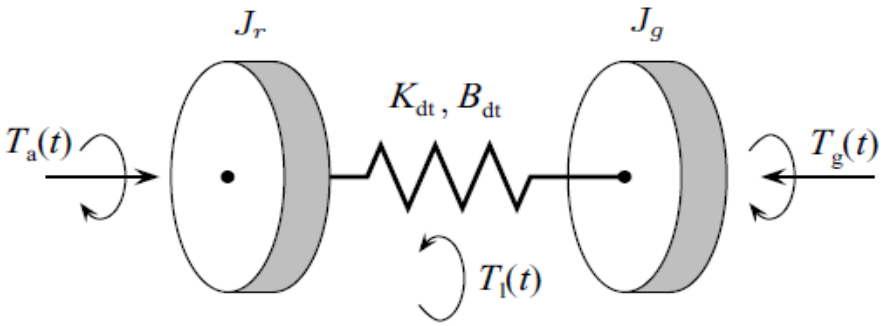

Figure 3.2: Drive-train

delay model, a common feature in most literature is used.

$$\dot{\beta} = \frac{1}{\tau_\beta}\beta + \frac{1}{\tau_\beta}\beta_{ref} \tag{3.6}$$

where β and β_{ref} are the pitch angle and the pitch control input respectively. Also, a simple first-order delay model is employed for the generator and converter dynamics given as:

$$\dot{T_g} = \frac{1}{\tau_g}T_g + \frac{1}{\tau_g}T_{g_{ref}} \tag{3.7}$$

T_g is the generator torque and $T_{g_{ref}}$, the control input from the generator. τ_g and τ_β are their respective delay time constants.

3.1.3 Aerodynamics model

The nonlinearity in the chosen wind turbine models emanates from the aerodynamic model. It consists of the thrust force on the rotor, F_T, and the aerodynamic torque T_a from captured aerodynamic power P_r available in wind power P_w that sweeps across the blades' surface. The forces T_a and F_T are given as:

$$T_a = \frac{P_r}{w_r} = \frac{1}{2}\rho A R C_p\left(\lambda(t), \beta(t)\right) V_w^2(t), \tag{3.8a}$$

$$F_T = \frac{1}{2}\rho A C_t\left(\lambda(t), \beta(t)\right) V_w^2(t). \tag{3.8b}$$

where ρ is the air density, A, the rotor swept area, V_w is the available wind speed and R, the radius of the rotor. The power and thrust coefficients are denoted as C_p and C_t respectively which are both functions of the pitch angle β and blade tip speed λ given as:

$$\lambda(t) = \frac{R w_r(t)}{V_w(t)}. \tag{3.9}$$

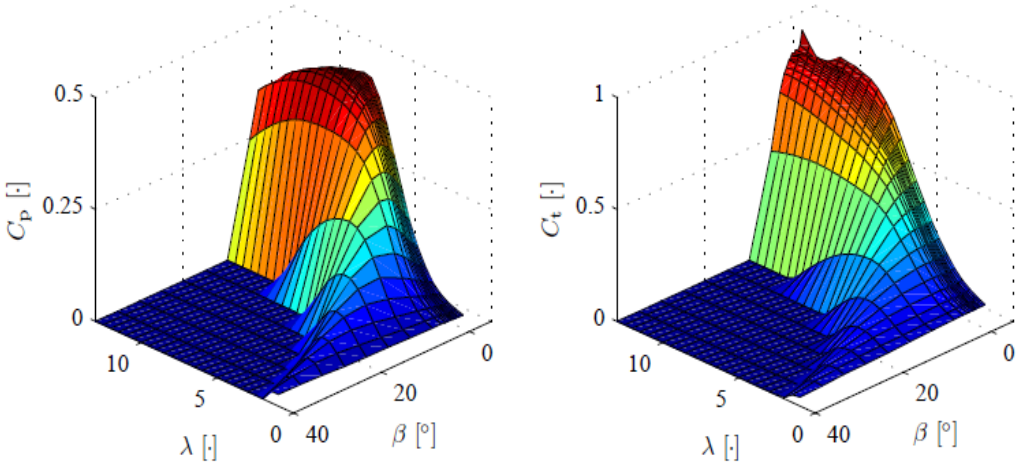

Figure 3.3: The C_p and C_t coefficients as functions of the pitch angle and the tip-speed ratio.

3.1.4 Complete state space model

Considering the torsion angle as a state, $\theta_s = \theta_r - \theta_g$ and the mechanical model in state space form from (3.1),

$$\ddot{q} = -M^{-1}C\dot{q} - M^{-1}Kq + M^{-1}Q \tag{3.10}$$

The complete model involving all the interacting sub-models is given by:

$$\dot{x} = Ax + Bu + f(x, V_w) \tag{3.11}$$

$$A = \begin{bmatrix} 0_{3\times3} & L_{3\times4} & 0_{3\times1} & 0_{3\times1} \\ -M^{-1}K & -M^{-1}D & 0_{4\times1} & \begin{bmatrix} 0_{3\times1} \\ -\frac{1}{J_g} \end{bmatrix} \\ 0_{1\times3} & 0_{1\times4} & -\frac{1}{\tau_\beta} & 0 \\ 0_{1\times3} & 0_{1\times4} & 0 & -\frac{1}{\tau_\beta} \end{bmatrix},$$

$$B = \begin{bmatrix} 0_{7\times1} & 0_{7\times1} \\ \frac{1}{\tau_\beta} & 0 \\ 0 & \frac{1}{\tau_g} \end{bmatrix},$$

$$f(x, V_w) = \begin{bmatrix} 0_{4\times1} \\ \frac{1}{Nm_B}F_T(x, V_w) \\ \frac{1}{J_r}T_a(x, V_w) \\ 0_{3\times1} \end{bmatrix}.$$

The states $x = [y_T, y_B, \theta_s, \dot{y_T}, \dot{y_B}, w_r, w_g, \beta, T_g]$ are the tower and blade displacements, torsion angle, tower, and blade velocity, rotor and generator speed, the pitch angle and the generator torque respectively. The inputs $u = \left[\beta_{ref}, T_{g_{ref}}\right]$ are the reference control pitch angle and generator torque. In the sequel, the nonlinearity from $f(x, V_w)$ is reformulated into a pseudo-linear form through LPV nonlinear embedding.[1]. An LPV model of the wind turbine is obtained from (3.11) by means of a non-linear embedding approach as described in (Rugh and Shamma, 2000). This allows to the introduction of a model that is linear in the state space, but nonlinear in parameter space offering an optimization problem where simple convex optimization tools can be applied.
A further reduced wind turbine by (Odgaard et al., 2015a) which considered only the pitch, torque, and rotor speed dynamics are considered in this chapter as the degradation as shown in the subsequent sections depends on these variables.

3.1.5 A further reduced model from (Odgaard et al., 2015a)

Neglecting torsion angle and friction and with the assumption that the low and high-speed shaft is one complete model, a simple wind turbine model is proposed as:

$$\dot{w_r} = \frac{1}{J}(T_a - N_g T_g) \tag{3.13a}$$

$$\dot{\beta} = \frac{1}{\tau_p}(-\beta + \beta_{ref}) \tag{3.13b}$$

$$\dot{T_g} = \frac{1}{\tau_g}(-T_g + T_{g_{ref}}) \tag{3.13c}$$

$$\tag{3.13d}$$

where w_r is the rotor speed, T_g is the generator torque and β the pitch angle for capturing wind depending on wind speeds V_w.

3.1.6 A general description of a wind turbine blade

Wind turbine blades are purposely designed for maximum extraction of kinetic energy from a minimum available wind, whilst taking into account their cost of fabrication, therefore ideally manufacturing an efficient blade from an economically viable material. Wind turbine blades as described by (Leon et al., 2017) are composed of composite materials, conventionally fibre reinforced polymers, and glass fibre or recently a hybrid of carbon and fibre. This is primarily due to their comparatively high stiffness, stiffness-to-density ratio, and toughness. The suction and pressure face is adhesively bounded together by shear webs joining the lower and upper parts of the blade shell. They may also be fabricated as a unit through the process of infusion. The convenient selection of appropriate composite materials enables the development of longer and larger blades which are cost-effective mainly due to their strength-to-mass utilization ratio (Chen

[1]Plant's model parameters can be found at `https://www.nrel.gov/docs/fy13osti/57228.pdf`

and Eder, 2020). Aerodynamic and structural considerations such as the designed blade shape, number of blades, aerofoil selection, and optimal attack angles play a major role in enhancing an optimal tip-speed ratio (ratio of the speed of the rotor tip to wind speeds over the blade) which is basically a metric to measure maximum captured energy from wind. Due to the exposure of the blades to the stochastic wind as well as forces such as gravity, these composite materials are liable to gradual degradation due to cracks. In the sequel, a method of determination of the material degradation through a stiffness degradation algorithm under stress is discussed.

3.1.7 Fatigue estimation Of wind turbine blades with stiffness degradation

Fatigue in structures occurs when subjected to repeated cyclic stress below their peak static strength resulting in a localized, progressive, and eventual permanent structural alteration (cracks or complete fracture) of a UUT (Krasnosel'skiĭ and Pokrovskiĭ, 1989). Estimating fatigue in wind turbine structures subjected to stochastic wind loadings and other forces has been a subject of study for

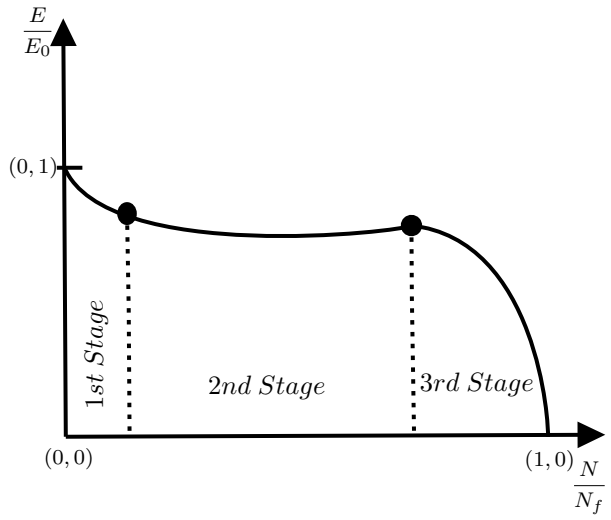

Figure 3.4: Curve showing stages of stiffness degradation.

many decades. These studies, therefore, present grounds to compute the fatigue life of components of wind turbines to enable predesigns, either active or passive, which averts rapid loss of structural strength for a longer operational lifetime enhancing the economic viability of wind energy technology. Ideally, wind turbine blades are designed to withstand up to about a 10^8 magnitude of load cycles during its stipulated target lifetime of 20-25 years. Directional and magnitudinous variation in stochastic wind results in the phenomenon of wind shear, a consequence of larger winds at the top of the structure compared to the bottom resulting in an unbalanced loading of the wind turbine structure resulting in structural stress (Blanke et al., 2006). Gyroscopic and gravitational forces also contribute to loadings on the structure. Attention to mitigating these fatigues in wind turbines has garnered even more prominence with the introduction of large wind turbines for higher power output. Large wind turbines inherently introduce an increase in masses of components exacerbating stress. For example, large blade sizes increase the surface of attack of

wind amplifying the effects of aerodynamic forces on the structure when subjected to turbulent wind. Longer and larger blades may also deflect causing destruction to the tower. Also, massive masses mean an increased effect of gravity on the structure leading to pronounced stress effects. Thus it is cogent to understand the behaviour of these occurrences to better maximize profits putting in mind that their cumulative effect over time leads to costly unplanned maintenance. Due to the difficulty in measurement of deterioration in materials over time, predictive tools dependent on specific material parameters in functions derived from rigorous experiments are considered. One such method is the stiffness degradation algorithm. According to (Vassilopoulos et al., 2010), the modulus decay of most fiber-reinforced composite materials occurs in three stages as shown in Figure 3: E_0 is undamaged stiffness, E is the stiffness at a specific point in the material fatigue life cycle, N is the total test cycles and N_f is the fatigue life in cycles. In the first stage, there is a rapid degrading of stiffness of about 2-5$\%$ mostly due to transverse matrix cracks, at this stage, microscopic cracks in the material start. Stage two involves a gradual degradation over the fatigue lifetime. Damage here is mostly caused by edge delaminations and additional longitudinal cracks. Eventually, in the final state, degradation occurs in abrupt steps, culminating in an overall fatigue failure of the specimen.

From (Van Paepegem and Degrieck, 2002), under the assumption that our UUT, the blade is a solid beam, the damage model considering compressive stress can be described as:

$$\frac{dD}{dN} = f_i(\phi, D) + f_p(\phi, D), \tag{3.14}$$

where f_i is the initial stage function of a steep decline in stiffness and f_p is the damage propagation function of the second and final stages. These two functions are given by

$$f_i(\phi, D) = \left[C_1 \Sigma(\phi, D) \exp(-C_2 \frac{D}{\sqrt{\Sigma(\phi, D)}}) \right]^3, \tag{3.15a}$$

$$f_p(\phi, D) = C_3 D \Sigma(\phi, D)^2 \left[1 + \exp(\frac{C_5}{3}(\Sigma(\phi, D) - C_4) \right]. \tag{3.15b}$$

where failure index $\Sigma(\phi, D)$ is a function of the damage D resulting in material strength reduction and the stress value ϕ

$$\Sigma(\phi, D) = \frac{\phi}{(1 - D)X_c}. \tag{3.16}$$

The constant X_c is the comprehensive static strength. The damage growth model from initiation to final fatigue failure is thus given as :

$$\frac{dD}{dN} = \left[C_1 \Sigma \exp(-C_2 \frac{D}{\sqrt{\Sigma}}) \right]^3 + C_3 D \Sigma^2 \left[1 + \exp(\frac{C_5}{3}(\Sigma - C_4) \right] \tag{3.17}$$

where C_1 and C_2 are the material constants, C_3 is the damage propagation rate, and C_4 is a threshold below which there is no initiation of fibre fracture. When the threshold C_4 is crossed, the initial

fibre fracture occurs on the specimen, which causes an exponential rapid decrease in strength and enables the final fatigue failure of the material. As long as the failure index is below the threshold C_4, the parameter C_5 assumes a large value to ensure a strongly negative exponential function. When C_4 is crossed, it assumes a large positive for accelerated degradation of the material. The third power is used for compressive stress as they show from experiments to have considerably less effect than tensile stress. From (Van Paepegem and Degrieck, 2002), the parameters for a damage model for a fibre-reinforced composite of which some wind turbine blades are made up of with the stiffness degradation algorithm is given in Table 3.1. Even though the UUT is presumed to have reached a predefined threshold of damage after this test, it is by no means an indication that the component is not usable. Ideally, the natural assumption is to run the algorithm till a 100 $\%$ deterioration of material strength, but it must be noted that since most of these predictive or statistical methods are thought of as not exact, under conditions of fluctuating mean stress or pronounced sequence effects, a value below 100% is normally chosen (Pedersen, 2018).

Table 3.1: Parameters for stiffness degradation model.

Parameter	**Value**	**Unit**
C_1	0.002	(1/cycle)
C_2	30	-
C_3	4×10^{-4}	(1/cycle)
C_4	0.85	-
C_5	93	-
X_c	341.5	Mpa

3.2 Mathematical Background

In this section, the zonotope is described for sections 3 and 6 as well as reachability analysis for chapter 3.

3.2.1 Zonotope

For clarity, calligraphic capital letters are used to represent sets, $\Delta(.)$ for the uncertain component of a variable, and lower letter cases for deterministic representations. $\square(.)$ signifies the interval hull of a set. Considering the Minkowski sum of two sets S_1 and S_2 as $S_1 \oplus S_2 = \{s_1 + s_2 | s_1 \in S_1, s_2 \in S_2\}$, with a unitary box of r unitary elements and $B^r \in \mathbb{R}^r$ given as $B^r = [-1, 1]^r$. A zonotope can be defined as a class of geometric set with a center p and a generator matrix $H \in \mathbb{R}^{n \times r}$ in a linear affine image as

$$\mathcal{Z} \coloneqq \langle p, H \rangle = p \oplus HB^r \tag{3.18}$$

The Minkowski sum of two zonotopes $\mathcal{Z}_1 = \langle p_1, H_1 \rangle$ and $\mathcal{Z}_2 = \langle p_2, H_2 \rangle$ is thus given as:

$$\mathcal{Z}_1 \oplus \mathcal{Z}_2 = \langle p_1, H_1 \rangle \oplus \langle p_2, H_2 \rangle = \langle p_1 + p_2, [H_1 H_2] \rangle \tag{3.19}$$

The linear mapping of a zonotopic set, $\mathcal{Z}$ by a vector or a matrix $\mathcal{K}$ is given as :

$$\mathcal{K} \odot \langle p, H \rangle = \langle \mathcal{K}p, \mathcal{K}H \rangle \tag{3.20}$$

and the smallest box (interval hull) containing the zonotope is described by $\square\mathcal{Z} = p \oplus rs(H)B^r$, where $rs(H)$ is a diagonal matrix such that $rs(H)_{i,j} = \sum_{j=1}^{m} |H_{i,j}|$. Hence, $\mathcal{Z} \subset \square\mathcal{Z}$.

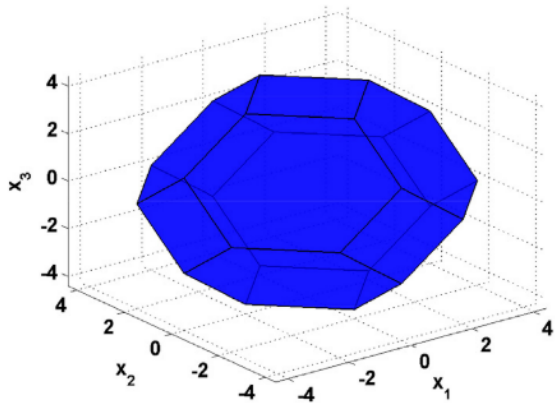

Figure 3.5: A 3D zonotope.

3.2.2 Reachability Analysis

Reachability analysis is a technique to evaluate resultant reachable sets which are computed through diverse means, mainly grouped into set propagation (Althoff et al., 2021) and simulation-based methods (Meslem and Martinez Molina, 2019). It fundamentally involves a union of all feasible trajectories under all possible input realizations and constraints that a dynamic system can reach within a finite or infinite time span, commencing from a bounded initial set (Amr et al.). There is a plethora of its applications, from real-time motion planning (Bansal et al., 2020); (Manzinger et al., 2021), stability analysis in control (Rakovic et al., 2012); (Desimini and Prandini, 2019), neural network verification(Xiang et al., 2018), multiplayer reach-avoid games (Yan et al., 2020), through backward reachability analysis, safety planning (Harno and Kim, 2019); (Bui et al., 2021) etc. For a feasible reachable set realization, there are requirements of initial and transition conditions that ensure computational feasibility and promote interpretability. Thus, this encourages the use of convex sets which are easily mathematically computable under linear reachability mapping and interpretation of final reachable sets either through conservatively inner or outer approximation through desirable bounding techniques. However, some methodologies such as the Hamilton-Jacobi reachability formalism encourages nonlinear reachability and non-convex input maps but

leads to exponential computational complexity when the number of variables involved increases (Bansal et al., 2017). Reachability analysis intrinsically involves uncertain conditions which differ from a deterministic case, such that transitions hereafter are not known but can be bounded as shown in Fig 3.6. For a continuous dynamic system given as :

$$\dot{x}(t) = f(x(t), w(t)) \tag{3.21}$$

where $x(t) \in \mathbb{R}^n$ is the n dimensional states, $w(t) \subset \mathcal{W}$, the exogenous input variable that takes its value from a compact convex set $\mathcal{W}$ and $f(.)$, the flow map. The reachable set $\mathcal{R}_t(.)$ for the time interval $t \subseteq [t_0,\ T] \in \mathcal{R}^+$ is defined by all possible trajectories $\xi\left(t, x_0, w\left(t_0,\ T\right)\right)$ defined on an initial set $\mathcal{X}_0$, $\forall x_0 \subset \mathcal{X}_0$ and inputs $w_{[t_0,T]} \subset \mathcal{W}$. The assumed resultant compact convex set can thus be described as a union of sets:

$$\mathcal{R}_{[t_0,\ T]}(\mathcal{X}_0,\ \mathcal{W}) = \bigcup_{t \in [t_0,\ T]} \mathcal{R}_t(\mathcal{X}_0,\ \mathcal{W})$$

(Althoff et al., 2021) formalises the set $\mathcal{R}_{[t_0,\ T]}(\mathcal{X}_0,\ \mathcal{W})$ in discrete time domain considering the semi-group property of differential equations, with sampling time τ as:

$$\mathcal{R}_{[0,\ N-1]}(\mathcal{X}_0,\ \mathcal{W}) = \bigcup_{k=0}^{N-1} \mathcal{R}_{k\tau}\left(\mathcal{R}_{[0,\ \tau]}(\mathcal{X}_0,\ \mathcal{W})\right) \tag{3.22}$$

which signifies a sequential construction of sets with memory at each time step k in $[0,\ T]$. This involves extensive use of Minkowski sums, thus the motivation of zonotopes as the preferred candidate set representation.

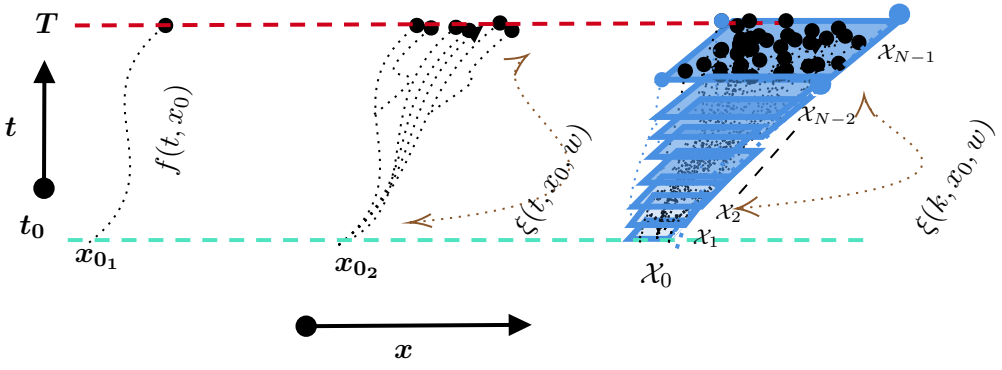

Figure 3.6: Illustration of reachability analysis temporally $[t_0,\ T]$, from left to right, showing deterministic reachability from a single point from state space, x_{0_1}; non-deterministic from x_{0_2} and a set-based reachability from the set $\mathcal{X}_0$.

3.2.3 LPV model

In order to obtain the effective stress value ϕ, which affects a damage event on the composite material, the flap-wise loadings are considered. Taking into account different wind conditions from the high fidelity FAST (Jonkman et al., 2009), (Sanchez et al., 2015) established a relationship between the flapwise root moment, the pitch angle, and the exogenous wind as follows:

$$\phi(t) = a_1\beta(t) + a_2 w(t). \tag{3.23}$$

(3.17) is thus included in the wind turbine model for the prognostic procedure. It must be converted from cycles to the time domain to be included in the wind turbine model. Since the rainflow counting algorithm produces a discontinuous output, from its algorithmic branches and loop policy, (3.17) can be thought of as a discontinuous function and thus problematic for direct online implementation. Luckily some works such as in (Löw et al., 2020) employ the assumption of the use of *Light Detection and Ranging* (LIDAR) devices to predict future wind conditions to circumvent this problem, by essentially taking advantage of the delay of wind contact with the blades. With a pre-knowledge of the wind profile from the LIDAR a pre-processing stage enables an online implementation. The delay given as the contact time (t_c) between wind and the structure is given as:

$$t_c = \frac{d}{v_w}. \tag{3.24}$$

where d is the measuring distance and v_w the mean flow velocity. Therefore with the known number of cycles, n_c within a time frame t_c in the pre-processing stage using rainflow counting, an estimated cycle per sampling time T_s is taken as:

$$\Theta(t) = \frac{T_s}{t_c} \times n_c.$$

The prognostic-based model is therefore given as :

$$\dot{w_r} = \frac{1}{J}(T_a - N_g T_g) \tag{3.25a}$$

$$\dot{\beta} = \frac{1}{\tau_p}(-\beta + \beta_r) \tag{3.25b}$$

$$\dot{T_g} = \frac{1}{\tau_g}(-T_g + T_{g_r}) \tag{3.25c}$$

$$\dot{D} = \Theta(t)(f_i(\phi, D) + f_p(\phi, D)) \tag{3.25d}$$

The non-linear model, (3.25) is posed as an LPV model by embedding the nonlinearity in scheduling parameters $\theta(k)$. As such, the resultant nonlinear time-varying degradation model is formulated mathematically into a pseudo-linear form through embedding. The LPV model in discrete time with a sampling time T_s is, therefore:

$$x(k+1) = A(\theta(k))x(k) + Bu(k) \tag{3.26}$$

where $x = [w_r\, \beta\, T_g\, D]^T \in R^n$ are the states, $u = [T_{g_r}\, \beta_r]^T \in R^m$ the inputs and $w(k) \in R^d$ the disturbance from the wind.
The system matrices are given as follows:

$$A(\theta(k)) = I + T_s \begin{bmatrix} k_1\theta_1(k) & 0 & -\frac{N_g}{J} & 0 \\ 0 & -\frac{1}{\tau_p} & 0 & 0 \\ 0 & 0 & -\frac{1}{\tau_g} & 0 \\ 0 & \theta_2(k) & 0 & \theta_3(k) \end{bmatrix},$$

$$B = T_s \begin{bmatrix} 0 & 0 \\ 0 & \frac{1}{\tau_p} \\ \frac{1}{\tau_g} & 0 \\ 0 & 0 \end{bmatrix},$$

$k_1 = \frac{1}{2}\rho\pi R^2$, and the variable scheduling parameters are: $\theta_1(k) = \frac{C_p(\lambda(k),\beta(k))}{\lambda(k)w_r(k)}$,
$\theta_2(k) = \Theta(k)(\frac{1}{(1-D(k)X_c}$)$^3(a_1^3\beta(k)^2 + 3a_1^2\beta(k)(a_2w(k)) + 3a_1(a_2w(k))^2 + (a_2w(k))^3)$ and $\theta_3(k) = \Theta(k)C_3\Sigma(k)^2\left[1 + \exp(\frac{C_5}{3}(\Sigma(k) - C_4)\right]$.

3.3 Model-based Prognostics under set-based uncertainty description

The proposed prognostics approach is primarily based on the generic model-based prognostics formalism, adapted to a set-based description of uncertainties. The plant model is subjected to control and exogenous disturbance (wind) inputs $u(k)$ and $w(k)$, under sensor noise $v(k)$ conditions, such that $w(k)$ and $v(k)$ are described as unknown but compact convex sets,

$$x(k+1) = f(x(k), \theta(k), u(k), w(k), k) \tag{3.27}$$

$$y(k) = h(x(k), \theta(k), u(k), v(k), k) \tag{3.28}$$

where $v(k) \in \mathcal{V}$ and $w(k) \in \mathcal{W}$, with the compact sets $\mathcal{V}$ and $\mathcal{W}$ described as zonotopic sets. The output data $y(k)$ and information from the model, under uncertainty is used in the ZKF estimation of zonotopic bounded states including the damage variable.
the description of this compact set is subsequently used as the premise to predict the EOL and RUL at a specific time instant k_p that take their values from resultant feasible compact uncertainty propagated sets that retain desirable properties for interpretability due to the initial zonotopic set. Future conditions during predictions are also considered bounded in sets and influence the penultimate degradation reachable set and thus the EOL and RUL, $\Box EOL(\Box x(k_p), \Box\theta(k_p)|\Box y(k_p))$ and $\Box RUL(\Box x(k_p), \Box\theta(k_p)|\Box y(k_p))$, respectively. Considering $T_{EOL} \in \mathbb{R}^{n_x} \times \mathbb{R}^{n_\theta}$ as a threshold

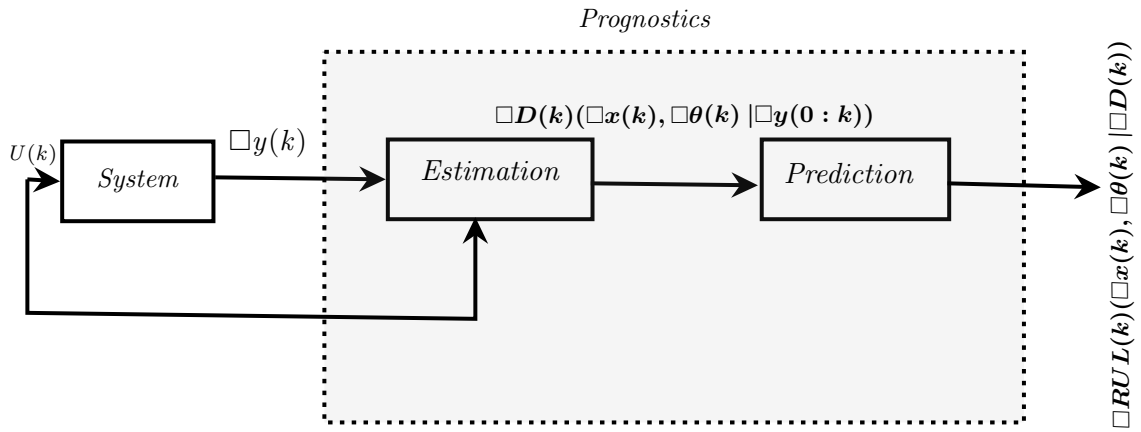

Figure 3.7: Illustration of a set-based model-based prognostics.

of failure, T_{EOL} maps to a Boolean domain, such that a failure is 1 and 0 otherwise. $T_{EOL} : \mathbb{R}^{n_x} \times \mathbb{R}^{n_\theta} \to \mathbb{B}$, the $EOL(k_p)$ is formalised in (Daigle et al. (2012)) as

$$\begin{aligned} EOL(k_p) &= \inf\{k \in \mathbb{N} : k \geq k_p \wedge \\ &T_{EOL}(x(k), \theta(k), u(k)) = 1\}, \end{aligned} \tag{3.29}$$

The remaining useful life, at k_p is thus given as (3.30) in set form:

$$\square RUL(k_p) = \square EOL(k_p) - k_p. \tag{3.30}$$

3.4 Implementation of Zonotopic Kalman filter

Considering the fact that the process of estimation of states is crucial in various procedures such as prognostics of systems, the effect of uncertainties on observed states is essential to examine. This warrants state estimation methods, such as the well-established Kalman filter which has seen an abundance of applications over the decades with variant modifications, to enhance its efficiency and alternative uses.

Different methods of representing these uncertainties motivate different types of estimation schemes. These are mainly through the stochastic paradigm and set-based formulations with the latter involving unknown disturbances and noise that are considered bounded in compact sets. Various geometrical representations for bounded uncertainty sets have been used in a number of works yielding good results. The resultant estimate of set-membership methods is feasible sets that are consistent with the states, inputs, and model output data, with the center of the resultant sets representing the reference point of the estimate (Evans et al., 2015). It is, therefore, necessary to represent them with compact sets that provide less complexity from a computational point of view. Convex sets such as the interval-based set (Xiong et al., 2013), ellipsoidal (Liu et al., 2016), poly-

topic or zonotopic sets (Wang et al., 2018) have been used which enables estimation of sets of admissible values of states at every time instant enabling robustness to the worst-case scenario with designated a priori bounds on uncertainties (Körber and King, 2010). Some works (Cembrano et al., 2011a) go a step further by merging the two paradigms of stochastic and set-membership methodologies to formulate a somewhat "hybrid" state estimation. Each geometrical representation offers different characteristics which may result in ease or setbacks in the computation of propagated uncertainty sets in set-based Kalman filter formulations. Zonotopes, a special class of polytopes, offers simplicity in the computation of sets and flexibility in operation.

As stated earlier, the stages of prognostics involve uncertainties. Due to the sensitivity of this process, it is important to quantify all uncertainty sources appropriately. The zonotopic uncertainties in this chapter are considered to be additive and constructed from symmetric interval sets. The quantified uncertainties are (i) the sensor noise, $v(k) \in [-\Delta v \ \Delta v]$ (ii) modelling uncertainties which are considered to emanate from the uncertain measured wind in the nonlinear embedded nonlinearities, from θ_1 and θ_2, which are calculated from appropriate interval analysis operation, such that, $\theta_1 \in [-\Delta\theta_1 \ \Delta\theta_1]$ and $\theta_2 \in [-\Delta\theta_2 \ \Delta\theta_2]$ and (iii) Uncertainty from the exogenous wind input, $w(k) \in [-\Delta w \ \Delta w]$. From the interval sets, the zonotopic sets are formulated for the Kalman filter procedure.

Considering that the dynamical LPV system can be represented as

$$x(k+1) = A(\theta(k))x(k) + Bu(k) + E_w w(k) \tag{3.31a}$$

$$y(k) = Cx(k) + E_v v(k) \tag{3.31b}$$

E_w and E_v are set up to represent the resultant uncertainty bounds from all the uncertainty sources. w and the noise v are assumed bounded in a unitary hypercube centered at the origin, $w \in [-1,\ 1]^{n_w} = \langle 0,\ I_{n_w} \rangle$ and $v \in [-1,\ 1]^{n_v} = \langle 0,\ I_{n_v} \rangle$, $I_{n_w} \in \mathbb{R}^{n_w \times n_w}$ and $I_{n_v} \in \mathbb{R}^{n_v \times n_v}$ are identity matrices. Considering the quasi-LPV model (4.1), a polytopic LPV model is used to formulate the estimation, such that the estimated states $\hat{x}(k)$ with n_θ varying parameters is given as:

$$\begin{aligned} \hat{x}(k+1) = &\sum_{i=1}^{2^{n_\theta}} \left(\mu_i(\theta(k))\right) \left(A_i(\theta(k))x(k) + Bu(k)\right) + \\ &+ \mathbb{L}\left(\theta(k)\right) \left(y(k) - \hat{y}(k)\right) \end{aligned} \tag{3.32}$$

The observer gain $\mathbb{L}\left(\theta(k)\right) \in \mathbb{R}^{n_x \times n_y}$ takes its solution from the convex hull of a 2^{n_θ} vertex polytope.

$$\mathbb{L}\left(\theta\right) = \sum_{i=1}^{2^{n_\theta}} \mu_i\left(\theta\right) \mathbb{L}_i \tag{3.33}$$

$$\sum_{i=1}^{2^{n_\theta}} \mu_i\left(\theta\right) = 1$$

$\mathbb{L}_i$ are the 2^{n_θ} observer gains for each of the polytope's vertices.

Assumption 1: The system matrices A($\theta(k)$) and C are observable for any realization of $\theta(k)$.

The gains $\mathbb{L}_i$ are obtained by solving an LQC duality problem. Let the observer gain tuning parameters be $\mathbb{Q} = \mathbb{Q}^T = \mathbb{H}^T\mathbb{H} \geq 0$ and $\mathbb{R} = \mathbb{R}^T > 0$ and A_i be for each vertex of the polytope. Thus, with an optimal bound γ, the polytopic observer gains are obtained by solving an LMI minimization problem to find Υ and $\mathbb{W}_i$.

$$\min_{\gamma,\Upsilon=\Upsilon^T,\mathbb{W}} \gamma \tag{3.34}$$

subject to

$$\begin{bmatrix} \gamma\mathbb{I}_n & \mathbb{I}_n \\ \mathbb{I}_n & \Upsilon \end{bmatrix} > 0 \tag{3.35}$$

$$\begin{bmatrix} -\Upsilon & \Upsilon\mathbb{A}_i - \mathbb{W}^T C & \Upsilon\mathbb{H}^T & \mathbb{W}^T \\ \mathbb{A}_i^T\Upsilon - \mathbb{C}^T\mathbb{W} & -\Upsilon & 0 & 0 \\ \mathbb{H}\Upsilon & 0 & \mathbb{I}_{n_x} & 0 \\ \mathbb{W} & 0 & 0 & -\mathbb{R}^{-1} \end{bmatrix} < 0 \tag{3.36}$$

$$\begin{bmatrix} -r\Upsilon & q\Upsilon + \mathbb{A}_i^T\Upsilon - \mathbb{C}^T\mathbb{W} \\ q\Upsilon + \Upsilon\mathbb{A}_i - \mathbb{W}\mathbb{C} & -r\Upsilon \end{bmatrix} < 0 \tag{3.37}$$

$q = 0$ and $r = 1$ are the center and radius of a unitary circle, respectively. (3.37) is included to guarantee the stability of the observer. The disturbances, ($\omega \in \mathbb{R}^{n_x}$) and measurement noise, ($\upsilon \in \mathbb{R}^{n_y}$) are unknown but assumed to be bounded and represented by zonotopes

$$\mathcal{W} = \langle c_\omega, R_\omega \rangle \tag{3.38a}$$

$$\mathcal{V} = \langle c_\upsilon, R_\upsilon \rangle \tag{3.38b}$$

where c_ω and c_υ are the centers of the sets with $R_\omega \in \mathbb{R}^{n_x \times n_x}$ and $R_\upsilon \in \mathbb{R}^{n_y \times n_y}$ as their generator matrices representing the uncertainties. The state is thus estimated as $\hat{x} = \langle c_x, R_x \rangle$.

$$c_x(k+1) = c_p(k) + \mathbb{L}\left(y(k) - Cc_p(k)\right) \tag{3.39a}$$

$$R_x(k+1) = \left[(\mathbb{I} - \mathbb{L}C)\, R_p(k), -\mathbb{L}E_\upsilon\right] \tag{3.39b}$$

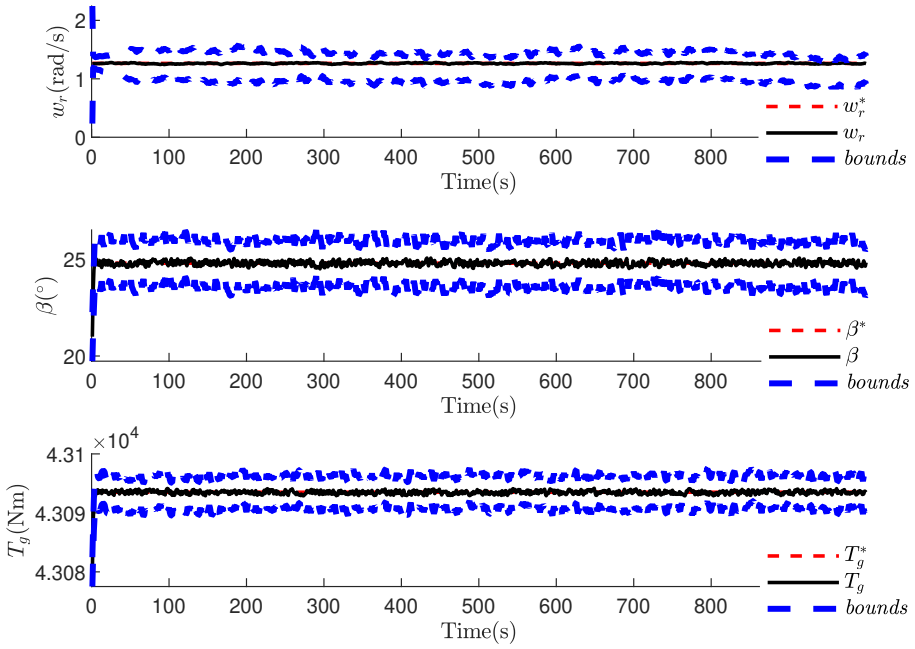

Figure 3.8: Estimation of states by ZKF with bounded sets.

$$c_p(k+1) = \sum_{i=1}^{2^{n_\theta}} \mu_i(\theta(k)) A_i(\theta(k)) x(k) + Bu(k) \tag{3.40a}$$

$$A(\theta(k)) = \sum_{i=1}^{2^{n_\theta}} \mu_i(\theta(k)) A_i(\theta(k)) \tag{3.40b}$$

$$R_p(k+1) = [A(\theta(k)) R_x(k) \quad E_\omega] \tag{3.40c}$$

$\mathbb{L}$ is given as in (3.33).

With the estimated c_x state and associated uncertainty R_x description as shown in Fig. 3.8, the prediction stage at each designated prediction time can be undertaken.

3.5 Prediction of the RUL

The time prediction distribution of the EOL at prediction instants k_p can be thought of as a reachability analysis problem based on set propagation considering initial set conditions from the estimator i.e $\hat{\mathcal{X}}_{k_p} \subset \langle c_{x_{k_p}}, R_{x_{k_p}} \rangle$, with inputs sourced through random sampling from an assumed known distribution of inputs. Assuming the matrices $A(\theta(k))$ are always shur, then the propagation of the sets with respect to the system ensures that a set of positive invariant sets,

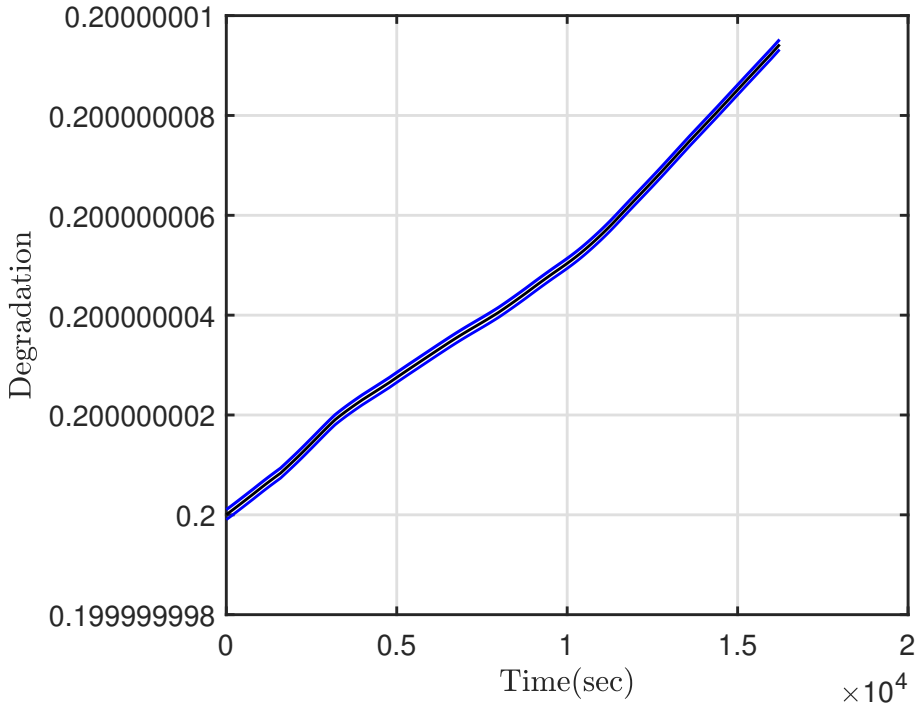

Figure 3.9: Monotonic degradation state with bounds.

$[\zeta(k_p), \zeta(k_p+1)....\zeta(k_{EOL})]$, can be constructed. Thus, the evolution of the centers of the set is guaranteed to be $x(k) \subset \zeta(k)$. The propagated positive invariant sets are just unions of the constituents convex sets (3.41) and the uncertainty sets constructed via Minkowski sums (3.42):

$$\zeta(k_{EOL}) \subseteq \mathcal{R}_{[k_p,\, k_{EOL}]}(\hat{\mathcal{X}}_{k_p},\, \mathcal{W}_{k_p}) = \bigcup_{k=k_p}^{k_{EOL}} \mathcal{R}_{k\tau}\left(\mathcal{R}_{[0,\,\tau]}(\hat{\mathcal{X}}_{k_p})\right) \tag{3.41}$$

$$\begin{aligned} &\Delta\mathbb{X}(k_p+j) \subseteq \textstyle\bigoplus_{j=1}^{k_{EOL}} A(\theta(j))^j \Delta x(k_p) \oplus A(\theta(j))^{(j-1)} \\ &B\Delta u(k_p+j-1) \oplus E_w \Delta w(k_p+j-1)) \end{aligned} \tag{3.42}$$

Since the control inputs are dependent on the wind conditions and the degradation is a function of only the wind, only a distribution of the wind is considered. $\mathcal{W}_{k_p} \supset [w(k_p) + \Delta w(k_p),\ w(k_p+1) + \Delta w(k_p+1), ...w(k_{EOL}) + \Delta w(k_{EOL})]$. The procedure is illustrated in Fig. 3.10.

Remark 1 Since the degradation model is strictly monotonous with respect to the initial state $x_0 \in \mathbb{R}^n$ and inputs $w_i \in \mathbb{R}^w \subset \mathcal{W}$, for all trajectories $\upsilon(t, x_0, w) : \mathbb{R}_{>0} \times X \times \mathbb{R}^w \to X, : x_2 > x_1, \upsilon(t_2, x_2, w_2) >> \upsilon(t_1, x_1, w_1)$. From (Althoff et al., 2021), it can be inferred, that $\forall x_0 \leq \overline{x}, w \leq \overline{w}$, each state trajectory can be constructively, bounded as in $\forall i \in \mathbb{N}^+, t > 0, \upsilon_i(t, x_{i,0}, w) < \upsilon_i(t, \overline{x_i}, \overline{w})$ and $\upsilon_i(t, x_{i,0}, w) > \upsilon_i(t, \underline{x_i}, \underline{w})$. The reachable zonotopic convex sets $\zeta(k)$ are therefore over-approximated with hypercubes. Hypercubes are themselves zonotopes, so the process involves a

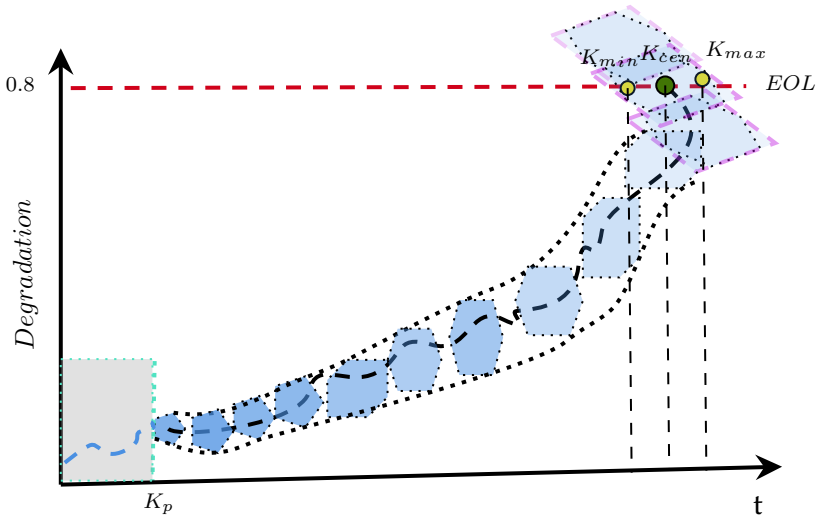

Figure 3.10: Evaluation of RUL with associated bounds via set propagation

mapping of a zonotope to another zonotope that invariably increases conservativeness but for the purposes of interpretability. The RUL prediction can be summarized in Algorithm 1.

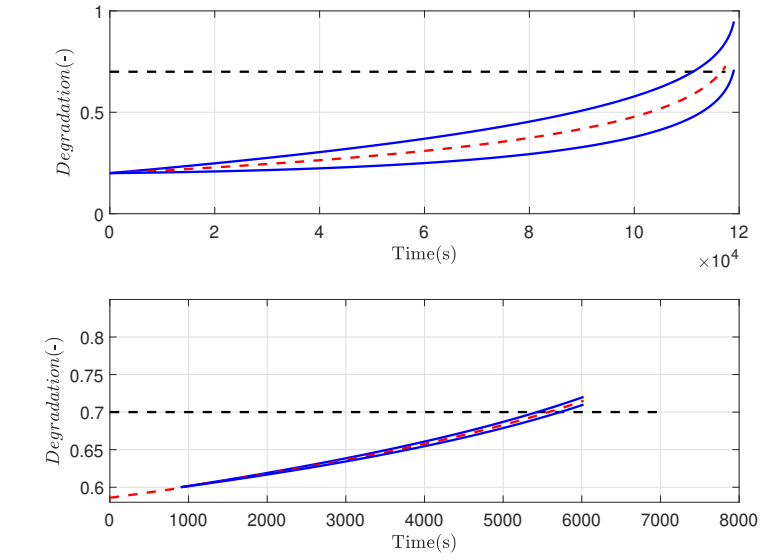

Figure 3.11: Propagation of degradation uncertainty set to EOL.

Algorithm 1 Proposed set-based prognostics procedure.

Inputs $\{(c_{x_{k_p}}, R_{x_{k_p}}, \mathcal{W}_{k_p}, A(\theta(k_p)), k_p\}$
Output $\{RUL, \overline{RUL}, \underline{RUL}\}$
$c(k) \longleftarrow c_{x_{k_p}}$, $R_x(k) \longleftarrow R_{x_{k_p}}$, $A(\theta(k)) \longleftarrow A(\theta(k_p))$
for $k = k_p, k_p + 1, ...$ **do**
  while $T_{EOL}(\underline{D_{k_{min}}}(k)) = 0$ **do**
    $D_{cen}(k) \longleftarrow D(c(k))$ ▷ Propagation of damage set's center
    $\underline{\underline{D_{min}}}(k) \longleftarrow D(c(k) - rs(R_x(k)))$ ▷ Propagation of damage set's lower bound
    $\overline{D_{max}}(k) \longleftarrow D(c(k) + rs(R_x(k)))$ ▷ Propagation of damage set's upper bound
    $c(k+1) = (A(\theta(k))c(k) + Bu(k)$ ▷ Propagation of states
    $R_x(k+1) = [(A(\theta(k))R_x(k) \quad E_w]$ ▷ Propagation of uncertainty bounds

    if $T_{EOL}(D_{k_{cen}}(k)) = 1$
      then $k_{cen} \longleftarrow k$
    if $T_{EOL}(\underline{D_{k_{min}}}(k)) = 1$
      then $\underline{k_{min}} \longleftarrow k$
    if $T_{EOL}(\overline{D_{k_{max}}}(k)) = 1$
      then $k_{max} \longleftarrow k$
  end while
  $RUL \longleftarrow k_{cen} - k_p$
  $\overline{RUL} \longleftarrow k_{min} - k_p$
  $\underline{RUL} \longleftarrow k_{max} - k_p$
end for

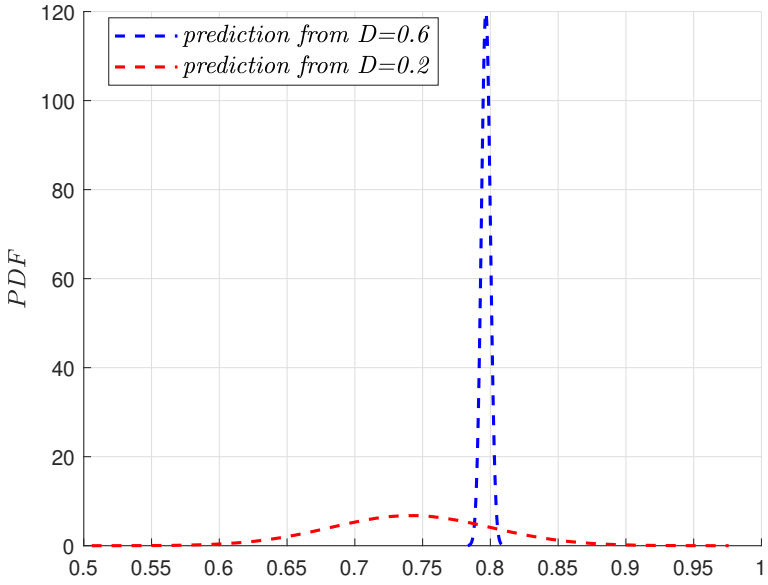

Figure 3.12: PDFs of degradation at the EOL.

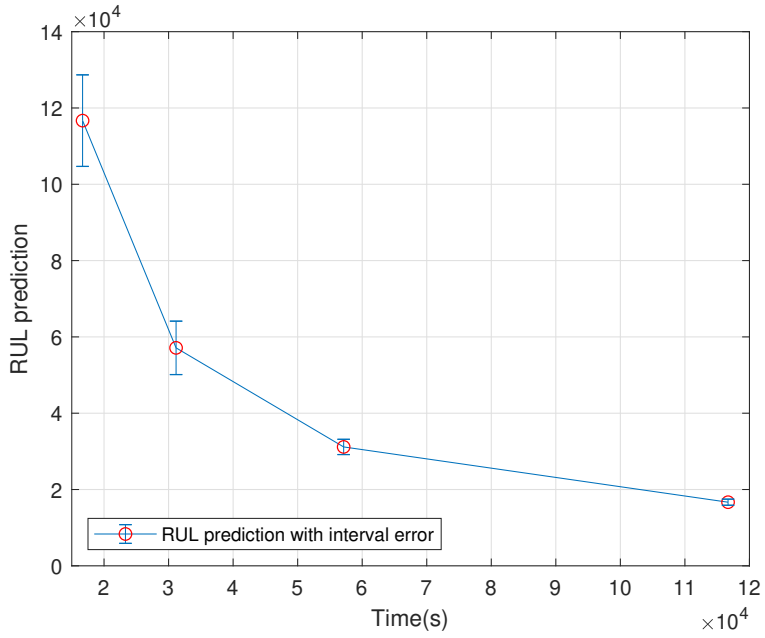

Figure 3.13: Remaining useful life Predictions .

To show the efficacy of the proposed methodology an accelerated degradation experiment is undertaken by amplifying the otherwise small degradation events. A degradation threshold of 0.7 is chosen and the degradation is assumed to start from 0.2 and 0.5. Fig. 3.11 mainly shows desirable results of a more certain EOL and thus remaining useful life when the degradation of the material is close to the threshold, conversely, the uncertainty is more distributed when prediction time is far from the threshold. This is also shown in Fig. 3.13 where the minimization of the width of the interval is realised. It must be noted that the prediction times are selected set of instants during the online operation of the plant with the estimator.

3.6 Conclusions

This chapter has proposed a model-based prognostics procedure using a zonotopic Kalman filter that is able to provide a set-based propagation of degradation, aiding in the quantification of the fated uncertainties associated with prognostics. The prognostics procedure is then applied to the degradation of a wind turbine blade material subjected to a forecasted bounded set description of the wind profile. To facilitate an online condition-based implementation, an otherwise nonlinear based Kalman filter from the nonlinear wind turbine model is presented in a pseudo-linear form, a polytopic linear parameter varying representation, decreasing computational cost and easing in the propagation of the positive invariant zonotopic uncertainty sets to a reachable set that triggers an end of life. Using this information on health, the remaining useful life with its associated uncertainties can be predicted. The proposed approach has been tested in a benchmark wind turbine using a high-fidelity simulator.

Chapter 4

Health-Aware LPV Model Predictive Control of Wind Turbines

The content of this chapter is based on the following works:

- Khoury et al. (2020a) Khoury, B., Nejjari, F., and Puig, V. (2020a). Health-aware lpv model predictive control of wind turbines. *IFAC-PapersOnLine*, 53(2), 826–831. doi: https://doi.org/10.1016/j.ifacol.2020.12.838.
- Khoury et al. (2022c) Khoury, B., Nejjari, F., and Puig, V. (2022c). Health-aware linear parameter varying model predictive control of wind turbines. *IEEE Transactions on Control Systems Technology (submitted)*.

In the quest to achieve a more environmentally sustainable global energy mix, wind energy has seen immense growth over the last decades, becoming one of the most promising renewable energy resources that exist today. From the latest global energy growth reports, total installed capacity as of 2020 stood at 65GW, an increment of 8% from 2019 (IEA, 2020) primarily due to government subsidies and incentives. However, in recent times these subsidies have seen substantial cuts (Quintana-Rojo et al., 2020) mainly due to the classification of wind technology as a matured one, thus presenting a challenge for wind energy suppliers to adapt to market changes. Therefore, there is a call for innovative operational schemes to make wind energy a more competitive energy source compared to its conventional counterparts such as fossil fuels, further enhancing its contribution to global energy participation and therefore promoting the mitigation of global warming. It is henceforth imperative to present cost-effective models of operation that seek to reduce levelized cost of energy (LCoE) and thus increase return on investment. One of the major costs involved in wind turbine operation is their operation and maintenance (O&M) cost. Considering that wind turbine structures are subjected to unforgiving extreme conditions, components are susceptible to rapid failure before their projected end of life (EOL) resulting in a number of costly, most often unplanned replacements during the plant's estimated 20-25 year lifespan. Also, wind turbines tend to be classified as not *easy-to-access* structures due to their predominately remote locations,

therefore, increasing O&M costs and downtime (Colak et al., 2015). This is further exacerbated in the case of offshore wind turbines which have structurally larger rotor diameters and a more slender tower, resulting in a more pronounced effect of dynamic loadings (Zhang et al., 2019). Based on reports (Colak et al., 2015), O&M costs account for roughly $15 - 20\%$ of total operational cost. In this chapter, a health-aware control (HAC) that takes into account information about the plant's health utilizing the technique of direct component deterioration incorporation is proposed. This involves specifically predicting through the method of stiffness degradation algorithm, the prognosticated degradation of the wind turbine's blade, our unit under test (UUT) with the objective of extending the useful life of the blades with MPC. Considering that wind turbines exhibit nonlinear dynamics and operate in different operating zones depending on the range of wind speeds, modelling, and control using parameter-varying models (Shirazi et al., 2012); (Inthamoussou et al., 2014) is motivated. The advantage of using this class of systems is the use of an extension of linear techniques to perform gain-scheduling control of non-linear systems. This enables the formulation of a convex optimization problem that is readily solved with an off-the-shelf solver whilst also providing the advantage of working in wide operational points, a limitation of Jacobian linearization as done in (Sanchez et al., 2015) for wind turbine control.

4.1 LPV modelling of a Wind turbine model

In this section, a brief description of wind turbine control is presented. Subsequently, with the nonlinear model of the wind turbine as described in (3.11) from chapter 3, two different LPV models are presented for the design of a two-level control scheme.

4.1.1 Wind turbine control

The control of wind turbines depends on the measured effective wind speed (see Figure 4.1). Below a cut-in wind speed ($4m/s$), the plant ceases to operate since wind speed is deemed inadequate for power production. The pitch angle is fixed at 0° to allow for a maximum extraction of power when the wind speed is above the cut-in wind speed but below the rated speed ($11.5m/s$), an alternating generator torque control is employed here. Above it, the pitch angle is varied to ensure a rated rotor torque albeit a fixed rated generator torque $T_{g,opt}$ such that the rated rotor speed $w_{r,rated}$ is achieved and hence the rated turbine power. Between these regions is a transition region ($[11.5m/s,\ 12m/s]$) where the generator torque is rapidly increased to maximum using a fast controller based on the control law $T_g \backsim w_r^2$. Above cut-off speed ($\leq 25m/s$), the blades are halted to avoid damage to the turbine structure.

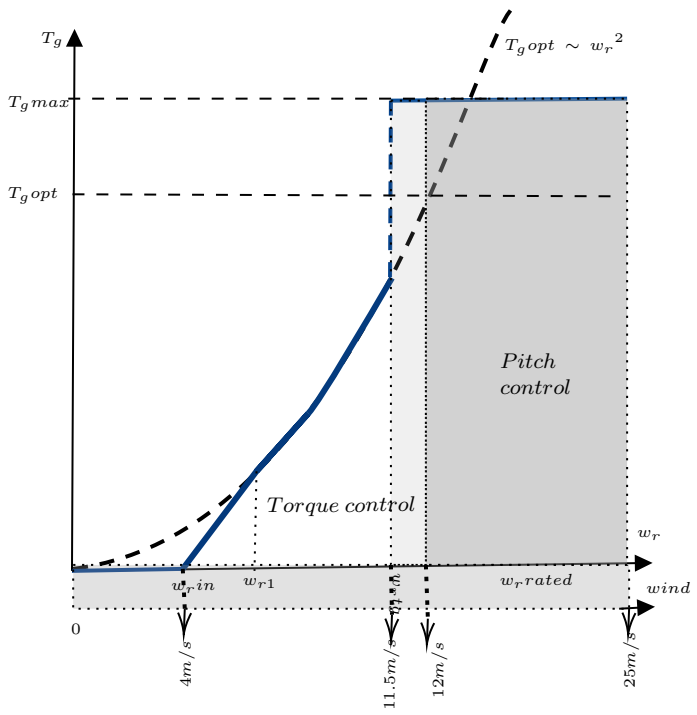

Figure 4.1: Regions of wind turbine control.

4.1.2 LPV model I

An LPV model is designed for the entire control region of the wind turbine. This is used for the lower level of the control scheme, which will be described in detail in the subsequent sections. Considering the nonlinearity in $f(x, V_w)$ from (3.11), with a sampling time of T_s and under Euler discretization, the dynamic model of the LPV can be expressed as follows:

$$x(k+1) = Ax(k) + Bu(k) + B_w(\theta(k))V_w(k), \tag{4.1}$$

where $V_w(k) \in R^d$ is the disturbance from the wind.
The system matrix containing the nonlinear embedding $B_w(\theta(k))$ (4.1) is as follows:

$$B_w(\theta(k)) = \begin{bmatrix} 0_{4\times 1} \\ \frac{1}{Nm_B}\vartheta\theta_1(k) \\ \frac{1}{J_r}\vartheta R\theta_2(k) \\ 0_{3\times 1} \end{bmatrix}. \tag{4.2}$$

(4.3)

where $\vartheta = \frac{1}{2}\rho A$ and the varying parameters are:
$\theta_1(k) = C_t(\lambda(k), \beta(k))V_w(k)$ and $\theta_2(k)$ =$C_p(\lambda(k), \beta(k))V_w(k)$.

4.1.3 LPV model II

In the 3rd region, the torque as has been shown in Fig. 4.1 is constant. Thus, the dynamic model can be reformulated into a simple model as done in (Georg, 2015) which considers only the dynamics of the rotor speed and the pitch angle avoiding the unnecessary excess computational time of control in this region. The state matrices of this model are as follows:

$$A = \begin{bmatrix} \frac{1}{J_r+J_g}(T_a(x_u, V_w) - T_g) & 0 \\ 0 & -\frac{1}{\tau_\beta} \end{bmatrix}, \tag{4.4}$$

$$B_u = \begin{bmatrix} 0 \\ \frac{1}{\tau_\beta} \end{bmatrix}. \tag{4.5}$$

In an LPV form, the matrix $A(\theta(k))$ is therefore:

$$A(\theta(k)) = \begin{bmatrix} \frac{1}{J_r+J_g}(\vartheta R\theta_2(k) - \frac{T_g}{\theta_3(k)}) & 0 \\ 0 & -\frac{1}{\tau_\beta} \end{bmatrix}. \tag{4.6}$$

$\theta_3(k) = w_r(k)$; $w_r(k) \neq 0$, where $x_u = [w_r,\ \beta]$.

Assumption 1 *The states $x(k)$ and the wind, $V_w(k)$ are assumed observable at each time instant k.*

At every time instant, depending on the region of operation, the dynamics of the system is obtained as linear in state space determined by the nonlinear parameter embedding $\theta_i(k)$ bounded in a box $\theta_i \in \left[\overline{\theta_i}, \underline{\theta_i}\right]$, that varies in a defined operational region, appropriately a convex polytopic set. Therefore, the system matrices are linear time variant and function of the scheduling parameters which are bounded in a compact polytopic set. Therefore with n_θ varying parameters for each case, a polytopic representation of the dynamic matrices is given as the linear combination of $n_v = 2^{n_\theta}$ vertices (θ_i) of a polytope as follows depending of the LPV model.
For LPV I:

$$B_w(\theta(k)) = \sum_{i=1}^{n_v} \alpha_i(k) B_w(\theta_i), \tag{4.7}$$

and LPV II:

$$A(\theta(k)) = \sum_{i=1}^{n_v} \alpha_i(k) A(\theta_i), \tag{4.8}$$

where in both cases

$$\sum_{i=1}^{n_v} \alpha_i = 1,\ \alpha_i = [0, 1]. \tag{4.9}$$

4.2 Offline Degradation Prognostics of a Wind Turbine Blade

The degradation of the wind turbine's composite material based on the stiffness degradation is presented in this section. The degradation vs accumulated stress is then segmented into zones based on the stress accumulated by the blade over time.

4.2.1 Prediction of degradation function

With the stiffness degradation algorithm as explained and represented mathematically in Chapter 3, the composite strength degradation of the wind turbine's blade subjected to accumulated stress is studied. Wind turbines are subjected to a simultaneous combination of stress components such as the flapwise, edgewise bending, and torsion forces that contribute to fatigue (Chen and Eder, 2020). However, in this work, only the flapwise root moment is considered. This blade root moment caused by aerodynamic forces acquired from the high fidelity OpenFAST is subjected in a cumulative manner on the component material till a predefined deterioration level (EOL). The EOL is chosen as 0.8 .i.e 80% loss in material strength as shown in Fig. 4.2. The degradation vrs accumulated stress function is then segmented into linear and bilinear functions that best fit, see Fig. 4.3 & Fig. 4.4, this is done to appropriately capture the dynamic behaviour in stages 1 and 3 of degradation. The 2nd stage of the blade lifetime degradation is largely minimal and considered as the most productive period of the blade's lifetime, therefore is not included in the controller's health-aware design. At any instant k, degradation Deg is represented per each j-segments with the following model

$$\varphi(k)_j \approx b_{2_j}\phi^2_{acc}(k) + b_{1_j}\phi_{acc}(k) + b_{0_j}$$

where $b_{0_j} = 0$ for a 1st degree polynomial fit. With respect to accumulated stress ϕ_{acc}, the degradation is given as

$$Deg(k) \approx \begin{cases} \varphi(k)_j \text{ for } \quad \phi_{acc_{min_j}} \leq \phi_{acc}(k) \leq \phi_{acc_{max_j}}. \end{cases} \tag{4.10}$$

where $\phi_{acc_{min_j}}$ and $\phi_{acc_{max_j}}$ are the bounds of segment j. A simple linear mathematical model proposed by (Sanchez et al., 2015) is chosen for the blade root moment. In this model, a mean flapwise root moment of the blades as a result of wind loadings is described as a function of the alternating pitch angle and the wind itself:

$$\phi(t) \approx f(\beta(t), w(t), t) = a_1\beta(t) + a_2 w(t). \tag{4.11}$$

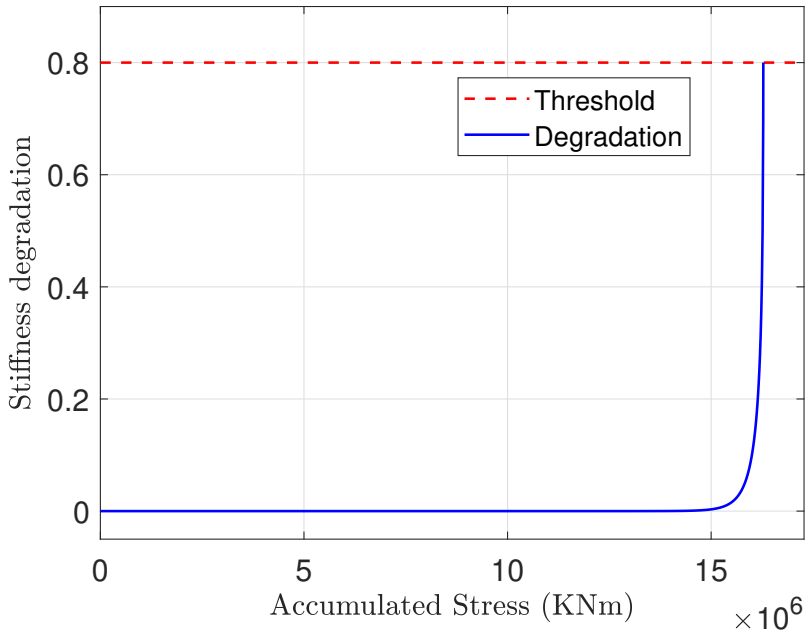

Figure 4.2: Curve showing stages of stiffness degradation.

4.2.2 Procedure of Rainflow Counting Integration

In this section, the integration of the discontinuous rainflow counting procedure is illustrated. Fatigue and thus degradation events occur as per the occurrence of a cycle of stress as evident in (3.17). In other to account for the effective cycle of stress from a history of mechanical stress on the blade, a cycle counting method must be employed. The go-to methodology in practice, the rain flow counting method (RFC) initially proposed by (Endo et al., 1967) is used. It interprets complex cyclic behaviour of stress as the probability of occurrence of load cycles in different ranges, ideally extracting closed loading reversals (or cycles). Fluctuating stress and strain on structures are represented as peaks in the RFC method. Counting these peaks results in a histogram of peaks in which the random history of stress (or strain) can be transformed into a statistical distribution of amplitudes of fluctuating stress or strain as a function of time. The algorithm has a complex sequential and nonlinear structure to decompose arbitrary sequences of loads into cycles, hence it is unsuitable for direct incorporation into control frameworks. In this context, some papers propose the externalization of the RFC from the control and present the output of the algorithm as external parameters to the control unit. This has been termed Parametric Online Rainflow-counting (PORFC) and has been successfully applied to wind turbines in (Löw et al., 2020). This chapter draws inspiration from this methodology, by basically identifying the instances of cyclic stress occurrences in the MPC prediction horizon. Assuming a stress history as given in Fig. 4.5, characteristics of the effective stress cycles (Fig. 4.6) either closed or unclosed is given from the RFC methodology. This is typically made up of the start, (k_{start}) and end times (k_{end}) of cycles, the range, mean stress values $(\sigma_r,\ \sigma_m)$ and a factor of 1 or $\frac{1}{2}$ signifying a complete or half cycle. Half

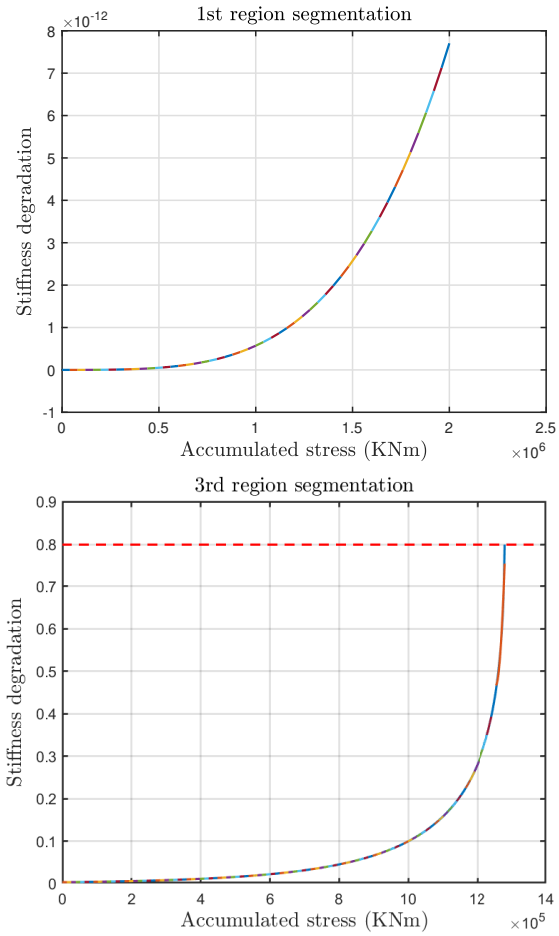

Figure 4.3: Segmented 1st and 3rd stages of the stiffness degradation vs accumulated stress curve.

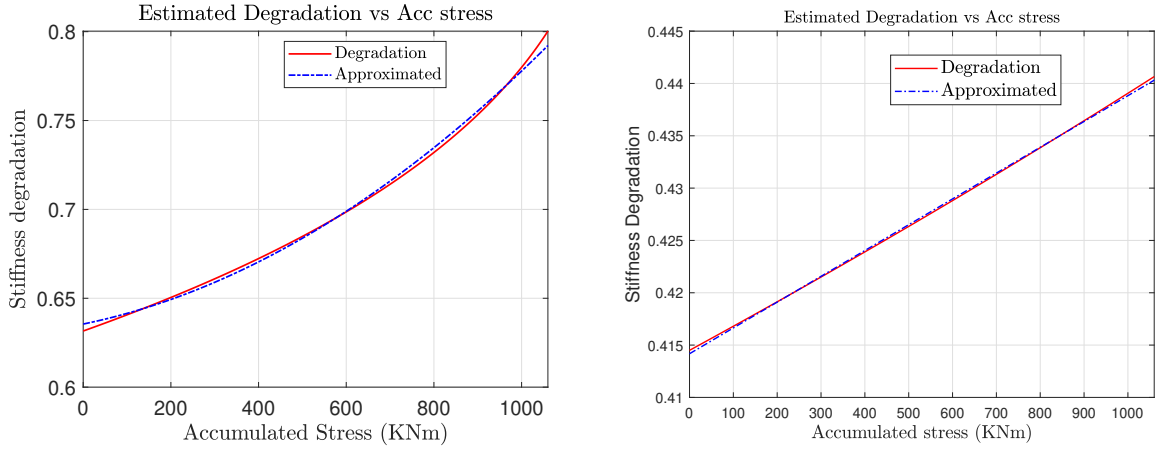

Figure 4.4: Estimated segments of the stiffness degradation vs accumulated stress curve.

cycles are long-term transition cycles that are not complete in the observed stress history. They are either neglected, conservatively treated as full cycles, or handled as residue carried along to a

future batch of stress. Neglecting half cycles may be an over-approximation since half cycles normally contribute to a high magnitude of effective damage when complete. A variant of the RFC proposed by (Downing and Socie, 1982) which allows for a better online RFC that does not require total knowledge of the stress history is used in this work. Unlike the generic RFC, the proposed methodology is not rearranged to begin and end with maximum peaks, thus avoiding most half cycles. The few half cycles are approximately treated as half of their original magnitude.

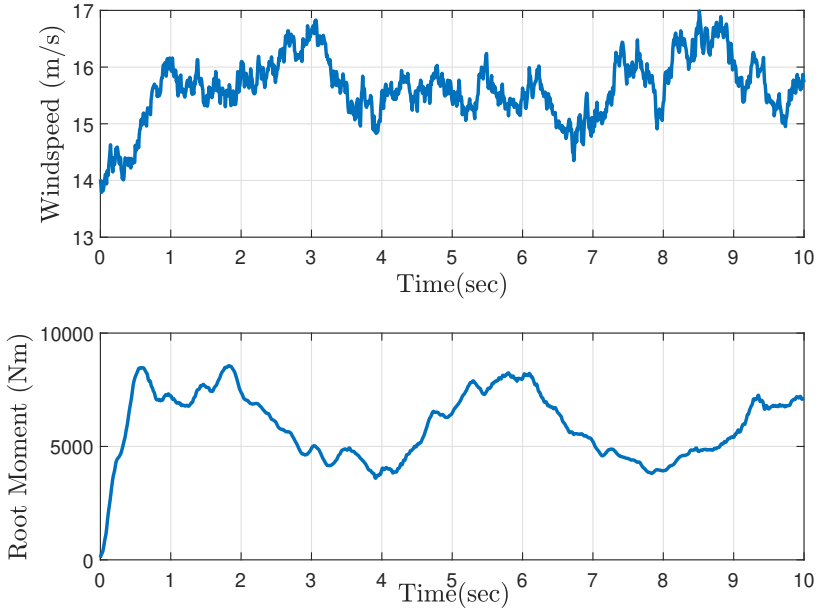

Figure 4.5: (Top) Wind speed. (Bottom) Blade root moment(stress).

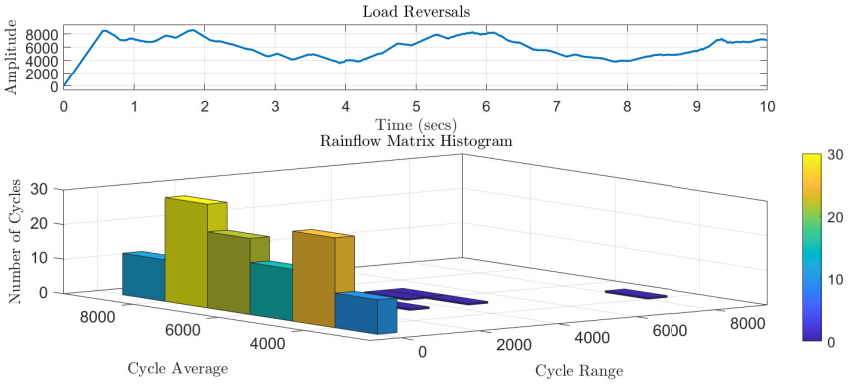

Figure 4.6: Information from rainflow counting from Matlab®.

Assuming a prior knowledge of 10 s wind information and stress (Fig. 4.5). The rainflow counting information is given in Table 2. The cycles' start and end times are then allocated on the prediction horizon of MPC as shown in Fig. 8.

Table 4.1: Rainflow information from stress input.

cycle #	Count	Range	Mean	Start	End
1	1	7	8534.5	0.008	0.016
2	1	2	7028	0.024	0.032
3	1	29	6880.5	0.04	0.048
4	1	1	6467.5	0.056	0.064
5	1	1	6455.5	0.072	0.08
⋮	⋮	⋮	⋮	⋮	
124	1	307	7583.5	1.936	1.992
125	1	1698	7622	1.68	1.896
126	0.5	8467.2	4328.4	0	1.64
127	0.5	8467.2	4328.4	1.64	2.016

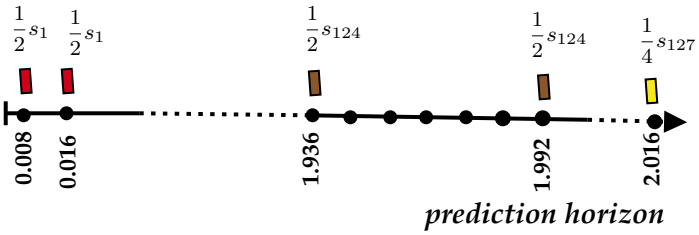

Figure 4.7: Allocation of cycles in MPC's prediction horizon.

4.3 Health-Aware Control

This section formulates the health-aware control, by presenting how the two-level control is designed.

4.3.1 Control configuration

The health management control is only considered for the above-rated wind speeds since it is in this region that requires pitch actuator action. Below rated wind speeds, the blade must be at fine pitch angle as discussed in earlier sections. Thus, the proposed control setup consists of a two-level control configuration where the upper level undertakes the function of Prognostics and Health Management (PHM) as shown in Fig.4.8. The lower level has the dual purpose of controlling the turbine below rated wind speeds and also preventing a complex optimization problem in the upper level which will be elaborated on in detail. For designing the controllers, the following assumptions are considered.

Assumption 2 *A considerable future wind information for a pre-simulation and MPC control is made available by a LIDAR.*

Assumption 3 *All other components' degradation is not considered. The chapter is based on the premise that plant life is only dependent on blade degradation.*

However, it must be noted that components such as the drive train is a strong contributor to the economics of a wind turbine operation.

Under these assumptions, the parameter values from the RFC and the segmented degradation as explained in Section 4.2.1 are fed into the upper-level MPC optimization setup for health management in stages 1 and 3 of the offline stiffness degradation test. Normal control operation occurs in the 2nd stage. The RFC parameter values are acquired through a pre-simulation considering future stress history from the stochastic wind.

4.3.2 Lower Level MPC

A set point tracking MPC is designed for the lower level control. This involves reference set points tracking of the pitch angle (β^*), rotor speed (w_r^*), and generator torque (T_g^*), with a quadratic cost function in an optimization loop as:

$$\mathcal{L}_l(k, u_l(k), x(k)) = \varphi_1(w_r(k) - w_r^*)^2 + \varphi_2(T_g(k) - T_g^*)^2..$$

$$... + \varphi_3(\beta(k) - \beta^*)^2 + \varphi_4 \Delta u_l$$

The optimization problem solved is hence:

$$\min_{\mathbf{u}_l(1...N_p), \hat{\mathbf{y}}(1...N_p)} \sum_{i=0}^{N_p-1} \mathcal{L}_l(k, u_l(k), x(k)) \tag{4.12}$$

subject to (4.13)

$$x(i+1|k) = Ax(i|k) + Bu_l(i|k) + B_w(\theta_{pi})V_w(i|k), \tag{4.14}$$

$$u_l(i|k) \subseteq \mathcal{U},$$

$$x(i+1|k) \subseteq \mathbb{X}, \tag{4.15}$$

$$\Delta u_l(i+1|k) = u_l(i+1|k) - u_l(i|k). \tag{4.16}$$

(4.17)

where $\mathcal{X}$ and $\mathcal{U}$ are box constraints of the states and inputs respectively. The lower level is designed to have a faster sampling time than the upper level ensuring that its output is available to the upper level. After every optimization loop, $\hat{y}$ is fed into the upper level and u_l as input to the plant for below-rated speed control and torque control during the health management control.

4.3.3 Upper level PHM-EMPC

An economic MPC is formulated in the upper level which involves the conflicting performance indices of maximizing power P to its rated value in the presence of varying wind $V_w(k)$ and minimizing the degradation of the blade composite material Deg. At each time instant, k, with

pre-simulated values of the cycle properties from the RFC and selected degradation parameters with prioritization weights as per the accumulated stress value, an economic MPC is solved for a pitch actuator input β_h. The pre-simulated inputs are: $\Psi(k) = [R_f, W_j, \Lambda, \hat{y}]$ where $R_f \in \mathbb{R}^{\frac{p_t}{T_u}}$ is a vector with entrants of $\frac{1}{2}$ for when a cycle occurs (start and end instances) at a sample time and 0 otherwise. p_t is the prediction horizon time and T_u, the upper-level sampling time. W_j is a selected weight depending on the current degradation segment j, Λ, is a set of degradation parameters at j and $\hat{y}$ the input from the lower level which serves as initial states and also pitch angle values β to prevent bilinear functions that arise for 2nd-degree polynomial fits from Section 4.2.1. Therefore the multi-objective criteria are setup as:

$$\mathcal{L}_u(k, u(k), x(k), \Psi(k)) = W_j Deg(k) - W_1 P(k) + W_2 \Delta u(k)$$

and the optimization solved is:

$$\min_{\beta_{\mathbf{h}}(1...N_p), \mathbf{x_u}(1...N_p), Deg(1...N_p)} \sum_{i=0}^{N_p-1} \mathcal{L}_u(k, u(k), x_u(k), \Psi(k)) \tag{4.18}$$

$$\text{subject to} \tag{4.19}$$

$$x_u(i+1|k) = A(\theta(k))x_u(i|k) + B_u\beta_h(i|k) \tag{4.20}$$

$$Deg(i+1|k) = Deg(i|k) + (R_f(i).f(\phi(k), \Lambda(k))).T_u, \tag{4.21}$$

$$P(i+1|k) = n_g T_{g_{opt}} w_g(i|k), \tag{4.22}$$

$$P(i|k) \leq P_{max}, \tag{4.23}$$

$$\beta_{min} \leq \beta_h(i|k) \leq \beta_{max}, \tag{4.24}$$

$$[w_{r_{min}}, \beta_{min}]^\intercal \leq x_u(i+1|k) \leq [w_{r_{max}}, \beta_{max}]^\intercal, \tag{4.25}$$

$$\Delta\beta_h(i+1|k) = \beta_h(i+1|k) - \beta_h(i|k). \tag{4.26}$$

$$\tag{4.27}$$

From the sequences $\beta_h(1, .., ., N_p)$ and $Deg(1, .., ., N_p)$, the first values represent the health-aware pitch angle control input to the plant and the initial degradation for the next sampling time.

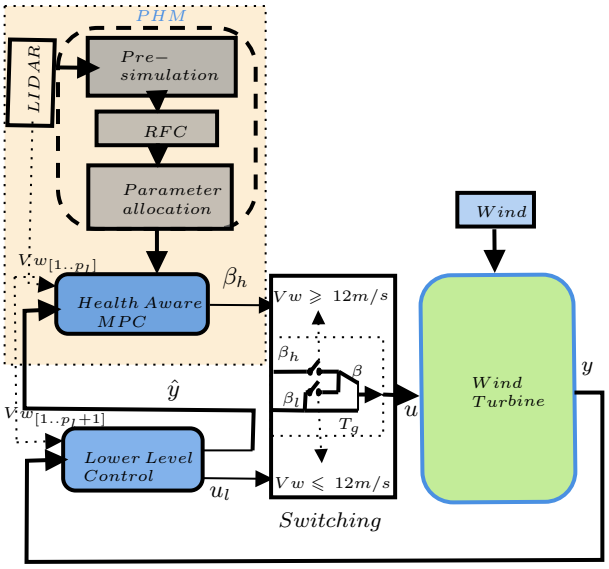

Figure 4.8: Control configuration of the proposed Health Aware scheme.

4.4 Simulation and results

In this section, graphical performance of the proposed health-aware scheme based on simulations is presented. The merit of the proposed scheme is illustrated. To illustrate the performance of the lower MPC, it is compared with the OpenFAST baseline control which is designed such as considering the actuator inputs as $T_{g_{ref}}$ and β_{ref} as follows

- For below rated wind speeds, β_{ref} is kept constant at $0°$ and the variable torque given as $T_{g_{ref}} = K_{opt} w_g^2$
- For above wind speed, $T_{g_{ref}}$ is constant and the pitch angle is controlled with a gain scheduled PI controller.

A comparison in Fig. 4.9 shows a relatively good fit between the two control schemes across all regions with selected means of wind speeds of $8m/s$ and $15m/s$ for the 2 regions of control, respectively. In the pitch control zone (mean wind of 15m/s), the MPC maintains a rated power of $5MW$ by alternating the pitch angle in the presence of the varying wind. For the torque control zone, the pitch is constant at $0°$ whilst the torque alternates. From the setup of the upper-level optimization problem, a minimization of degradation, must invariably result in a degradation of the plant as shown in Fig. 4.10, which involves 3 selected segments of degradation with different weights from a mean wind speed of $18m/s$. The pitch angle increases to decrease the sweeping area of the stochastic wind which results in a minimized degradation, but this results in a decrease in aerodynamic energy extraction and thus a reduced power is produced.
The upper level acts as a complementary control for health management in certain periods in the plant's lifetime. Hence, weights can be arbitrarily selected per operators' discretion for each

segment of the degradation with respect to accumulated stress levels. Table 4.2 shows the trade-off in numbers between the steady state power and it is associated accumulated stress with respect to different selected weights W_j at the end of the simulation run for an extended period.

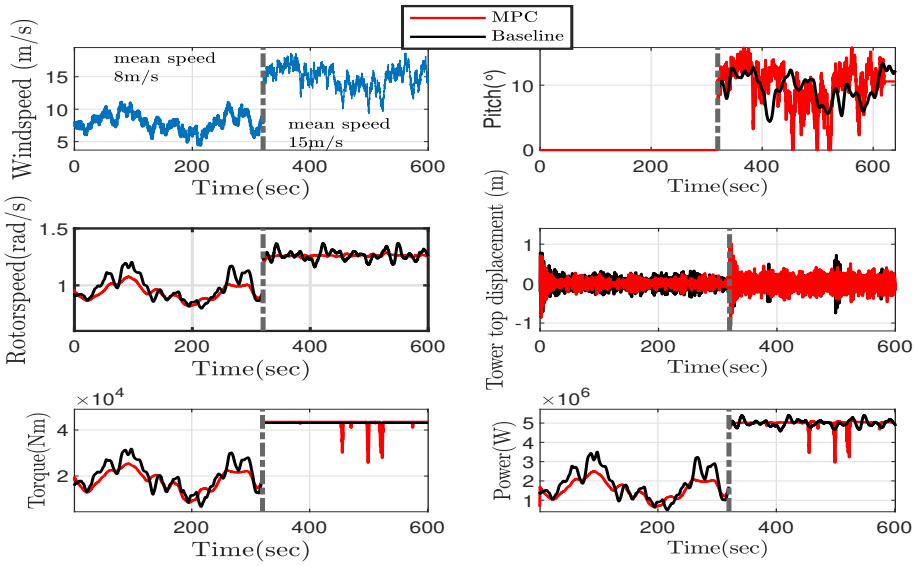

Figure 4.9: The lower level MPC in the two regions of control.

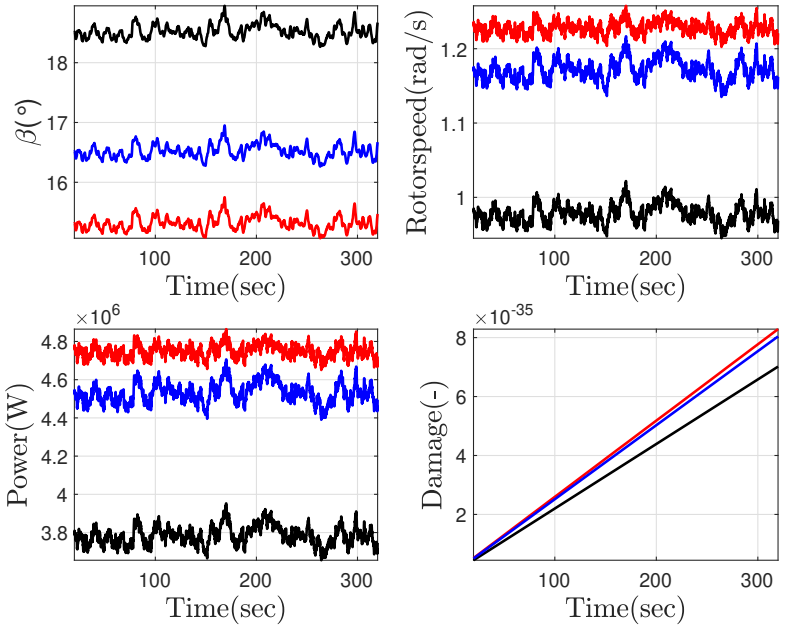

Figure 4.10: Operation of the upper-level control.

Varying weights W_j, the Pareto front presented in Figure 4.11 can be obtained that for reduced

Table 4.2: Table showing power and accumulated stress with varied weights, W_j.

W_j	**Power(MW)**	**Acc. Stress**
$W_{j,1}$	5	4.11×10^{10}
$W_{j,2}$	4.54	3.74×10^{10}
$W_{j,3}$	4.164	3.43×10^{10}
$W_{j,4}$	3.97	3.26×10^{10}

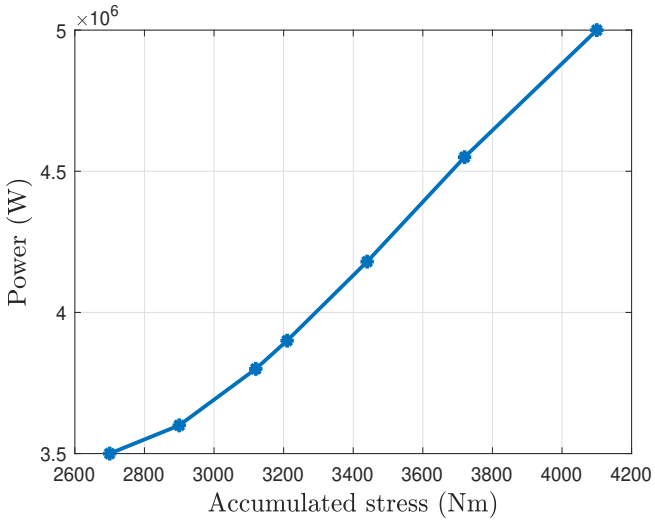

Figure 4.11: Pareto front of power and accumulated stress

accumulated stress on the blades, the control actions from the MPC results in the deration of power, which involves an increase of pitch angle to decrease the blades exposure to varying wind loading, decreasing aerodynamic thrust in the process.

4.5 Conclusions

This chapter presented a mechanism to directly include the health of a wind turbine blade in its control framework. It involved the design of a two-level control scheme; a lower-level MPC for normal control below rated wind speed and torque control above rated speed. An upper-level economic MPC is designed for pitch control above rated wind speeds that take into account the degradation of the blade, modeled via the stiffness degradation algorithm. Given the nature of the degradation curve, it is segmented into zones to attenuate degradation in each region represented with models that are included in the optimization setup according to accumulation stress levels. Considering that stress is a cyclic phenomenon, the method of rain flow counting is used to extract externally through a pre-simulation the occurrence of the effective cycle of degradation along a moving prediction horizon. The scheme shows its efficacy and practicality in illustrated results.

Chapter 5

Data-driven Prognostics Of Power Semiconductor Devices

The content of this chapter is based on the following works:

- Khoury et al. (2022b) Khoury, B., Bessa, I., Puig, V., Nejjari, F., and Palhares, R.M. (2022b). Data-driven prognostics based on evolving fuzzy degradation models for power semiconductor devices. In *Proceedings of the 7th European Conference of the Prognostics and Health Management Society 2022.* PHM Society, 241 Woodland Drive, State College, PA 16803.
- Khoury et al. (2022a) Khoury, B., Bessa, I., Nejjari, F., and Puig, V. (2022a). A set-based uncertainty quantification of evolving fuzzy models for data-driven prognostics. In *15th International Conference on Diagnostics of Processes and Systems*.

The Insulated gate bipolar transistor (IGBT) has long established itself as a competent successor to prior power semiconductors such as the power bipolar junction transistor (BJT), Darlington transistor, and metal oxide semiconductor field-effect transistor (MOSFET). It functions by combining the desirable properties of a high input impedance and high switching speeds of the MOSFET with the low saturation voltage of the BJT, enabling a voltage-controlled transistor that is capable of containing large collector-emitter currents with a virtually zero-gate current drive. The product is a transistor variant that offers medium to high power application abilities, low ON-resistance, and fast switching compared to its predecessors.
As with any component in a system, IGBTs are prone to failure under certain operating conditions, primarily from electrical and thermal stress caused by conditions such as high temperature and cycling effects (Lu and Sharma, 2009). However, the critical nature of power semiconductors in the chain of operation of most systems may cause a total shutdown emanating from an otherwise inexpensive source. From an industrial survey by (Yang et al., 2011), the majority of respondents indeed assert that power electronic devices are one of the most fragile components in most industries and the need for increased research interest in reliability monitoring and improvement. This monitoring is essential, especially in critical systems such as aviation, where the neglecting cost

may be more than just monetary. In lieu of this, there is a need for reliable and robust diagnostic and prognostic techniques that seek to avert to a low degree any spontaneous call for maintenance that introduces unplanned expenditures and manages faults or deterioration during inception before they escalate to disruptive levels. Using a model-based method, a failure precursor's features or both, a fault source can be detected, isolated, and the RUL of an IGBT predicted for maintenance responses such as planned replacements undertaken at an optimal time before its EOL.
Some common failure modes in IGBTs are gate diode degradation, body diode degradation, the bond wire, and solder layer fatigues (Nguyen and Kwak, 2020). For appropriate health management algorithms, it is desirable to study a component's observable parameters that conspicuously show deviation from their normal behaviour reflecting an associated anomaly, i.e., a failure mode when in operation. For instance, during failure modes such as the bond wire and solder layer fatigues, there is an associated increase in measured Collector- gate voltage (VCE), which results from an increased bond wire resistance for bond wire fatigues and thermal resistance associated with the latter due to the lack of effective heat dissipation between adjacent layers. The transistor turn-off time has also been identified as a parameter of interest for latch-up faults in (Brown et al., 2010). These parameter-failure mode pairings are acquired through a procedure termed FMMEA (Failure Modes, Mechanisms and Effects Analysis) under accelerated aging procedures. The criteria for choosing a specific prognostics parameter depends on its sensitivity to the failure mode and also the ease of attaining accurate measurements from sensors. For example, the junction temperature as a precursor is indicative of most thermal failure modes. Still, the difficulty in sensor integration during predesigns and inaccurate measurements limits its applicability. Therefore, works such as (Eleffendi and Johnson, 2016) considers the junction temperature as a failure precursor but are obtained through a lookup table considering measured VCE. With appropriately measured precursors from IGBTs, different prognostic procedures have been studied in the literature.
In (Saha et al., 2009), a model-based prognostics procedure using a particle filter is used based on a fitted model on the collector-emitter leakage current obtained from an accelerated aging procedure. However, in (Haque et al., 2018) an auxiliary particle filter proved to have a better variance and robustness of RUL predictions compared to particle filters using the VCE as a failure precursor, a predominant choice in most papers. Data-based algorithms have also been extensively studied, both statistically and in the area of artificial intelligence. Statistically, for data-based prognostics of IGBTs, (Ismail et al., 2019) employed the Gaussian process regression, while later in (Ismail et al., 2020) the authors used a modified maximum likelihood method to predict the RUL. The results show that the Gaussian process regression has better prognostic metrics than the modified maximum likelihood method. With the VCE as a chosen precursor in (Ahsan et al., 2016), Neural Network (NN) and Adaptive Neuro-Fuzzy Inference System (ANFIS) models are used to predict the RUL, the NN showed better performance compared to the ANFIS. In (Alghassi et al., 2016), the authors proposed a time delay neural network algorithm in tandem with a probabilistic function with VCE as the precursor parameter, which proved to be more efficient than a stand-alone NN model. Comprehensive reviews exist in the literature on the broad subject, encompassing the

type of failures (Nguyen and Kwak, 2020; Hanif et al., 2019), precursor parameter attainment, and prognostics methods (Degrenne et al., 2019; Kabir et al., 2012) employed on power semiconductors in general.

Although adaptive prognostics methods are able to modify their parameters according to the data stream behaviour to reduce the modelling error, their structure is fixed and there is no clear relationship between their evolving degradation stage and their parameters Angelov (2012). Otherwise, evolving systems are known for their ability to modify both parameters and structure to provide explainable representations for data streams. While their parameters are adapted to minimize the modelling error, the structure becomes more complex to represent novel dynamics which can be related to the achievement of novel degradation stages in prognostics problems. Recently, evolving fuzzy degradation models are proposed for aiding data-stream-driven PHM systems Camargos et al. (2020); (Camargos et al., 2021); (Ahwiadi and Wang, 2022). In particular, those models are used to capture the degradation dynamics and predict the equipment RUL. In this regard, evolving prognostic approaches have been successfully applied to ball bearings (Camargos et al., 2020) and lithium-ion batteries providing (Camargos et al., 2021); (Ahwiadi and Wang, 2022) competitive results with some interpretability features. This motivates the application of those methods for the challenging IGBT prognostic problem. Properties such as monotonicity and trendability of a chosen extracted feature or dimensionally reduced subspace of selected features are a strong prerequisite for attaining a good RUL prediction, employed in prognostics algorithms. However, the downside of this procedure is that the granularity of the degradation data is diminished or lost when smoothing tools are applied to attenuate these properties. This result in algorithms that sacrifice interpretability for improved RUL predictions. Even though it is agreed that the primary end goal of prognostics algorithms is to improve the RUL prediction, there must be a motivation to consider characteristics of the degradation trend, which may be used for secondary purposes or aid in a better RUL prediction. This especially comes in handy when considering degradation data as used in this chapter, a stage-based degradation process, where classification of the stages may prove to be important for better estimating the RUL.

The approach in this chapter considers a data-based evolving fuzzy model that uses two classes of input features: an interpretable feature as a premise variable and an RUL prediction-friendly counterpart in the auto-regressive consequent of the fuzzy model. In particular, the degradation representation is based on the Evolving Ellipsoidal Fuzzy Information Granules (EEFIG), which has already been applied for clustering (Cordovil et al., 2020), fault diagnosis (Cordovil et al., 2020), and leaning-based control (Cordovil et al., 2022) approaches. The merit of this methodology over others is that it provides a platform with a dual function mode: (1) Providing a good RUL prediction in conjunction with (2) classifying the different stages of degradation, as shown in Figure 5.1, enabling interpretability. Given the importance of uncertainty quantification, an extension on the topic of set-based quantification was undertaken in (Khoury et al., 2022a).

5.1 IGBT Aging and Degradation

As stated in the prequel, for prognostics, it is imperative to acquire parameters that explicitly represent the failures, such that a study of their behaviour can inherently constitute knowledge of the failure mechanism. To measure all useful related precursor parameters, the IGBT is subject to aggressive thermal or electrical cycles of stress in an experimental environment until a failure happens. In this work, a run-to-failure experiment on 4 IGBT undertaken by (Sonnenfeld et al., 2008) is considered. The experiment involves subjecting power transistor devices to DC square wave signals at the gate, placing the devices under thermal stress. This aging process is undertaken until a latch-up or thermal runway (EOL) when signals are switched steadily between $0V$ and $4V$, with temperature controlled between $329°C$ and $330°C$ outside the rated temperature of the test transistors. The transient data collected when the devices switch are the (i) Collector-emitter turn-on Voltage; (ii) Gate Voltage; and (iii) Collector current.

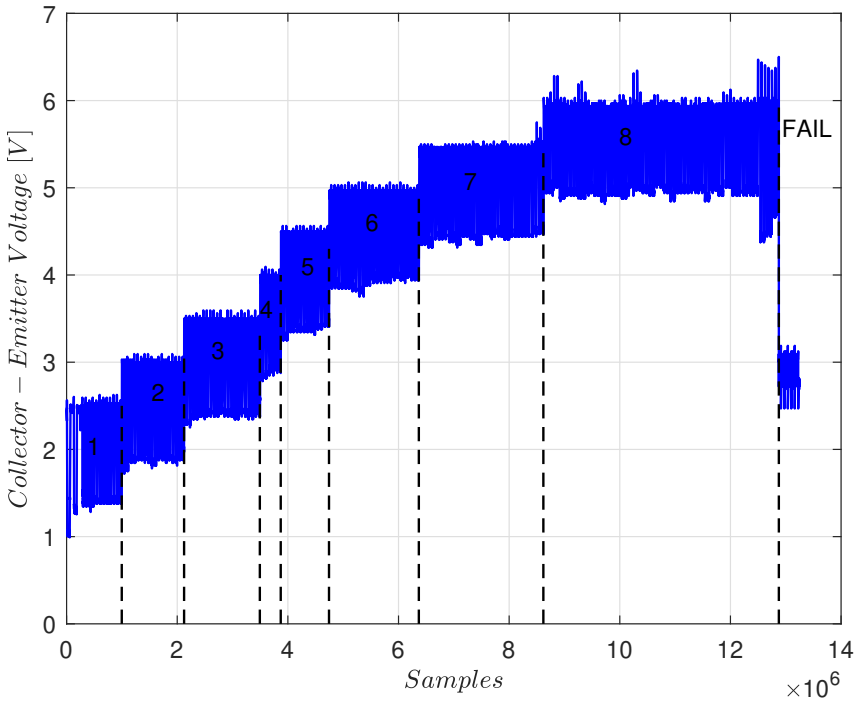

Figure 5.1: Measured collector-emitter voltage from aging test of IGBT1 showing stages of degradation.

5.2 Data-driven Prognostics based on evolving fuzzy degradation model

5.2.1 Degradation features extraction and selection

From the literature, the VCE is the predominantly chosen precursor, which has proven its efficacy as well as practicability compared to other parameters, with various pre-evaluated metrics sup-

porting its selection. Therefore, the VCE is selected as the parameter of interest in this chapter. With VCE as the selected condition-based Monitoring (CM) data, features are extracted serving as a pseudo-representation of the degradation behaviour. The raw data, shown in Figure 5.2, are almost always noisy, an undesirable characteristic for a RUL prediction. These features, either frequency or temporal based, must exhibit desirable characteristics that ensure accurate RUL extrapolations with less uncertainty (Gouriveau et al., 2016b). Two types of characteristics of input data into the proposed algorithm are considered. First, a feature that satisfies the traditional desirable properties of monotonicity, trendability, and prognosticability for an accurate and less uncertain RUL prediction is considered, and a feature that represents the shape of degradation shows the different stages. Unlike the first case, the accuracy of the RUL is not deemed a factor. Thus, for the auto-regressive consequent feature, a feature construction from (Javed et al., 2015) is considered. The authors employ the standard deviation (SD) of a Cumulative trigonometric (C-trig) function on the data set. This was proven to possess overall better prognostic characteristics backed with more accurate RUL compared to generic features when tested on a case study. Two C-trig functions, as proposed in (Javed et al., 2015), are considered and the best selected based on the suitability metric (5.1), as proposed in (Celaya et al., 2011).

$$\text{Suitability} = \begin{bmatrix} \text{Monotonicity} \\ \text{Trendability} \\ \text{Prognosability} \end{bmatrix}^{\top} \begin{bmatrix} 1 \\ 0.976 \\ 1 \end{bmatrix} \tag{5.1}$$

For the premise variable of the fuzzy model, features of the mean and the root mean square are considered for selection presented in Table 5.2. Smoothing is done with the moving average and the window length selected equal to the number of samples in each test set performed on individual IGBT. Considering a data-stream $X = [x_1, x_2, \ldots, x_n] \in \mathbb{R}^n$ the selected features are presented in Table 5.1.

Table 5.1: Trigonometric features for the premise variable.

Feature	Formula
SD of asinh(X)	$\sigma\left(\log\left[x_i + (x_i^2+1)^{\frac{1}{2}}\right]\right)$
SD of atan(X)	$\sigma\left(\frac{i}{2}\log\left(\frac{i+x_i}{i-x_i}\right)\right)$

Table 5.2: Features for the auto-regressive consequent variable.

Feature	Formula
Energy	$\sum_{i=1}^{n} E(x_i)$
Root Mean Square (RMS)	$\sqrt{\frac{1}{n}\sum_{i=1}^{n} x_i^2}$

The cumulative function as from (Javed et al., 2015), is done by considering a simultaneous point-wise running total and scaling of a time series:

$$\mathrm{CF}_i(X) = \frac{\sum_{i=1}^{n} X(i)}{|\sum_{i=1}^{n} X(i)|^{\frac{1}{2}}} \tag{5.2}$$

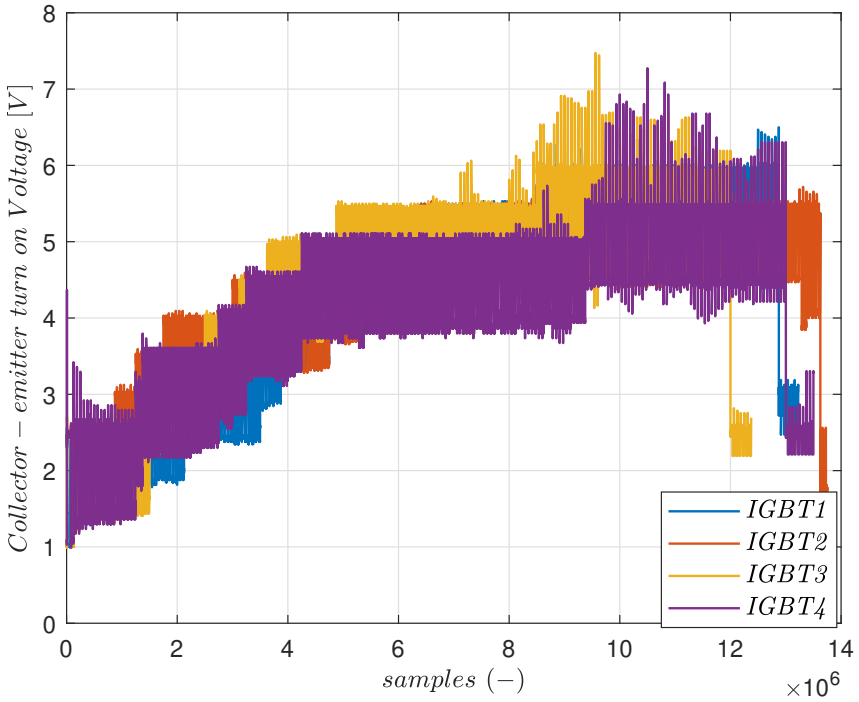

Figure 5.2: Measured collector-emitter voltage from aging test of 4 IGBT.

Feature selection: For the auto-regressive consequent feature of the fuzzy model, the *cumulative SD of* $(atan)$ is selected, with a suitability score of 2.972 compared to 2.957 of $(asinh)$. For the premise variable, the RMS feature was selected based on the best results from the two features (i.e Table 5.2) as inputs.

5.2.2 Evolving Ellipsoidal Fuzzy Information Granules

In (Cordovil et al., 2020), the Evolving Ellipsoidal Fuzzy Information Granules (EEFIG) model and its evolving granular learning algorithm are introduced. The learning algorithm is an online data processing that employs evolving fuzzy information granules based on the parametric principle of justifiable granularity (Pedrycz and Wang, 2016). In this chapter, we propose employing the EEFIG algorithm to model the degradation of the IGBT.

An EEFIG is a collection of N granules $\mathbb{G}_k = \{\mathcal{G}_k^1, \ldots, \mathcal{G}_k^N\}$, where each granule is a fuzzy set $\mathcal{G}_k^i =$

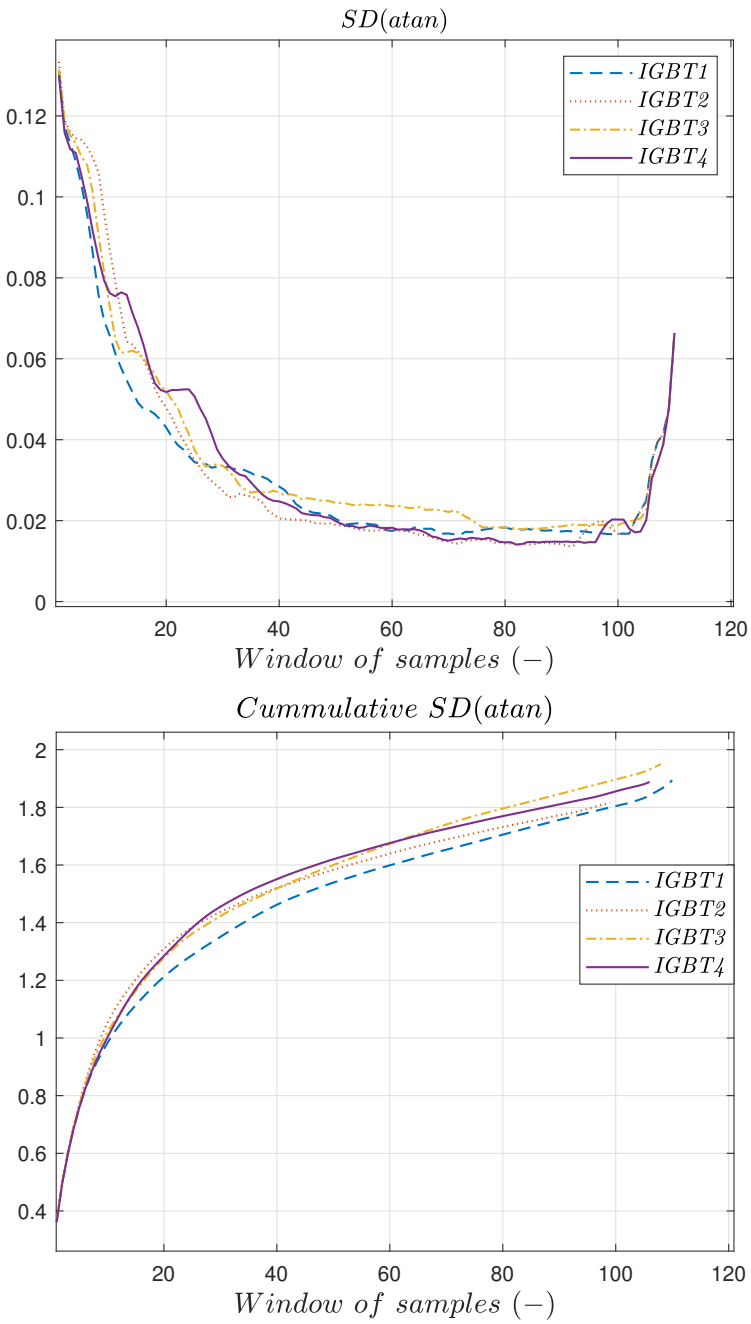

Figure 5.3: Selected auto-regressive consequent feature of the 4 IGBTs. (Top.) SD(atan) (Bottom.) C-SD(atan).

$\left(\mathbb{R}^{n_z}, g_k^i\right)$, where $g_k^i : \mathbb{R}^{n_z} \rightarrow [0,1]$ is the membership function of the EEFIG $\mathcal{G}_k^i$. The membership function ω_k^i is parameterized by the granular prototype $\mathcal{P}_k^i$ of the i-th granule at the time instant k, which is also a numerical evidence basis for the granulation process. The granule prototype is defined as follows:

$$\mathcal{P}_k^i = \left(\underline{\mu}_k^i, \mu_k^i, \overline{\mu}_k^i, \Sigma_k^i\right), \tag{5.3}$$

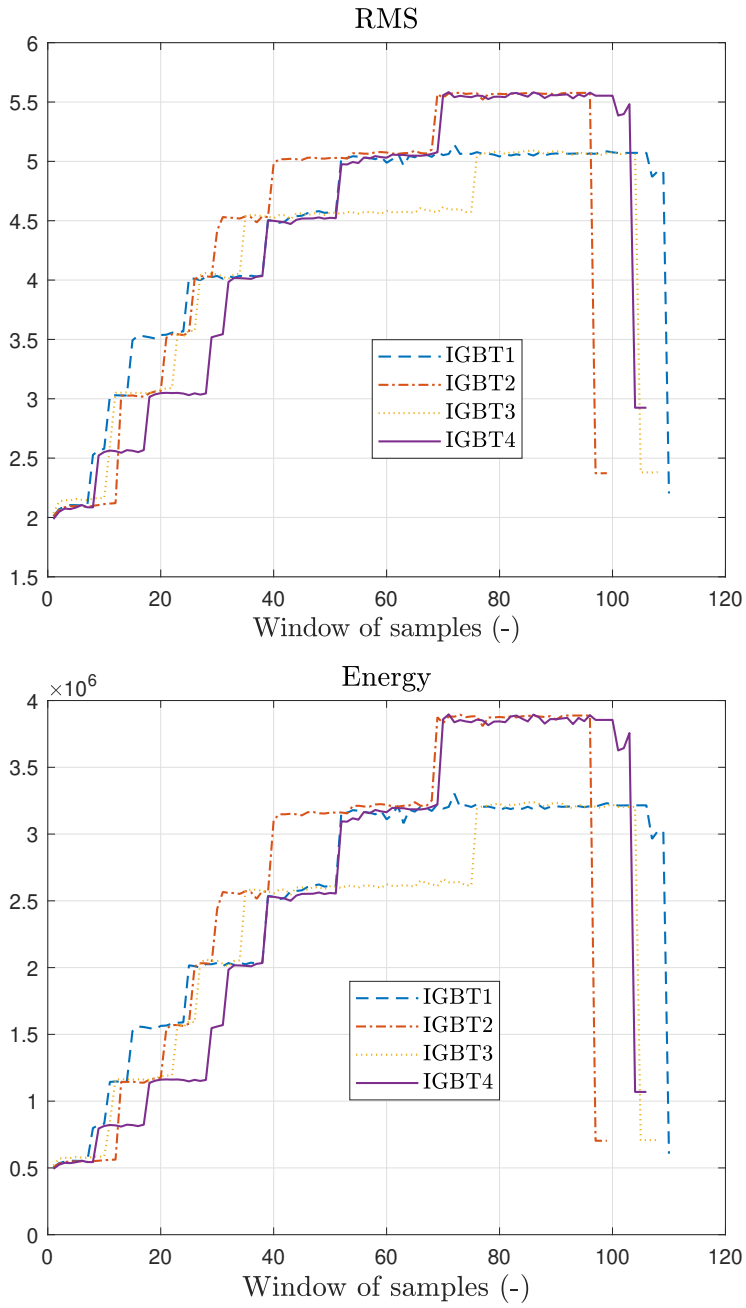

Figure 5.4: Considered premise features of the 4 IGBTs.

where $\underline{\mu}_k^i$, μ_k^i and $\overline{\mu}_k^i$ are the lower, mean, and upper bound vectors of the i-th EEFIG at time k and Σ_k^i is the inverse of its covariance matrix. Given the granule prototype $\boldsymbol{\mathcal{P}}_k^i$, the membership function of an EEFIG is parameterized as

$$\omega_k^i\left(z_k\right) = \exp\left\{-\left[\left(z_k - \mu_k^i\right)^\top \left(\Delta_k^i\right)^{-1}\left(z_k - \mu_k^i\right)\right]^{\frac{1}{2}}\right\}, \tag{5.4}$$

where, for $p \in \mathbb{N}_{\leq n_z}$,

$$\Delta_k^i = \text{diag}\left\{ \left(\frac{\overline{\mu}_{k,1}^i - \underline{\mu}_{k,1}^i}{2} \right)^2, \ldots, \left(\frac{\overline{\mu}_{k,p}^i - \underline{\mu}_{k,p}^i}{2} \right)^2 \right\},$$

being $\overline{\mu}_k^i$, and $\underline{\mu}_k^i$ the semi-axes of the i-th EEFIG prototype such that $\underline{\mu}_k^i < \mu_k^i < \overline{\mu}_k^i$ (Wang et al., 2014). The normalized membership functions g_k^i at the k-th time instant for i-th granule is

$$g_k^i(z_k) = \frac{\omega_k^i(z_k)}{\sum_{i=1}^N \omega_k^i(z_k)}. \tag{5.5}$$

Moreover, the distance of a given data sample $z_k \in \mathbb{R}^{n_z}$ to the i-th EEFIG is given by the square of Mahalanobis distance:

$$d(z_k, \mu_k^i) = (z_k - \mu_k^i)^\top \Sigma_k^i (z_k - \mu_k^i). \tag{5.6}$$

The granulation process is the updating of the EEFIG model based on the data stream. The updates are performed aiming to improve the so-called granular performance index with respect to a data sample. The performance index of the i-th granule with respect the sample z_k, denoted $\bar{\mathcal{Q}}_k^i$, is defined as

$$\bar{\mathcal{Q}}_k^i(z_k) = d(z_k, \mu_k^i)|\mathcal{G}_k^i| \tag{5.7}$$

where $|\cdot|$ is the fuzzy cardinality operator of the i-th EEFIG, whose update is performed as follows

$$|\mathcal{G}_k^i| = |\mathcal{G}_{k-1}^i| + g_k^i(z_k) - \frac{\partial g_k^i(z_k)}{\partial \mathcal{P}_k^i}, \tag{5.8}$$

where the term $\frac{\partial g_k^i(z_k)}{\partial \mathcal{P}_k^i}$ is computed as described in (Cordovil et al., 2022). The total EEFIG performance index is the sum of the data sample contribution index of each granule:

$$\mathcal{Q}_k^i = \frac{1}{k} \sum_{j=1}^k \bar{\mathcal{Q}}_j^i(z_j). \tag{5.9}$$

To decide whether a granule must be updated or not, the concept of data sample admissibility is used. A data sample z_k is said to be admitted by a given granule prototype $\mathcal{P}_k^i$ if it is used to update the granule prototype parameters. In this sense, two criteria are used to evaluate the data sample admissibility:

$$d(z_k, \mu_k^i) < \nu, \tag{5.10}$$

$$\mathcal{Q}_k^i > \mathcal{Q}_{k-1}^i, \tag{5.11}$$

where $\nu = \left(\chi^2\right)^{-1}(\gamma, n)$ is a threshold parameterized by the inverse of chi-squared statistic with $n+m$ degrees of freedom, leading EEFIG prototype to cover around $100\gamma\%$ of the stream sample. A data sample z_k which does not meet the first condition (5.10) for some granule is denominated an anomaly. In parallel, as the data samples are available and evaluated, a structure named tracker whose objective is to follow the data stream dynamics to indicate change points is established.

The tracker is parameterized by a mean vector μ_k^{tr} and an inverse covariance matrix Σ_k^{tr}, which are recursively updated (Moshtaghi et al., 2016). A new granule is created if the following conditions hold:

1. The tracker is c-separated from all the existing granule prototypes. The c-separation condition is expressed as follows

$$\|\mu_k^{\text{tr}} - \mu_k^i\| \geq c\sqrt{n_z \max(\bar{\xi}(\Sigma_k^{\text{tr}}), \bar{\xi}(\Sigma_k^i))}, \tag{5.12}$$

   for all $\mathcal{G}_k^i \in \mathbb{G}_k$, where $\bar{\xi}\left(\Sigma_k^{\text{tr}}\right)$ is the largest eigenvalue of Σ_k and, $c \in [0, \infty)$ specifies the separation level. Here, c is assumed as 2.

2. The number of consecutive anomalies is $n_a > \zeta$ where ζ is a hyper-parameter defined by the user to control the minimum amount of anomalies that may enable the rule creation.

5.2.3 EEFIG-based degradation modelling and RUL estimation

Based on the EEFIG model described in the previous section, the following Takagi-Sugeno fuzzy model is proposed for the degradation modelling

$$\begin{aligned} &\textbf{Rule } i: \text{IF } \ z_k \text{ is } \mathcal{G}_k^i \\ &\qquad \text{THEN } y_k^i = \vec{\theta}_k^{i\top} \left[y_{k-1}, y_{k-2}, \ldots, y_{k-L}\right]^\top, \end{aligned} \tag{5.13}$$

for $i \in \mathbb{N}_{\leq C_k}$, where $y_k \in \mathbb{R}$ is the health index, $z_k \in \mathbb{R}^{n_z}$ is the vector of premise variables, $\vec{\theta}_k^i \in \mathbb{R}^L$ are the coefficients of the i-th fuzzy rule at instant k, $L \in \mathbb{N}$ is the number of regressors in the auto-regressive consequent, and $C_k \in \mathbb{N}$ is the number of rules at instant k. Using the center-of-gravity defuzzification for (5.13), the health index y_k is

$$y_k = \sum_{i=1}^{C_k} g_k^i\left(z_k\right) \vec{\theta}_k^{i\top} \left[y_k \ y_{k-1} \ \cdots \ y_{k-L+1}\right]^\top \tag{5.14}$$

$$\vec{\Theta}_k h_k\left(\vec{y}_k\right), \tag{5.15}$$

where

$$\vec{\Theta}_k = \left[\vec{\theta}_k^{1\top} \ \dots \ \vec{\theta}_k^{C_k\top}\right],$$
$$\vec{y}_j = \begin{bmatrix} y_j \\ \vdots \\ y_{j-L+1} \end{bmatrix}, \ h_k\left(\vec{y}_l\right) = \begin{bmatrix} g_k^1\left(z_k\right)\vec{y}_j \\ \vdots \\ g_k^{C_k}\left(z_k\right)\vec{y}_j \end{bmatrix}.$$

As described in (Cordovil et al., 2020); (Cordovil et al., 2022), the consequent parameters $\vec{\Theta}_k$ are estimated based on Recursive Least Squares (RLS) methods. In particular, here we use the Sliding-windowed Fuzzily Weighted Recursive Least Square (SFWRLS) where the weights are the membership degrees and the data window contains the last φ samples:

$$H_k = \left[h_k\left(\vec{y}_{k-1}\right) \ \dots \ h_k\left(\vec{y}_{k-\varphi}\right)\right] \tag{5.16}$$
$$X_k = \left[y_k \ \dots \ y_{k-\varphi+1}\right] \tag{5.17}$$

Therefore, the recursive equations for the SFWRLS estimator are provided as follows

$$\Upsilon_k = P_k H_k \left(\eta I_\varphi + H_k^\top P_k H_k\right)^{-1} \tag{5.18}$$
$$P_{k+1} = \eta^{-1}\left(P_k - \Upsilon_k H_k^\top P_k\right) \tag{5.19}$$
$$\vec{\Theta}_{k+1} = \vec{\Theta}_k + \left(X_k - \vec{\Theta}_k H_k\right)^\top \Upsilon_k^\top \tag{5.20}$$

where $P_k \in \mathbb{R}^{LC_k \times LC_k}$ is an estimate of the inverted regularised data autocorrelation matrix, $\Upsilon_k \in \mathbb{R}^{n_x}$ is the SFWRLS gain vector and $\eta \in (0, 1]$ is the forgetting factor.
Given the estimate of the parameters of (5.13), the one-step ahead prediction of the degradation at instant k is computed as follows

$$\hat{y}_{k+1|k} = \sum_{i=1}^{C_k} g_k^i\left(z_k\right)\vec{\theta}_k^{i\top}\left[y_k \ y_{k-1} \ \dots \ y_{k-L+1}\right]^\top \tag{5.21}$$

For any $N \in \mathbb{N}$, define

$$\hat{\vec{y}}_{k+N|k} = \begin{cases} \left[y_k, y_{k-1}, \dots, y_u\right]^\top, & \text{if } N = 1, \\ \left[\hat{y}_w, \dots, \hat{y}_{k+1}, y_k, \dots, y_u\right]^\top, & \text{if } 1 < N < L, \\ \left[\hat{y}_w, \dots, \hat{y}_u\right]^\top, & \text{if } N \geq L, \end{cases} \tag{5.22}$$

where $u = k + N - L$ and $w = k + N - 1$. The N-step ahead health index prediction $\hat{y}_{k+N|k}$ is computed as follows:

$$\hat{y}_{k+N|k} = \vec{A}_k \hat{\vec{y}}_{k+N|k}, \tag{5.23}$$

where $\vec{A}_k = \sum_{i=1}^{C_k} \omega_k^i\left(z_k\right)\vec{\theta}_k^{i\top}$.

Based on the long-term prediction described in (5.23), the RUL can be estimated by predicting the future health state of the system given the current and past system's condition, which are provided by $\hat{\vec{y}}_{k+N|k}$ and z_k. Indeed, the RUL can be defined as the amount of time until the system's health index reaches a predefined threshold, that is:

$$\hat{\mathrm{RUL}}_k = \inf\{N \in \mathbb{Z}_{\geq 0} : \hat{y}_{k+N|k} \leq \eta\}, \tag{5.24}$$

where $\hat{\mathrm{RUL}}_k \in \mathbb{Z}_{\geq 0}$ denotes the RUL estimate computed at instant k given the observations of degradation state until k, and η is the end of life threshold, which must be defined based on historic data.

5.2.4 Uncertainty quantification

Consider a state transition function given by a TS model, with rules as in (5.13). The degradation propagation (5.23) can be rewritten as

$$\hat{y}_{k+N|k} = \vec{A}_k \vec{y}_{k+N|k} + \epsilon_{k+N}, \quad \forall N > 0. \tag{5.25}$$

To account for prediction uncertainties, white Gaussian noise is added to (5.25) from

$$\epsilon_k \sim \mathcal{N}\left(0, \sigma_\epsilon^2\right), \tag{5.26}$$

where σ_ϵ^2 is considered constant. The noise variance can be estimated through Monte Carlo simulations using the consequent parameters' covariance matrix estimated via RLS until time instant k (Camargos et al., 2020) or by recursively tracking the covariance of estimation errors through the online learning operation, i.e., for time instances $n \in \mathbb{N}_{\leq k}$ (Camargos et al., 2021). In the univariate case, the mean error is recursively tracked as

$$\Delta_{\epsilon,k} = \epsilon_k - \hat{\mu}_{\epsilon,k-1}, \tag{5.27}$$

$$\hat{\mu}_{\epsilon,k} = \hat{\mu}_{\epsilon,k-1} + \frac{1}{k}\Delta_{\epsilon,k}. \tag{5.28}$$

The initial mean error is $\hat{\mu}_{\epsilon,0} = 0$. Given the estimated mean error, the sum of squares is obtained recursively from

$$s_{\epsilon,k} = s_{\epsilon,k-1} + (\epsilon_k - \hat{\mu}_{\epsilon,k-1})^2, \tag{5.29}$$

being $s_{\epsilon,0} = 0$. The variance σ_ϵ^2 in (5.26), used for long-term prediction, is then approximated by the error covariance matrix at time instant n:

$$\sigma_\epsilon^2 = \frac{s_{\epsilon,k}}{k-1}. \tag{5.30}$$

5.2.5 Uncertainty propagation

After obtaining the initial uncertainty in one-step estimates, its long-term propagation considers the input vector (5.22) to be a vector composed of estimated random variables. Note that if $N = 1$, the previous degradation states are known and, naturally, are non-random variables. Accordingly, the output $\hat{x}_{k+N}$ of the state transition relation (5.25) is also a random variable. Computing variances in a multi-step prediction framework is needed for uncertainty propagation. The first step gives

$$\begin{aligned} \text{Var}\left(\hat{y}_{k+1|k}\right) &= \vec{A}_k \text{Cov}(\vec{y}_{k+1|k})\vec{A}_k^\top + \sigma_\epsilon^2 \\ &= \vec{A}_k \vec{\Lambda}_1^L \vec{A}_k^\top + \sigma_\epsilon^2 \\ &= \sigma_\epsilon^2 \\ &= \lambda_1^2, \end{aligned} \tag{5.31}$$

in which $\vec{\Lambda}_N^L \triangleq \text{Cov}(\vec{y}_{k+N|k})$, and $\lambda_N^2 \triangleq \text{Var}(\hat{y}_{k+N|k})$. Note that $\vec{\Lambda}_1^L = 0$, since previous degradation states are known at $N = 1$. Then, the $\vec{N}$**-step variance** is computed recursively as

$$\text{Var}(\hat{y}_{k+N|k}) = \vec{A}_k \vec{\Lambda}_N^L \vec{A}_k^\top + \sigma_\epsilon^2. \tag{5.32}$$

The covariance matrix of the random vector $\vec{y}_{k+1|k}$ is

$$\vec{\Lambda}_N^L = \begin{bmatrix} \lambda_{N-1}^2 & \cdots & \lambda_{N-L}\lambda_{N-1}\hat{\rho}_{L,1} \\ \vdots & \ddots & \vdots \\ \lambda_{N-1}\lambda_{N-L}\hat{\rho}_{1,L} & \cdots & \lambda_{N-L}^2 \end{bmatrix}. \tag{5.33}$$

Moreover, $\lambda_i^2 = 0$ when $i < 0$, meaning that x_{k+N} is known. The covariance matrix (5.33) is weighted by Pearson correlation coefficients, $\hat{\rho}$, estimated through historic data.
Considering the degradation to be a random variable with Gaussian distribution whose expected value is propagated by successive iterations of (5.25), then RUL lower and upper bounds at an $\alpha(100)\%$ significance level are given as

$$\hat{\text{RUL}}_k^{\text{lb}} = \inf\left\{N \in \mathbb{Z}_{\geq 0} : \hat{y}_{k+N|k} + z_{1-\frac{\alpha}{2}}\, \lambda_N \leq \eta\right\}, \tag{5.34a}$$

$$\hat{\text{RUL}}_k^{\text{ub}} = \inf\left\{N \in \mathbb{Z}_{\geq 0} : \hat{y}_{k+N|k} + z_{\frac{\alpha}{2}}\, \lambda_N \leq \eta\right\}. \tag{5.34b}$$

5.3 Experimental Setup

To evaluate the proposed data-driven prognostics based on evolving fuzzy degradation model, we use the accelerated aging IGBT dataset from the NASA Ames Research Center[1]. This dataset contains sensor data from four devices. In particular, there are aging time series for the VCE,

[1]The dataset is available for download in `ti.arc.nasa.gov/project/prognostics-data-repository`

gate-emitter voltage, collector current, thermal and electrical resistance, and the times at which the switch is on and off. The health index y_k is selected to be

$$y_k = SD\left(\arctan\left(V_{\mathrm{CE_{on}}}\right)\right), \tag{5.35}$$

and the premise variables vector is

$$z_k = \left[\bar{E}_k \; \bar{E}_{k-1} \; \bar{E}_{k-\tau+1}\right]^\top \tag{5.36}$$

where $\bar{E}_k$ is the energy of VCE described in Table 5.2.

The proposed evolving fuzzy prognostics require the tuning of some hyper-parameters, namely: L, the number of lags in the autoregressive model for the health index y_k (cf. (5.13)); τ, the number of lags of E_k used in the premise vector z_k; η, the forgetting factor of SFWRLS (cf. (5.18), (5.19) and (5.20)); φ, the size of the data windows used in SFWRLS (cf. (5.16) and (5.17)); and ζ, the number of necessary consecutive anomalies to enable the granule creation.

For choosing the hyper-parameters of the proposed algorithm, we designate a test dataset regarding one of the four devices and perform a grid search to solve the following problem

$$\ell(D) =_l \quad \sum_{k=1}^{\mathrm{EOL}_D} k\mathrm{ra}_k(D,l) \quad \text{s.t.} \quad l \in \mathcal{L} \tag{5.37}$$

where $l = (L, \tau, \eta, \varphi, \zeta)$ is the vector of hyper-parameters, $\mathcal{L} = [2,5] \times [2,5] \times [0.96,1] \times [2,6] \times [2,6]$ is the search space, EOL_D is the end of life of the D-th device, and $\ell(D)$ are the optimal parameters within the the search space $\mathcal{L}$, and the ra is

$$\mathrm{ra}_k = 1 - \frac{\left|\mathrm{RUL}_k - \hat{\mathrm{RUL}}_k\right|}{\mathrm{RUL}_k}, \tag{5.38}$$

5.4 Experimental Results

In this section, the results for the RUL prediction for IGBTs based on evolving fuzzy models are presented and discussed. For evaluating the results, the Mean Absolute Percentage Error (MAPE) is used as figure of merit:

$$\mathrm{MAPE}_k = \frac{100}{\mathrm{EOL} - k + 1} \sum_{i=k+1}^{\mathrm{EOL}} \left| \frac{\mathrm{RUL}_i - \hat{\mathrm{RUL}}_i}{\mathrm{RUL}_i} \right|, \tag{5.39}$$

where EOL is the end of life of the UUT; RUL_k and $\hat{\mathrm{RUL}}_k$ are the current and estimated RUL at k, respectively.

Table 5.3 provides the MAPE results computed from $k = 20$. Notice that the EEFIG-based prognostics were able to guarantee MAPE results below 50% for the IGBT devices 1, 2, and 4. However,

the third IGBT presents more challenging data which results in higher MAPE for any parameter set.

Table 5.3: MAPE_{20} results

UUT dataset \ Parameter tuning dataset	1	2	3	4
1	20.3560	31.5868	59.6492	48.3150
2	23.0306	15.1883	34.4047	15.2904
3	67.4113	76.0535	70.8395	74.9962
4	40.7839	31.4586	37.6570	28.2187

Figures 5.5-5.7 depict the RUL prediction results in α-λ plots with accuracy cones of $\pm 30\%$. In particular, Figure 5.5 presents the results for the second IGBT using the parameters obtained by solving (5.37) for the dataset extracted from the fourth IGBT. Figure 5.11 presents the results for the first IGBT using the parameters obtained by solving (5.37) for the dataset extracted from the second IGBT. And, Figure 5.7 presents the results for the second IGBT using the parameters obtained by solving (5.37) for the dataset extracted from the third IGBT.

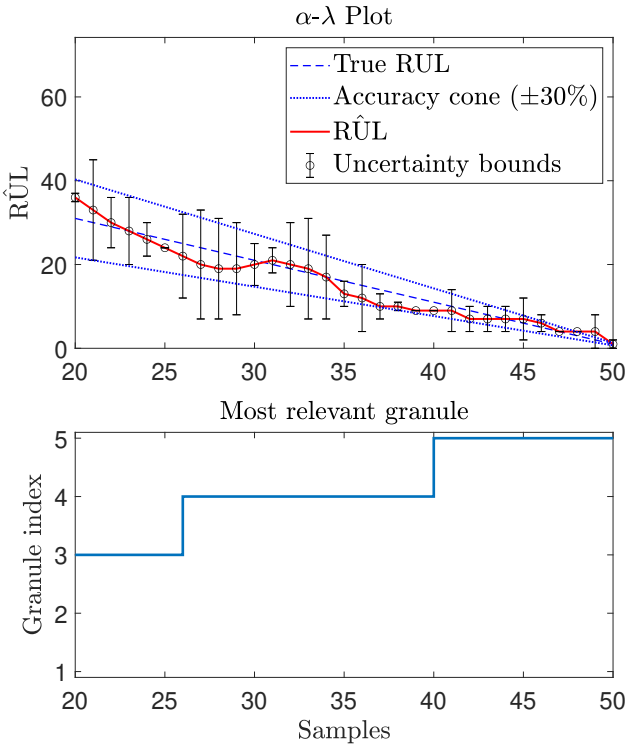

Figure 5.5: RUL prediction for the 2nd IGBT with parameters obtained for the test dataset with data from the 4th IGBT.

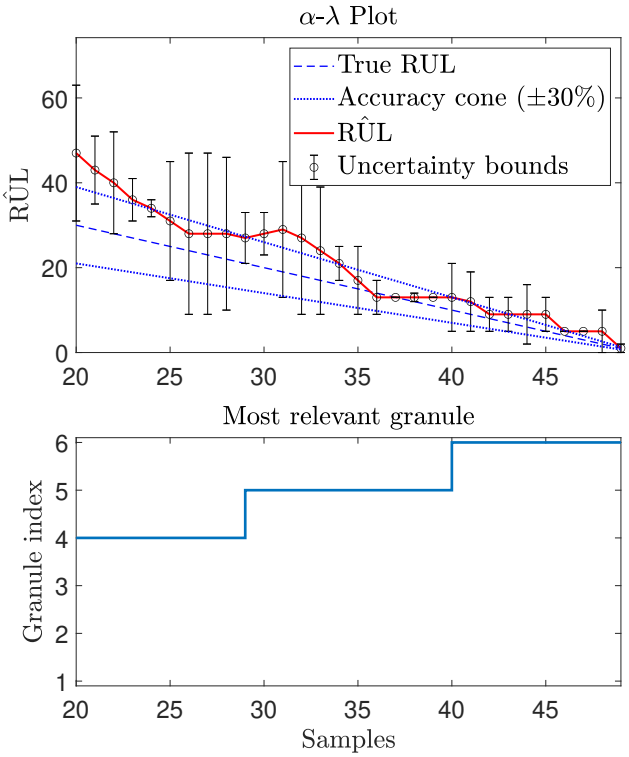

Figure 5.7: RUL prediction for the 2nd IGBT with parameters obtained for the test dataset with data from the 3rd IGBT.

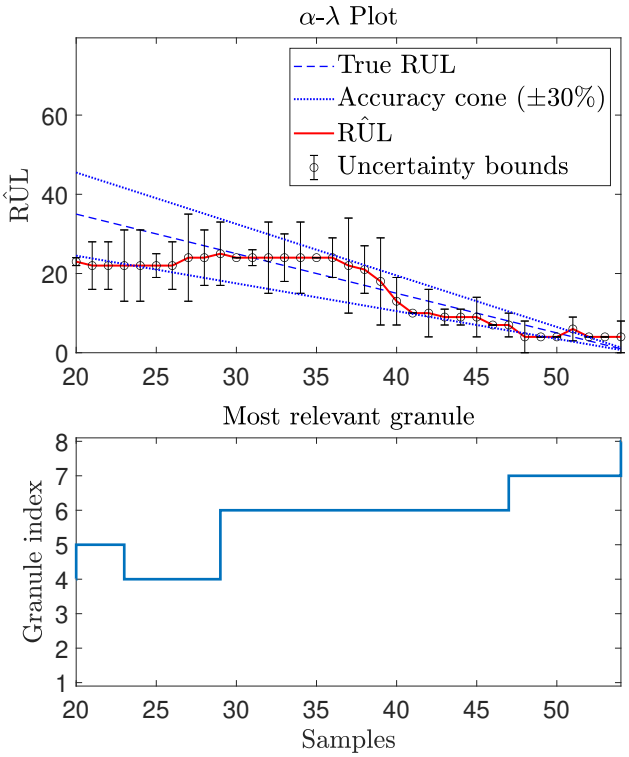

Figure 5.6: RUL prediction for the 1st IGBT with parameters obtained for the test dataset with data from the 2nd IGBT.

In Figures 5.5 and 5.11, notice that the RUL predictions remain inside of the accuracy cone in most of the time, and the true RUL tends to be within the predicted RUL bounds. However, the results become considerably worse for Figure 5.7, as already indicated in Table 5.3.

One of the key advantages of applying evolving fuzzy methods is interpretability. In this regard, the bottom plots of Figures 5.5, 5.11, and 5.7 indicate the granule with maximum membership degree at each sample. It is possible that new granules are being created and becoming more relevant since they are capturing novel degradation stages. Indeed, the transitions between the most relevant granules could be used as a failure or degradation stage indicator.

5.5 Set-Based Uncertainty Quantification

In this section, a set-based approach is proposed for uncertainty quantification and subsequent set propagation for prognostics. As a matured field of study, the set-based methodology offers ease of quantifying all uncertainty sources which is then propagated with minimal computational effort. The uncertainty is quantified aided by the interval predictor estimation methodology and represented by boxes. Manipulations are undertaken with relevant interval analysis (IA) properties to arrive at an appropriate uncertainty representation. This is applied to Evolving Ellipsoidal Fuzzy Information Granules (EEFIG).

5.5.1 Interval Arithmetic

This section presents the main concepts and notations used. Calligraphic capital letters are used to represent sets and lower letter cases for deterministic representations. Assuming an uncertainty set $\mathcal{X}$, $\Delta x = [\underline{x}, \overline{x}]$ is the uncertain part with a center x^c i.e. $\mathcal{X} = x^c + \Delta x$. The sets of real and integer numbers are defined by $\mathbb{R}$ and $\mathbb{Z}$. $[(.)]$ signifies the interval hull of a set and $\mathbf{I}(\mathbb{R})$, real interval of a variable.

5.5.2 Interval predictor estimation

Uncertain models bounding

Bounding uncertain mathematical models into interval forms has seen a number of applications in the field of robust system identification, robust fault detection as well as stability and performance robustness of uncertain feedback systems. Different geometric forms such as polytopes, ellipsoids, and zonotopes have been successfully employed for this purpose. Interval models are used in prognostics in the spirit of interval bounds aided by set-based parameter estimation theorem which is mostly used in robust fault detection. For estimating these intervals, two options are normally considered; the interval predictor approach and the bounded error approach, the difference between the two is dependent on how the types of uncertainties are algorithmically handled. In this chapter, the interval predictor approach is considered. For a comprehensive comparison of the two approaches, the reader is referred to Blesa et al. (2011a).

Considering a model in a regressor form that is linear in parameter space as:

$$y(k) = \theta(k)\phi(k) + w(k) \triangleq \hat{y}(k) + w(k)\ ,\ y(k) \subseteq \mathcal{Y} \tag{5.40}$$

$$w(k) \leq \sigma(k)$$
$$\sigma(k) \geq 0\ ,\ k \in \mathbb{Z}_+.$$

where $\theta(k)$ and $\phi(k) \subseteq \Phi$ both $\in \mathbb{R}^{n_\theta}$ are the regressor and parameter vectors, respectively. The additive errors such as sensor noise and modelling uncertainties are considered bounded to a limit $\sigma(k)$. Φ is therefore a set that is constructed with interval parameter estimation elaborated in the sequel to bound parametric uncertainties in state predictions which is described with interval boxes as:

$$\Phi \in \mathbf{I}(\mathbb{R}^{n_\theta}) = \left[\underline{\phi}_1,\ \overline{\phi}_1\right] \times \cdots \times \left[\underline{\phi}_i,\ \overline{\phi}_i\right] \times \cdots \times \left[\underline{\phi}_{n_\phi},\ \overline{\phi}_{n_\phi}\right] \tag{5.41}$$

where $\underline{\phi_i} = {\phi_i}^c - \lambda_i$ and $\overline{\phi_i} = {\phi_i}^c + \lambda_i$, $\lambda_i \geq 0$. ${\phi_i}^c$ is the center and λ_i, the endpoint of a symmetric interval set.

Interval predictor parameter estimation algorithm

Given a sequence of interval regressor values, $\theta(k) \in \mathbf{I}\mathbb{R}^{N_{n_\theta}}$ and measurements $y(k)$. The set Φ should be constructed to ensure the inclusion of all possible realization of uncertainties. Hence it is desirable to consider the worst-case scenario of an uncertainty descriptive set that represents a complete membership of all uncertainties. Hence from (5.40), a suitable worst-case set description can be described as:

$$y(k) \in \left[\underline{\hat{y}}(k) - \sigma,\ \overline{\hat{y}}(k) + \sigma\right]\ \forall k \leq \mathbb{Z}_{[1,\ldots,N]} \tag{5.42}$$

(5.42) is thus equivalent to :

$$\underline{\hat{y}}(k) \leq y(k) + \sigma \text{ and } \overline{\hat{y}}(k) \geq y(k) - \sigma$$

where $\overline{\hat{y}}(k) = \max_{\phi(k)\in\Phi}(\theta(k)\phi(k))$ and $\underline{\hat{y}}(k) = \min_{\phi(k)\in\Phi}(\theta(k)\phi(k))$. As such, the uncertainty set Φ can be described as an intersection of unbounded admissible sets resulting from the half-spaces $\underline{\Phi}_k$ and $\overline{\Phi}_k$ considering the worst case scenario (5.42):

$$\underline{\Phi} = \bigcap_{k=1}^{N} \{\theta \in \mathbb{R}^{n_\theta} : \theta(k)\phi(k) \leq y(k) + \sigma\} \text{ and } \overline{\Phi} = \bigcap_{k=1}^{N} \{\theta \in \mathbb{R}^{n_\theta} : \theta(k)\phi(k) \geq y(k) - \sigma\} \tag{5.43}$$

Hence, the ultimate uncertainty set is satisfied where $\Phi \cap \overline{\Phi} \neq \emptyset$ & $\Phi \cap \underline{\Phi} \neq \emptyset$ in the parameter space. The uncertainty set is therefore:

$$\Phi = \bigcap_{k=1}^{N} \{\theta \in \mathbb{R}^{n_\theta} : |y(k) + \theta(k)\phi(k)| \leq \sigma\}.$$

Assuming a symmetric interval set $[-\Delta\hat{y},\ \Delta\hat{y}]$ with center y^c. Then the maximum endpoints for any variation from the nominal regressors can be described as:

$$\overline{\hat{y}}(k) = \hat{y}^c + \theta(k)\Delta y$$
$$\underline{\hat{y}}(k) = \hat{y}^c - \theta(k)\Delta y$$

where $\hat{y}^c = \theta(k)\phi^c$; $\phi^c = \left[\phi_1^c, \ldots,\ \phi_{n_\phi}^c\right]$ is the nominal model devoid of uncertainty. Therefore, assuming a predefined symmetric interval $\Delta y_0 = [-\Delta y_0,\ \Delta y_0]$, a mathematical problem is formulated such that an optimal λ is evaluated ensuring that all uncertainties are accounted for when $\Delta y = \lambda \Delta y_0$. This is achieved by solving an optimization problem with a cost function considering:

$$f(\lambda) = \sum_{k=1}^{N} \mathcal{W}(\Delta\hat{y}(k)) = 2\lambda \sum_{k=1}^{N} \theta(k)\Delta y_0\ ,\ \lambda > 0 \tag{5.44}$$

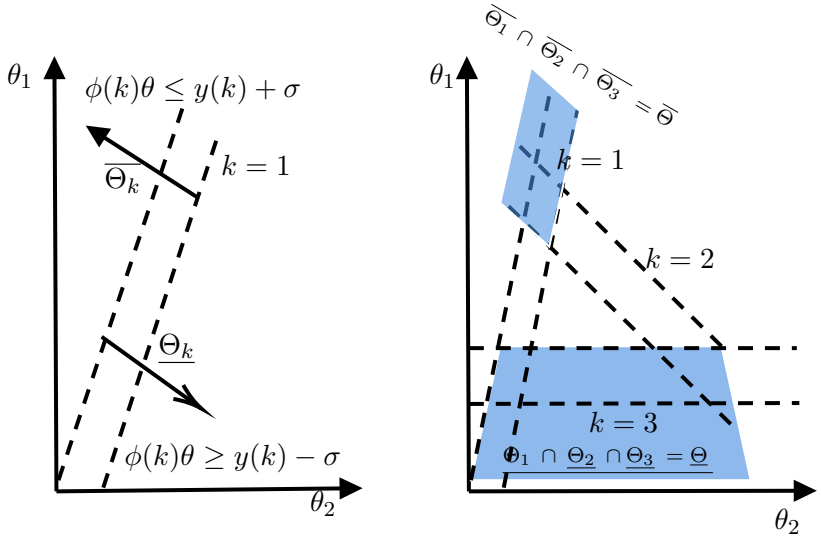

Figure 5.8: Left shows half spaces of $\underline{\Theta_k}$ and $\overline{\Theta_k}$ for 1 dimension and right shows $\underline{\Theta_k}$ and $\overline{\Theta_k}$ from dimensions 1 to 3 from Blesa et al. (2011a).

where $\mathcal{W}()$ is the width of the uncertainty set $\Delta\hat{y}$ and the constraint is as follows from (5.42):

$$\lambda\theta(k)\Delta y_0 \geq |y(k) - \hat{y}^c(k)| - \sigma \longrightarrow \lambda \geq \frac{|y(k) - \hat{y}^c(k)| - \sigma}{\theta(k)\Delta y_0} \tag{5.45}$$

Thus, the optimization problem to be solved is:

$$\begin{aligned} \min_{\lambda} \quad & f(\lambda) \\ \text{s.t.} \quad & \lambda \geq \tfrac{|y(k)-\hat{y}^c(k)|-\sigma}{\theta(k)\Delta y_0} \;\forall\; k \in \mathbb{Z}_{[1,\ldots,N]} \end{aligned} \tag{5.46}$$

The optimal solution is therefore:

$$\lambda = \sup_{k \in \mathbb{Z}_{[1,\cdot,N]}} \left(\frac{|y(k) - \hat{y}^c(k)| - \sigma}{\theta(k)\Delta y_0} \right) \tag{5.47}$$

In summary, this methodology is henceforth used to evaluate a factor λ which ensures a worst-case set Φ that bounds all uncertainties with regards to the present and modelling uncertainties σ under initial set conditions Δy_0. Since the constraint in (5.46) is an epigraph of a piecewise linear function, the optimization problem is convex, therefore finding a solution can be done with ease with common solvers. The bounded set is then propagated to a future predefined End Of Life (EOL).

5.6 Interval set-based uncertainty description.

For quantifying and propagating the uncertainty sets, the following conditions are assumed:

Assumption 4 *The unknown uncertainties in the process and measurement can be represented with an appropriate convex set.*

Assumption 5 *From Assumption 1, since the one-step ahead degradation fuzzy model* (5.21) *is linear, then a multi-step propagation with a convex uncertainty initial set ensures conservation of convexity. Thus the final uncertainty set is convex and easily interpretable.*

The initial noise and parametric uncertainties are quantified by finding an optimal λ solving the optimization problem (5.47). This allows to bound all realization of the considered uncertainty sources. For a one-step propagation i.e. $N = 1$, the input as from (5.22), considers only a certain measurement vector $\hat{\vec{y}}_{k+N|k} \in \mathbb{R}^{k+N-L}$ with its uncertain component of prediction (5.23) described as:

$$\Delta\hat{y}_{k+N|k} = \Delta\vec{A}_k\hat{\vec{y}}_{k+N|k}, \tag{5.48}$$

where $\Delta\hat{y}_{k+N|k}$ and $\Delta\vec{A}_k$ are the uncertain components described as symmetric intervals. For a multi-step forecast to the EOL, the uncertain set is constructed recursively considering propagation of the recursive sum of sets as:

$$\Delta\hat{y}_{k+N|k} = \Delta\vec{A}_k\hat{\vec{y}}_{k+N|k} + \Delta\vec{A}_k\Delta\hat{\vec{y}}_{k+N|k} + \Delta\vec{A}_k\Delta\hat{\vec{y}}_{k+N|k} + \Delta\epsilon_k. \tag{5.49}$$

Where $\Delta\hat{y}_{k+N_{EOL}|k}$ as the uncertainty set at $k+N_{EOL}|k$ of the UUT's EOL and $\Delta\epsilon_k$ as the bounded noise value during forecasting. For clarity, two noise components are considered, first from sensor noise in the prediction of the states and another ϵ_k for noise in future times of prognostication. The upper and lower bounds of the RUL are therefore given as:

$$\overline{RUL} = \sup\left(x \in \mathbb{R} \cup \{-\infty,\ +\infty\} \mid \Delta\hat{y}_{k+N_{EOL}|k} \in \hat{y}_{k+N_{EOL}|k},\ x \leq \hat{y}_{k+N_{EOL}|k}\right) \tag{5.50}$$

$$\underline{RUL} = \inf\left(x \in \mathbb{R} \cup \{-\infty,\ +\infty\} \mid \Delta\hat{y}_{k+N_{EOL}|k} \in \hat{y}_{k+N_{EOL}|k},\ \hat{y}_{k+N_{EOL}|k} \leq x\right) \tag{5.51}$$

Since the parametric uncertainty and the propagation noise (ϵ_k) are propagated in time, the future uncertainty and predicted uncertainty as stated in the introduction are considered in part taken care of in the prognostics process.

5.7 Results and discussion

The bound on the noise value ϵ_k is taken as the maximum variation of each cycle of stress from the given data Fig. 5.2 given their respective mean values Fig. 5.4 and . Whilst the uncertainty $\Delta y_0 \subseteq \sigma(k)$ is taken as a varying error between predicted and original feature at the propagation stage. The prognostic model is trained with data from IGBT2 and two test scenarios considered.

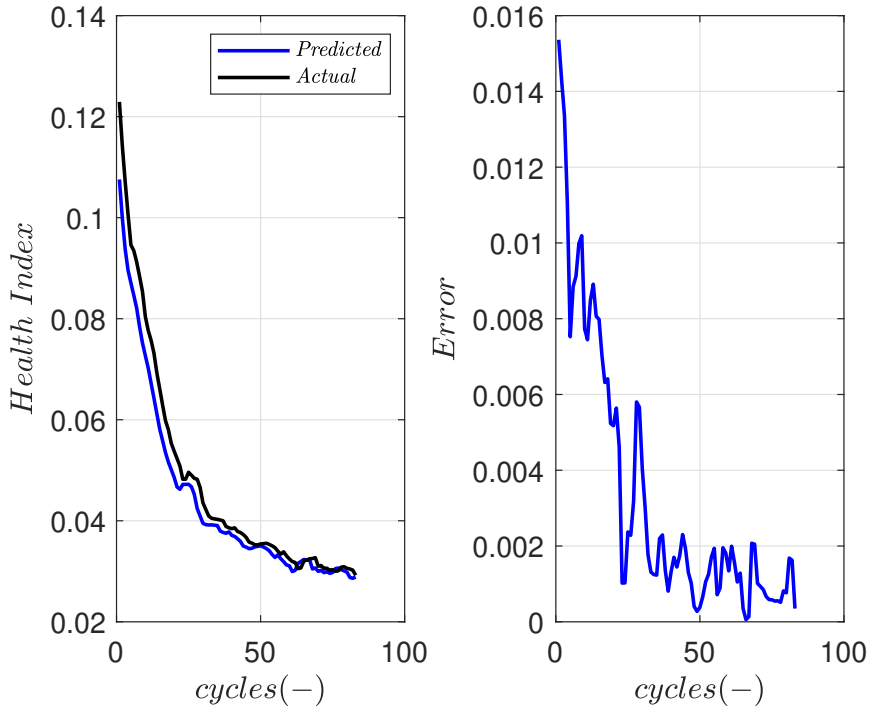

Figure 5.9: Predicted and real health index with error at each cycle..

First, the model is used for RUL prediction of the IGBT2 itself and a more realistic prediction on a different device, the IGBT1. Fig. 5.9 depicts the real and the estimated health index, whose error at each prognostic time instant is quantified with the process noise in a hyperbox for propagation, performed for each test scenario. The final uncertainty set at each prognostic time differs in width which depends on the initial uncertainty set and the duration of the EOL. As evident from Fig 5.11, the width of the uncertainty set generally decreases as more data are available for a better prediction by the algorithm. That is because the model becomes better as more data is available for training and thus fewer uncertainties in the prediction stage. Considering that unknown future conditions constitute uncertainties, the farther away from the EOL, the bigger the size of the interval sets. As expected, the magnitude of prediction error is greater in RUL prediction of the IGBT1, therefore the uncertainty set is wider than the self-test case as shown in Fig.5.12. The convergence of the sets from both scenarios shows a desirable property of the algorithm.

5.8 Conclusions

This chapter presented a novel data-driven prognostics approach based on the evolving granular fuzzy models denominated EEFIG for IGBTs. The EEFIG is able to learn degradation processes from the data stream adapting the parameters of the degradation process representation and modifying its structure by means of granule creation for representing novel stages of the degradation

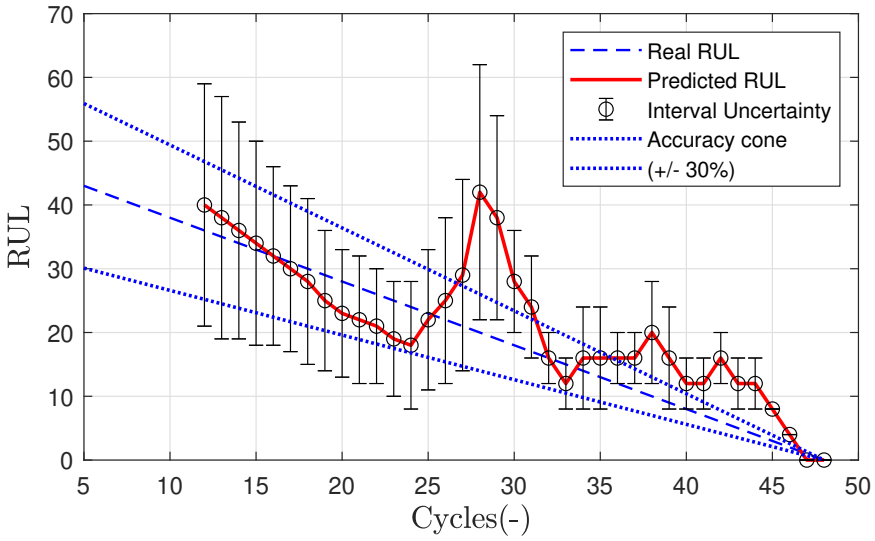

Figure 5.10: RUL prediction and uncertainty set description for the IGBT2 with parameters obtained for the test dataset with data from the IGBT2.

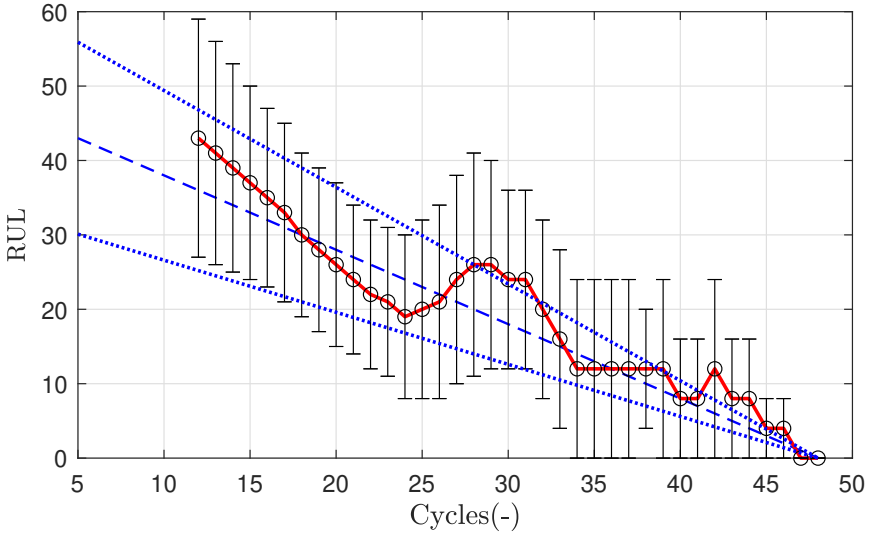

Figure 5.11: RUL prediction and uncertainty set description for IGBT1 with parameters obtained for the test dataset with data from the IGBT2.

process. The results indicate that the application of EEFIG for data-driven prognostics of IGBTs is promising, mainly due to its interpretability features. To tackle the inevitable presence of uncertainty in prognostics a novel set-based quantification and propagation for data-based prognostics, enabled by set-membership theory is proposed. The methodology proves its merits as easy to employ with reasonable uncertainty description. For future research, more complicated geometric

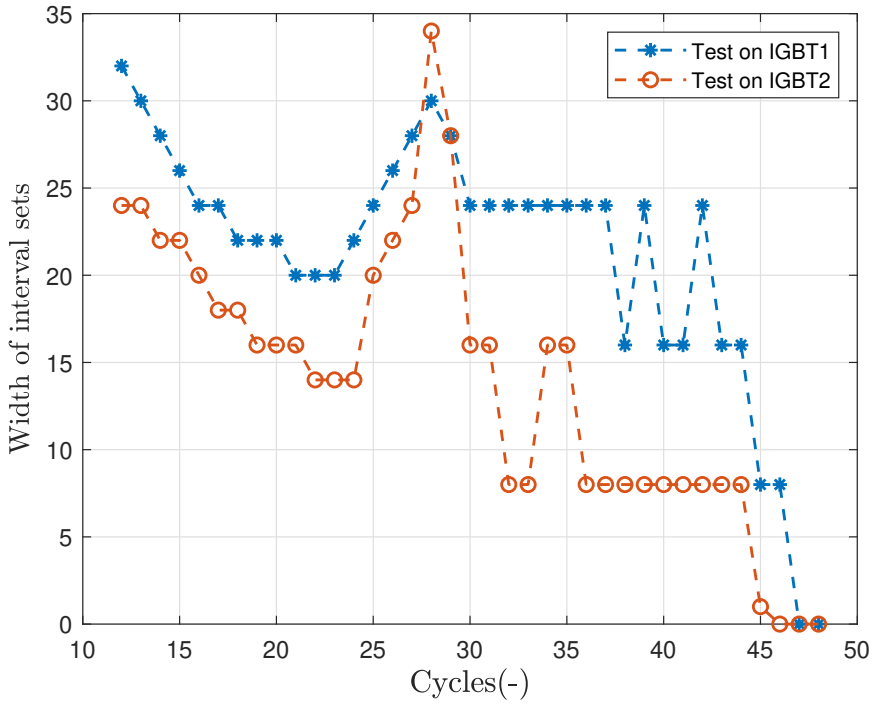

Figure 5.12: Width of uncertainty set at each RUL prediction cycle.

options such as zonotopes will be used for less conservative results. It would also be interesting to have a comparative analysis with different uncertainty quantification methods using the metrics as proposed in Saxena et al. (2017). The methodology will also be extended to other data-driven techniques such as deep learning.

Chapter 6

Reliability-Aware Zonotopic Tubed-Based MPC Of A DWN

The content of this chapter is based on the following works:

- Khoury et al. (2022d) Khoury, B., Nejjari, F., and Puig, V. (2022d). Reliability–aware zonotopic tube–based model predictive control of a drinking water network. *Int. J. Appl. Math. Comput. Sci.*, 32(2), 197–211. doi: 10.34768/amcs-2022-0015. URL `https://doi.org/10.34768/amcs-2022-0015`.

- Boutros et al. (2020) Boutros, K., Puig, V., and Nejjari, F. (2020). Robust economic model predictive control of water transport networks. In *28th Mediterranean Conference on Control and Automation, MED 2020, Saint-Raphaël, France, September 15-18, 2020*, 121–126. IEEE. doi: 10.1109/MED48518.2020.9183029. URL `https://doi.org/10.1109/MED48518.2020.9183029`.

For reliability modelling of interconnected components, there exist methods based on statistical inferences that present desirable mathematical representation of such stochastic processes. Popular amongst them are the Markov chain process, Stochastic Petri Nets and the use of Bayesian networks. Bayesian networks are by far the most common method applied in literature mainly due to the fact that Markov chains leads to combinatorial explosions of the number of states required when the number of model components increases. This makes such a method undesirable for evaluating the cumulative reliability of complex large networks such as a DWN, which contains many interacting components (Zeller and Montrone, 2018). Also since Stochastic Petri Net depends on Monte Carlo simulations, it may demand massive simulations for very low probability evaluations (Philippe and Lionel, 2006). Therefore, for reliability tests on a complex interconnected system of a power network, (Haghifam, 2015) opted for Bayesian networks leading to improved system efficiency evaluations as compared to other methods. (Philippe and Lionel, 2006) goes a step further by applying the concept of a Dynamical Object Oriented Bayesian Networks (DOOBN) modelling on a not so complex system, a water heater process. Comparison with

a Markov chain method by the authors shows that DOOBN yields good results for reliability evaluation, which is also deemed to be more compact and readable than Markov chains.

Model-based controllers such as MPC offer a suitable platform to include in its multi-objective optimization framework, a reliability index or/and reliability constraint function with the purpose of alleviating degradation against other competing criterion. Recently, the concept of incorporating directly an economic stage cost of an industrial processes in an MPC design termed economic MPC (eMPC) has garnered interest. This procedure involves an update of the generic cost function which normally involves tracking a set-point to one which explicitly involves economic terms such as energy, cost of production etc. eMPC allows an improvement during transients and the ability to manipulate control variables to satisfy various economic requirements (Müller et al., 2013). eMPC in the area of water supply has been extensively studied with numerous papers to that effect (e.g. (Cembrano et al., 2011b); (Wang et al., 2017a)). As the name suggests, the formulated control problem constituted by economic variables (e.g. cost, price or demand) which are mostly exogenous. Some of these variables are undoubtedly subject to stochastic variations which requires further control design considerations for a suitable operation. For example, and in relation to our case, in the design of an eMPC for a DWN with variable demand as done in (Wang et al., 2017a), a forecast of water demands is required to enable future predictions of states in an MPC optimization loop. But, forecasted demand as a variable is subject to human behaviour which can be described as uncertain at best. Therefore, there is the need to ensure that controllers are built robust considering these design variations, which are inevitable in real life situations. Methods of stochastic MPC (Wang et al., 2017b), the Min-Max Robust formulation (Löfberg, 2003), the tree-based method (Velarde et al., 2016) and other proposed concepts have been successfully applied to problems of uncertainties in MPC.
In this chapter, a robust eMPC that takes into account reliability modelled with Bayesian networks is proposed. The topology of the network showing flow relationships between actuators linked by pipes is utilized in the Bayesian probability formulations. The reliable robust eMPC is applied to a DWN, specifically in the Barcelona Drinking Water Network, considering uncertainties in the forecasted demand. The variations in demands are considered unknown but bounded in zonotopic sets. Zonotopic sets show desirable characteristics of less complexity, flexibility and reliable computation of linear transformation and Minkowski sums compared to other geometric counterparts such as interval or ellipsoidal sets (Le V. and Camacho, 2013). It must be noted that even though a robust MPC (RMPC) is achieved after this procedure, there is a certain degree of robustness for some magnitude of uncertainty beyond which the optimization problem ceases to be feasible.

6.1 Problem formulation and Preliminaries

In this section, a brief description of the selected DWN model and its condensed version will be discussed. Then an account of the primary predictive control for DWNs is given. Finally, as a

precursor to the sequel, some important mathematical preliminaries are introduced.

6.1.1 A general description of a control oriented DWN model

There exist in literature some models of DWNs that seek to capture key dynamics at different levels of a DWN's architecture. There are however, two predominant models that are commonly used in controller designs with numerous successful outcomes. Through graph theory, flow directions of water at network nodes as well as interactions at the tanks leading to a simple flow-based model description of the network is studied in (Grosso et al., 2014), whilst in (Wang et al., 2017b), some considerations are made from both the network's flow and pressure characteristics, specifically taking into account the interactions when flow and hydraulic head equations are considered in the modelling process.

Considering only the transport sub-level, the flow-based model offers an easier option to work with, largely due to its linearity but fails to capture key pressure dynamics which is important to present a complete mathematical behaviour of the network. Inclusion of pressure in the DWN dynamics introduces non-linearity from the pressure-flow affine equality equation into the optimization problem's constraints formulation resulting in a non-convex problem. Some works have been successful in designing nonlinear MPC (Wang et al., 2017b) for the control of these nonlinear models, whilst (Wang et al., 2018a) considers nonlinear constraints relaxation to produce a set of linear inequality constraints for a linear eMPC formulation. Despite its complexity, the nonlinear pressure-flow model offers a more realistic case to work with. The purpose of this chapter is primarily to illustrate the ability of a control law to enhance the reliability of DWNs whilst considering the real life scenario of demand uncertainties via a set-based method (zonotope) of robust MPC, henceforth the comparatively less complex flow based model will be used.

In (Puig et al., 2015), a flow-based model of the Barcelona water network is presented, which has been extensively used in literature, primarily for control design purposes. Basic relationships between elements considering mass balance at tanks and equilibrium of flow directions at nodes, give rise to a discrete-time invariant system as follows:

$$x(k+1) = Ax(k) + B_u u(k) + B_d d(k), \tag{6.1a}$$

$$0 = E_u u(k) + E_d d(k). \tag{6.1b}$$

where $x(k) \in \mathbb{R}_+^{n_x}$ is the vector of system states, denoting tank volumes at each time instant k. $u(k)$ $\in \mathbb{R}^{n_u}$ denotes the manipulated input from actuators affecting changes in states in combination with the non-negative model disturbance $d(k) \in {\mathbb{R}_+}^{n_d}$, the consumer demand. A, B_u, B_d, E_u and E_d are time-invariant matrices of suitable dimensions. From (6.1b), it can be inferred that the control variable $u(k)$ does not take its value from $\mathbb{R}^{n_u}$ but in a linear variety. This inference enables an affine parameterisation of the control variables in terms of a minimum set of disturbance, map-

ping the control problem to a space with a smaller decision vector and with less computational burden due to the elimination of the equality constraint (6.1b).

Proposition 1 (Wang et al., 2017a): Considering that there are more control variables than algebraic equations (i.e. $n_q < n_u$), the matrix E_u in (6.1b) has a maximal rank. Assuming that the equation has a solution, it can be expressed in a reduced staggered form using the Gauss-Jordan elimination.

From Preposition 1, the control variable is parameterized such that:

$$u(k) = \tilde{P}\tilde{M}_1\hat{u}(k) + \tilde{P}\tilde{M}_2 d(k). \tag{6.2}$$

The model can be represented as (6.3) by replacing (6.2) into (6.1a)

$$x(k+1) = Ax(k) + \hat{B}\hat{u}(k) + \hat{B}_d d(k). \tag{6.3}$$

where $\hat{B} = B\tilde{P}\tilde{M}_1$ and $\hat{B}_d = B\tilde{P}\tilde{M}_2 + B_d$.

From (6.2), $\hat{u}(k) \in \mathbb{R}^{n_{\hat{u}}} \subseteq \mathbb{R}^{n_u}$ can be expressed as a function of the demand variable *d(k)* and *u(k)*. Then, an evaluation of the control invariant set from the affine relationship between the input and demand can be developed. Reader is referred to (Wang et al., 2017a) for an in-depth description of how (6.3) is formulated from Proposition 1.

6.1.2 Conventional eMPC as applied to DWNs

The operation of a DWN is such that network elements, active (pumps and valves) or passive (pipes and tanks) interact to satisfy operational network objectives. Thus, the MPC paradigm offers a platform to introduce in a multi-objective framework, a control scheme that encompasses all these objectives whilst respecting system constraints. These control objectives include:

Minimization of operational cost (Economic term): The dominant objective index in the MPC optimization problem is the minimization of the cost of operation in relation to constant water production and variable electricity cost used for pumping water between source and demand. The MPC is designed such that an optimal cost is achieved whilst servicing demand under process constraints. Thus, the function is given as :

$$\mathcal{J}_E(k) = (\alpha_1 + \alpha_2(k))^T u(k), \tag{6.4}$$

where $\alpha_1 \in \mathbb{R}^{n_u}$ and $\alpha_2(k) \in \mathbb{R}^{n_u}$ represent respectively the constant water production costs and variable daily electricity costs. $u(k)$ is the actuator activity at each sample time k.

Guarantee of safe water storage: For operational security, it is imperative to maintain a safe level of water in tanks to ensure a consistent supply of water to demand nodes between two consecutive

time instants of the MPC and also to keep a safe stock of water in the event of any uncertainties related to supply availability. A penalty equal to the sum of the squares of the deviation of the volume in each tank from a predefined safety threshold is therefore posed as:

$$\mathcal{J}_s(k) = \begin{cases} \|x(k) - x_s\|^2 & \text{if } x(k) \leq x_s \\ \\ 0 & \text{otherwise} \end{cases} \tag{6.5}$$

A vector of safety levels of each tank is denoted by x_s. The cost function is reformulated as (6.6) with the inclusion of a slack variable $\varepsilon(k)$ and an introduction of constraint (6.7) in a bid to circumvent the occurrence of a problematic piece-wise affine cost

$$\mathcal{J}_s(k) = \|\varepsilon(k)\|^2, \tag{6.6}$$

$$x(k) \geq x_s - \varepsilon(k) \tag{6.7}$$

Penalization of actuator slew rate: For purposes of increasing the lifespan of actuators (pumps and valves) which is generic in MPC formulations, the deviation between two consecutive time instants of control actions is penalised for a smooth operation of control :

$$\mathcal{J}_{\triangle U}(k) = ||\triangle u(k)||^2, \tag{6.8}$$

where $\triangle u(k) = u(k) - u(k-1)$.
The volume of water in the tanks, $x(k)$ and the actuator actions, $u(k)$ are bounded in compact polyhedral sets $\mathbb{U}$ and $\mathbb{X}$ defined by

$$x(k) \in \mathbb{X} = \{x(k) \in \mathbb{R}^{n_x} | \underline{x} \leq x(k) \leq \overline{x}\} \tag{6.9a}$$

$$u(k) \in \mathbb{U} = \{u(k) \in \mathbb{R}^{n_u} | \underline{u} \leq u(k) \leq \overline{u}\} \tag{6.9b}$$

With the aforementioned objectives and constraints, a finite horizon optimal control problem which minimizes a cost

$$\mathcal{L}(k, \hat{u}, x) = \Lambda_1 \mathcal{J}_s(k) + \Lambda_2 \mathcal{J}_{\triangle \hat{U}}(k) + \Lambda_3 \mathcal{J}_E(k) \tag{6.10}$$

where $\mathcal{L}(k, \hat{u}(k), x(k)) \in \mathbb{N}_+ \times \mathbb{R}^{n_{\hat{u}}} \times \mathbb{R}^{n_x} \rightarrow \mathbb{R}_+$ is formulated taking into account that Λ_1, Λ_2 and Λ_3 ($\Lambda_i > 0 \ \forall i$) are design weights for each objective criterion that can be tuned following the procedure presented in (Toro et al., 2011). Thus, at each time instant k, considering the condensed dynamic equation (6.3), the optimization problem to be solved is:

$$
\begin{aligned}
&\min_{\hat{\mathbf{u}}(k),\mathbf{x}(k)} \sum_{i=0}^{N_p-1} \mathcal{L}(k, \hat{u}(k), x(k)) \\
&\text{subject to} \\
&x(i+1|k) = Ax(i|k) + \hat{B}\hat{u}(i|k) + \hat{B}_d d(i|k), \\
&\hat{u}(i|k) \subseteq \mathcal{U}(i|k), \\
&x(i+1|k) \subseteq \mathbb{X}, \\
&x(i|k) \geq x_s - \varepsilon(i|k),
\end{aligned} \tag{6.11}
$$

Remark 1: Considering that the control variable $\hat{u} \in \mathcal{U} \subseteq \mathbb{U}$ is mapped to a reduced space from Proposition 1. For the inclusion of an input constraint, a novel time-varying input domain set $\mathcal{U}(k+i|k)$ is introduced such that

$$\{\hat{u}(k) \in \mathbb{R}^{n_{\hat{u}}} | \underline{u} - \tilde{P}\tilde{M}_2 d(k) \leq \tilde{P}\tilde{M}_1 \hat{u}(k) \leq \overline{u} - \tilde{P}\tilde{M}_2 d(k)\}$$

under the assumption that the optimization problem (6.11) is feasible, i.e., there exists a non-empty solution given by the optimal sequence of control inputs $(\hat{u}^*(0), \hat{u}^*(1), ..., \hat{u}^*(N_p-1))$, where N_p is the prediction horizon. From the principles of receding horizon, only the first control action $\hat{u}^*(0|k)$ of the sequence N_p values obtained from the solution of the MPC optimization problem is applied to the plant,

$$\hat{u}(k) = \hat{u}^*(0|k),$$

disregarding the rest of control actions. At the next time instant k, the optimization problem is solved again using the current measurements of states and disturbances, with the most recent forecast of the latter over the next future horizon.

Definition 1: (*Robust Positive Invariant (RPI) set*): Assuming a solution $\varphi(x_0, k)$ exists for a discrete time-invariant system : $x(k+1) = Ax(k) + Bu(k) + w(k), \forall w(k) \in \mathbb{W}$. $\Omega \subseteq \mathbb{X}$ is defined as an RPI set if $\varphi(x_0, k) \in \Omega \; \forall x_0 \in \Omega$ for all $k = \mathbb{N}_{[1,..,\infty)}$, such that $(A+BK)\Omega \oplus \mathbb{W} \subseteq \Omega$.

Definition 2: *(minimal RPI (mRPI) set:)* a mRPI, Ω_∞ set is a set contained in all possible RPI sets of a system as described in Definition 2.

6.2 Tube-based MPC

The fundamental intent of designing a robust MPC controller must be such that the designed controller satisfies the tenets of *robust stability and recursive feasibility*, *robust constraint satisfaction* and *robust performance* for all realization of a system behaviour Σ = *f(k, x(k), u(k), d(k))*, subjected to

unaccounted variations of function variables; in essence, the system must operate at near normal in the event of some extent of uncertainties. Assuming an additive demand uncertainty in (6.3), the effects of unknown uncertainties on the exogenous known demand variable $d(k)$, $\Delta d(k) \subseteq \delta\mathbb{D}$ results in a subsequent variation in the state $\Delta x(k) \subseteq \delta\mathbb{X}$ and input variables $\Delta u(k) \subseteq \delta\mathbb{U}$ as evidenced from the affine relationships of the variables in equations (6.2) and (6.3). These variations can result in feasibility as well as stability issues. The model variables can therefore be thought of as a composition of an uncertainty *'free'* and an unknown uncertain component dependent on the demand uncertainty, with the latter involving a realization of variables at each time instant from bounded uncertainty sets ($\delta\mathbb{X}$, $\delta\mathbb{U}$, $\delta\mathbb{D}$) with the assumption that the uncertain demand is unknown but bounded. State and input uncertainty sets ($\delta\mathbb{X}$, $\delta\mathbb{U}$) are accordingly described as zonotopes generated from the known zonotopic bounded set of the demand uncertainty $\delta\mathbb{D}$. RPI sets are subsequently utilized in the tightening of original state and input constraints. Also considering that in the presence of uncertainty, asymptotic stability to an equilibrium point cannot be achieved like the nominal case, robust asymptotic stability is guaranteed with a terminal set Ω_∞. Ω_∞ presents a suitable region of attraction for the perturbed system ensuring stability and recursive feasibility.

Assumption 1. *The states $x(k)$ and demands $d(k)$ are considered known at each time instant k and the pair (A,$\hat{B}$) is controllable.*

$\delta\mathbb{D}(k)$ is generated from a symmetric interval set considering bounded demand uncertainty under additive uncertainty assumptions at each time instant k such that $\delta d(k)_l \in$ [-$\delta d(k)_l$, $\delta d(k)_l$], where l denotes a particular demand node in the network. The description of the set $\delta\mathbb{D}(k)$ is chosen appropriately to ensure that $\delta\mathbb{X}(k) \subset interior(\mathbb{X})$ and $\delta\mathbb{U}(k) \subset interior(\mathbb{U})$ (Mayne et al., 2005). The uncertain set $\delta\mathbb{D}(k)$ can therefore be represented in a zonotopic form as:

$$\delta\mathbb{D}(k) \triangleq [0]^{n_d} \oplus H_d(k)B^{n_d}. \tag{6.12}$$

where $[0]^{n_d}$ is a column vector of dimension n_d (n_d is the number of demand nodes), considered as the center the zonotope and $H_d(k)$ is a time varying diagonal matrix of the generators representing the bounds of variations at each demand node *j* at each time instant $k \in \mathbb{N}_{\geq 0}$: B^{n_d}; $B = [-1, 1]$. Consider $\tilde{x}$, $\tilde{\hat{u}}$ and $\tilde{d}$ as the real dynamic states, inputs and demand, respectively. Taking into account the uncertainty effects, appropriate decomposition of model variables are therefore given as: $\tilde{x} = x + \Delta x$, $\tilde{\hat{u}} = \hat{u} + \Delta\hat{u}$ and $\tilde{d} = d + \Delta d$.
$\Delta(.)$ is the uncertain component of each variable. The DWN model considering uncertainty in the demand variable is therefore given as from (6.2) and (6.3) as:

$$\tilde{x}(k+1) \triangleq A\tilde{x}(k) + \hat{B}\tilde{\hat{u}}(k) + \hat{B}_d\tilde{d}(k), \tag{6.13a}$$

$$0 \triangleq E_u\tilde{\hat{u}}(k) + E_d\tilde{d}(k). \tag{6.13b}$$

Nominal states and inputs, $x \in {\mathbb{R}_+}^{n_x}$, $\hat{u} \in {\mathbb{R}_+}^{n_u}$ are considered bounded in a compact polyhedron $\mathbb{X}$ and $\mathbb{U}$, containing the origin in their interiors, with $\hat{u} \subseteq \mathbb{U}$ and $x \subseteq \mathbb{X}$. In the presence of uncertainty, it is desirable to generate a tube of trajectories, meaning a sequence of *RPI* reachable sets such that for every transition of states and inputs of the nominal system, the resultant states and inputs after the effect of uncertainty remain in a closed and bounded set of the system constraints $(\mathbb{X}, \mathbb{U})$ as well as is asymptotically stable to an approximate equilibrium set $\tilde{\Omega}$; with RPI sets ($\delta\mathbb{X}(k) \subseteq \mathbb{X}, \delta\mathbb{U}(k) \subseteq \mathbb{U}, \tilde{\Omega} \subset \mathbb{X}$). A state RPI tube, $\tilde{X} = \{\tilde{X}_0, \tilde{X}_1, ..., \tilde{X}_N\}, \forall\ \tilde{X}_k = x(k) \oplus \delta\mathbb{X}(k)$ and an accompanying control tube $\tilde{U} = \{\tilde{U}_0, \tilde{U}_1, ..., \tilde{U}_N\}, \forall\ \tilde{U}_k = \hat{u}(k) \oplus \delta\mathbb{U}(k)$, is constructed online considering the bounded uncertainty description and the center of measured demands at k. $x(k)$ and $\hat{u}(k)$ are centers of the respective propagated state and control RPI tubes. The mismatch between nominal and real states influenced by uncertainties are mitigated by a local feedback controller K, in our case an LQR controller, such that the selection of this feedback gain, K satisfies a system with the assumption that $\tilde{d}(k) = 0$;

$$\Delta x(k+1) \triangleq (A + \hat{B}K)\Delta x(k). \tag{6.14}$$

with $\Delta x(k) \subseteq \delta\mathbb{X}(k)$. The local controller ensures that the deviation of the system dynamics in the closed-loop with $(A+\hat{B}K)$ is asymptotically stable. The primary aim is to have an optimal control problem, which keeps trajectories around the neighbourhood of the nominal optimal trajectory in the presence of uncertainties, for $\tilde{x}(0) \in x(0) + \delta\mathbb{X}$, therefore minimizing the spread of trajectories.

Remark 2: *Considering that $(A + \hat{B}K)$ is strictly stable and $\tilde{x} = x + \Delta x$, with an uncertain dynamic part $\Delta x(k+1) \triangleq (A + \hat{B}K)\Delta x(k) + \hat{B}_d\Delta d(k)$. Since $\delta\mathbb{X}$ is an RPI, $(A + \hat{B}K)\delta\mathbb{X} \oplus \hat{B}_d\delta\mathbb{D} \subseteq \delta\mathbb{X} \subset \mathbb{X}$, then it can be inferred that the transition of states from one time instant to another with any control law $\pi(u(x))$ depends on the dynamics of the centers, $x(k+1) = Ax(k) + \hat{B}\hat{u}(k) + \hat{B}_d d(k)$.*

6.2.1 Online computation of zonotopic reachable sets

The feedback gain K is computed and kept constant at each time instant k throughout the prediction horizon of the MPC controller to minimize the deviation of the perturbed state and ensures asymptotic stability to a predefined terminal set. An optimal local controller for state error minimization,

$$J_{[\tilde{\hat{u}}_0,.,\tilde{\hat{u}}_\infty)} = \sum_{i=0}^{\infty} (\tilde{x}(k) - x(k))^T Q(\tilde{x}(k) - x(k)) + \tilde{\hat{u}}(k)^T R\tilde{\hat{u}}(k) \tag{6.15}$$

where Q is semi-positive definite and R, a positive definite matrices of appropriate dimensions is proposed. $\tilde{x}(k)$ is the real state at time k from the plant under uncertainty and $\tilde{\hat{u}}$, the actual inputs, with $x(k)$ as the nominal state prediction from the MPC at time instant k. From the real state, $\tilde{x}(k)$ (i.e. $\tilde{x}(k) = x(k) + \Delta x(k)$), the uncertain dynamic part is:
$\Delta x(k+1) \triangleq (A + \hat{B}K)\Delta x(k) + \hat{B}_d\Delta d(k)$,

where $\Delta\hat{u} = K\Delta x$.
From the uncertain component, a corresponding $N_p \in \mathbb{N}_{>0}$ length of tube is computed at every k, where N_p is the selected prediction horizon of the MPC controller. Therefore, a set $\delta\mathbb{X}$ from which the realization of the error Δx assuming that initial deviation, $\Delta x(0) = 0$ can be described as:

$$\delta\mathbb{X}(k+i) \subseteq \bigoplus_{j=1}^{i} (A + \hat{B}K)^{i-j} \hat{B}_d \delta\mathbb{D}(i). \tag{6.16}$$

Given that $\delta\mathbb{D}(i) = 0 \oplus H_d(i)B^{nd}$, and from Properties 1 and 2 of zonotopes from 3, it therefore follows that:

$$\delta\mathbb{X}(k+i) \subseteq 0 \oplus \Psi_{[1,i]}(i)B^{n_d}, \tag{6.17}$$

$$\Psi_{[1,i]}(i) = \bigoplus_{j=1}^{i} (A + \hat{B}K)^{i-j} \hat{B}_d H_d(i). \tag{6.18}$$

The control variable $\tilde{\hat{u}}$ at each time instant can be described as:

$$\tilde{\hat{u}}_k = \hat{u}_k + K\Delta x_k, \tag{6.19}$$

where $\hat{u}(k)$ is the certain control variable obtained from the nominal MPC at time instant k. From equation (6.2), and under decomposition into certain and uncertain parts, considering that the actual control variable $\tilde{\hat{u}}_k$, $\tilde{\hat{u}} \in \delta\mathbb{U}$, the uncertain control RPI set is given as:

$$\delta\mathbb{U}(k+i) \subseteq \tilde{P}\tilde{M}_1 K \delta\mathbb{X}(k+i) \oplus \tilde{P}\tilde{M}_2 \delta\mathbb{D}(k+i), \tag{6.20}$$

The sequence of cross-sections of the control tube can therefore be described in a zonotopic form as:

$$\delta\mathbb{U}(k+i) \subseteq 0 \oplus [\tilde{P}\tilde{M}_1 K \Psi_{[1,i]}(K+i), \tilde{P}\tilde{M}_2 H_d(k+i)]B^{2n_d}. \tag{6.21}$$

6.2.2 Terminal state constraint set

For robust stability and recursive feasibility, a terminal constraint set is formulated considering a mRPI as done in (Raković et al., 2005). A terminal mRPI set $\tilde{\Omega}$, which is compact and convex is constructed as an outer approximation of the exact equilibrium state set

$$\Omega_\infty \triangleq \bigoplus_{j=0}^{\infty} (A + \hat{B}K)^j \hat{B}_d \delta\mathbb{D}, \tag{6.22}$$

where $\Omega_\infty \subseteq \tilde{\Omega}$. $(A + \hat{B}K) = \hat{A}$ and $\hat{B}_d\delta\mathbb{D} \subseteq \mathcal{W}$, under the assumption that $\hat{A}$ is strictly stable. An outer set approximation of Ω_∞ is defined if there exist a certain $k \in \mathbb{N}_{>0}$ such that, $(\hat{A})^k \mathcal{W} \subseteq \alpha\mathcal{W}$, $\forall\alpha = [0, 1)$. The infinite Minkowski sum of sets (6.22) under strict stability conditions ensures that

convergence is guaranteed. Considering the infinite Minkowski sum,

$$\bigoplus_{j=0}^{\infty}(\hat{A})^j\mathcal{W} \subseteq \bigoplus_{j=0}^{k-1}(\hat{A})^j\mathcal{W} \oplus \bigoplus_{j=k}^{2k-1}(\hat{A})^j\mathcal{W} \oplus \bigoplus_{j=2k}^{3k-1}(\hat{A})^j\mathcal{W} \oplus ..., \tag{6.23}$$

(6.23) can be simplified to achieve the condition $(\hat{A})^k\ \mathcal{W} \subseteq \alpha\mathcal{W}$ as follows:

$$\bigoplus_{j=0}^{\infty}(\hat{A})^j\mathcal{W} \subseteq \bigoplus_{j=0}^{k-1}(\hat{A})^j\mathcal{W} \oplus \bigoplus_{j=0}^{k-1}(\hat{A})^j(\hat{A})^k\mathcal{W} \oplus$$

$$\bigoplus_{j=0}^{k-1}(\hat{A})^j(\hat{A})^{2k}\mathcal{W} \oplus ..... \tag{6.24}$$

From $(\hat{A})^k\mathcal{W} \subseteq \alpha\mathcal{W}$, it can be stated that $(\hat{A})^{nk}\mathcal{W} \subseteq \alpha^n\mathcal{W}$. $\bigoplus_{j=0}^{k-1}(\hat{A})^j\mathcal{W}$ is thus convex and compact since $\delta\mathbb{D}$ is assumed to hold the same properties. Assigning $\bigoplus_{j=0}^{k-1}(\hat{A})^j\mathcal{W}$ as ζ. Ω_∞ is approximated from a truncation of (6.24) as:

$$\tilde{\Omega} \subseteq (1 + \alpha + \alpha^2 + ...)\zeta, \tag{6.25}$$

which results in an approximated set:

$$\tilde{\Omega} \subseteq \frac{1}{1-\alpha}\zeta. \tag{6.26}$$

The set in a zonotopic form is given as:

$$\tilde{\Omega} \subseteq 0 \oplus (1-\alpha)^{-1}\Psi_{[0,k]}B^{n_d}. \tag{6.27}$$

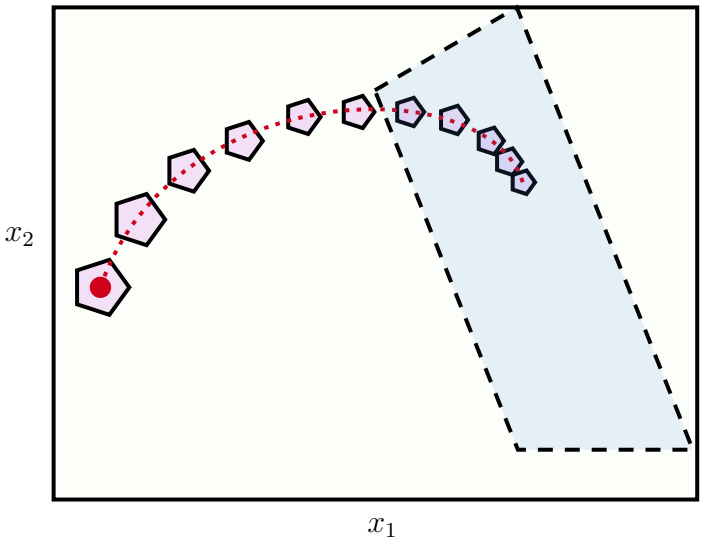

Figure 6.1: RMPC's state transition in 2D, showing the constraint set (outer box), the *mRPI*(inner box) and *RPIs* (interior polygons)

where

$$\Psi_{[0,k]} = \bigoplus_{j=0}^{k-1} (\hat{A})^j \hat{B}_d \hat{H}_d.$$

$\hat{H}_d$ is taken as the worst case demand uncertainty in reference to the demand profile of each node. The size of the set is therefore dependent on the design parameter α, the description of the uncertainty set $\delta\mathbb{D}$ and the appropriate selection of k.

Remark 3: The constructed approximated mRPI approaches the actual mRPI if for a significantly small $\alpha \in (0, 1]$, there exists a finite k chosen large enough, such that $(\hat{A})^k \mathcal{W} \subseteq \alpha \mathcal{W}$ holds. Appropriate selection of α and k is discussed in (Raković et al., 2005).
The constructed sequence of uncertain zonotopic sets and the terminal set will then be used in the the design of the robust eMPC by considering only alterations in the constraints and inclusion of the terminal set.

6.3 Evaluation of a DWN reliability

Definition 4: Reliability is defined as the ability of an item to perform a required function, under given environmental and operational conditions and for a stated period of time (ISO8402).

Evaluating the reliability of a system is a complex stochastic undertaking that calls for the application of appropriate statistical inference techniques in order to model such a phenomenon (Cai et al., 2020). In this section, the concept of Bayesian Networks (BN), fundamentally based on the structure of the DWN using graph theory, considering conditional dependencies between graph nodes (i.e. actuators in the network) related through arcs (flow in pipes) is considered.

For a BN parameter, we make use of a quantitative index of failure rate $\lambda(t)$ which assists to evaluate individual reliabilities of components, that is the probability of each component to function for a specified time. This information is then used in the broad BN modelling according to the structure of the network. Keeping in mind that the ultimate goal is to inculcate the reliability in the performance index and the constraints, a resultant dynamic nonlinear network reliability model from a dynamic BN is represented in a pseudo-linear form, avoiding any additional computational burden, basically escaping a laborious nonconvex problem.

6.3.1 Reliability based on component failure rate

Consider a continuously distributed random variable T denoting a time to failure having a distribution function $F(t)$, where $F(t)$ signifies the probability of a component to fail within the time interval $(0, t]$ (Rausand and Hoyland, 2004). Then with an associated probability density function,

$f(t)$, $F(t)$ can be described as:

$$F(t) = P_r(T \leq t) = \int_0^t f(u)\, du,\ \forall t \geq 0, \tag{6.28}$$

Conversely, the reliability of the component $R(t)$ is accordingly represented as the probability of survival in time interval $(0, t]$ and subsequently functioning at t.

$$R(t) = P_r(T \geq t) = 1 - \int_0^t f(u)$$

$$= \int_t^\infty f(u), du\, \forall t \geq 0. \tag{6.29}$$

Similarly, to evaluate the failure rate, the instance of an element functioning at t is considered, such that the probability of failing between the interval $[t, t + \Delta t]$ having survived to t is represented with a conditional probability as :

$$P_r(t < T \leq t + \Delta t | T > t) = \frac{Pr(t < T \leq t + \Delta t)}{Pr(T > t)}$$

$$= \frac{F(t + \Delta t) - F(t)}{R(t)} \tag{6.30}$$

dividing both sides by Δt, and as $\Delta t \to 0$, the failure rate of the component is thus:

$$\lambda(t) = \lim_{\Delta t \to 0} \frac{F(t + \Delta t) - F(t)}{\Delta t} \frac{1}{R(t)} = \frac{f(t)}{R(t)} \tag{6.31}$$

A relationship can therefore be established between the failure rate $\lambda(t)$ and the reliability function $R(t)$ from (6.31) considering the probability density function of the failure distribution in (6.28) as:

$$f(t) = \frac{dF(t)}{dt} = \frac{d(1 - R(t))}{dt} = \frac{-d(R(t))}{dt} \tag{6.32}$$

It follows from the formula of the failure rate (6.31) that:

$$\lambda(t) = \frac{dR(t)}{dt} . \frac{1}{R(t)} = -\frac{d}{dt} \ln R(t) \tag{6.33}$$

Note that $R(0) = 1$, therefore:

$$\int_0^t \lambda(t)\, dt = -\ln R(t) \tag{6.34}$$

$$R(t) = e^{-\int_0^t \lambda(u)\, du} \tag{6.35}$$

where (6.35) provides a relationship between the reliability of a component and the failure rate.

A plethora of methods have been proposed for finding a suitable function for failure rates that

approximately represents a component's functional property decay over time. In this chapter, we consider the effect of loadings on the failure rate as done in (Karimi Pour et al., 2019) and establish a load versus failure rate relationship, such that an exponential function establishing the relationship between each actuator, i-th failure rate and their corresponding loadings is given

$$\lambda_i(t) = \lambda_i^0 e^{(\beta_i u_i(t))} \tag{6.36}$$

where λ_i^0 is the baseline failure rate, $u_i(t)$, the control effort of each actuator and β_i is a constant parameter that depends on the actuator characteristics. Therefore under nominal operating conditions, the reliability is characterized as

$$R_{0,i}(t) = e^{(-\lambda_i^0(t))} \tag{6.37}$$

The equation below therefore holds for the probability of a component avoiding failure between the time interval $(0, t]$ considering the failure rate and the nominal failure rate

$$R_i(t) = R_{0,i} e^{-\int_0^t \lambda_i(u)\, du} \tag{6.38}$$

Consequently, a discrete-time representation, taking into account loading at different time instances, k sampled at T_s is as follows

$$R_i(k) = R_{0,i} e^{(-T_s \sum_{s=0}^{k} \lambda_i(u(s)))} \tag{6.39}$$

6.3.2 The Bayesian Network Theory

Consider the 3-tuple, $B_N = (P, A_B, N_B)$, representing a BN. B_N is therefore a Bayesian network, essentially a Directed Acyclic Graph (DAG) composed of a set of nodes N_B, with corresponding set of arcs, A_B accounting for direct dependencies between nodes. Each node $n_i \in N_B$ is subse-

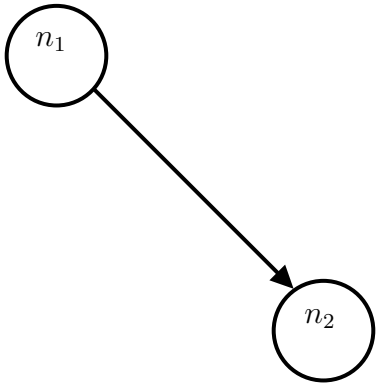

Figure 6.2: Two nodes in a simple acyclic graph,showing direct dependencies between nodes

quently associated with a probability distribution from the set P. From Fig. 6.2, the relationship

between nodes n_1 and n_2 is such that, $(n_1, n_2) \in A_B$, n_1 is therefore defined as the parent of n_2, hence n_2 possesses a direct dependency to n_1. A set of parent nodes of each node n_i in the network is indicated as $P_a(n_i)$. The direct dependencies of each node with its parents $P_a(n_i)$ is consequently computed considering the conditional probability distribution, $P_r(n_i|P_a(n_i))$, $P_a(n_i) \neq \emptyset$.

Assigning a discrete random variable Y_i to each node $n_i \subset N_B$, a finite number of m states set, S^n can be established for each node such that $S^n \triangleq \{s_1^n, s_2^n, ..., s_m^n\}$, under trivial Bayesian assumptions of, $s_i^n \cap s_j^n = \emptyset$, $\forall i \neq j$, $P_r(s_i^n) \geq 0$ and $P_r(\bigcup_{i=1}^{m} s_i^n) = 1$, where $P_r(Y_i = s_i^n)$ is the marginal probability that the state of node n_i is s_i^n. Therefore for an acyclic graph $B_N(P, A_B, N_B)$, $\forall n(N_B) = N$ with designated probability distributions $Pr(Y_1, Y_2, ..Y_N)$, the joint probabilities of the nodes under conditional probability assumptions and chain rule is simplified as:

$$P_r(n_i, n_2, ...n_N) = P_r(n_1) \prod_{i=2}^{N} P_r(n_i|P_a(n_i)) \tag{6.40}$$

where, n_1 is considered a root node, $\therefore P_a(n_1) = \emptyset$. Note that only prior probabilities are assigned to these nodes.

Dynamic Bayesian Network:

The Bayesian representation thus far presented in (6.40) is static, therefore to successfully include the reliability dynamics in the MPC, a temporal dimension that describes the time connection between two time instances of actuator loadings is added, hence an introduction of temporal dependencies in the modelling. For temporal dependencies in BN, the assumption is made that the system is a first order Markov, that is: (1.) Arcs between nodes are located in the same time period between instances or 2 neighbouring ones. (2.) Time homogeneous parameters of conditional probability are time invariant. Henceforth, the transition probability of a random variable X_i of reliability of each nodes $n_i \in N_b$ between two time instances say $k+1$ and k, with two states, F as a failed state and A as active is given as :

$$P_r(X_i(k+1)) = (A|X_i(k) = A) = R_{0,i} e^{(-T_s \sum_{s=0}^{k} \lambda_i(u,k))} \tag{6.41a}$$

$$P_r(X_i(k+1)) = (F|X_i(k) = A) = 1 - R_{0,i} e^{(-T_s \sum_{s=0}^{k} \lambda_i(u,k))} \tag{6.41b}$$

6.3.3 Bayesian network structure modelling of a DWN

The procedure of BN representation of a system primarily depends on the structuring and parameter definition stages, with the later dependent on the acyclic graphical representation of the system under study. The DWN as with its modelling as discussed in 6.1 involves a graphical

representation of actuators as nodes that are linked by unidirectional flow through pipes as arcs, hence an acyclic graph is duly presented. From the graph, based on minimum path sets in the network, that is the set of successful paths from the source to the demand, a resultant series-parallel arrangement is attained for the network reliability model. The BN parameter definition however is defined on the pair of probabilities of the root nodes and the conditional probabilities of nodes and their parents in individual minimum paths of the network. Therefore, the network reliability with the conditions prescribed at a certain time instant k according to the structure of the network is:

$$R_s(k) = 1 - \prod_{j=1}^{s}(1 - \prod_{i \in P_j} R_i(k)) \tag{6.42}$$

where, P_j is a minimum path set and R_i, the reliability of each node in the set considering prior and conditional probabilities.

The reliability term R_i from (6.37) includes exponential terms from the failure rate, introducing nonlinearities. To aid in including the reliability term in the MPC, the log of both sides is taken and subsequently represented in a pseudo-linear form such that:

$$\log(R_s(k)) = \log(\prod_{j=1}^{s}(1 - \prod_{i \in P_j} R_i(k)). \tag{6.43}$$

Assigning

$$(1 - \prod_{i \in P_j} R_i(k))$$

as $\varphi_j(k)$, then

$$\log(R_s(k)) = \sum_{j=1}^{s} \log \varphi_j(k). \tag{6.44}$$

where

$$\log(\varphi_j(k)) = \frac{\log(\varphi_j(k))}{\log(1 - \varphi_j(k))} \sum_{i \in P_j} \log(R_i(k)) \tag{6.45}$$

Thus, with $\frac{\log(\varphi_j(k))}{\log(1-\varphi_j(k))}$ as $\vartheta_j(k)$, the reliability of the network is given as:

$$\log(R_s(k)) = \sum_{i \in P_j}^{s} \vartheta_j(k) \sum_{i \in P_j} \log R_i(k) \tag{6.46}$$

Therefore, considering the DBN formulations in (6.41) and the baseline reliability, the dynamic model is

$$\log(R_s(k+1)) = \log(R_s(k)) + \sum_{i \in P_j}^{s} \vartheta_j(k) \sum_{i \in P_j} \log R_i(k) \tag{6.47}$$

6.4 Reliability Aware eMPC of DWN

In this section, finally the reliability aware Robust control problem, considering all procedures in the preceding sections is discussed. Considering that the reliability model in (6.47) is nonlinear, a quasi-LPV (qLPV) nonlinear representation of the nonlinear model through the embedding of nonlinearities in scheduling parameters $(\theta(k))$ is formulated. The time varying matrices of appropriate dimensions representing the qLPV approximate model are hence:

$$A_r(\theta(k)) = \begin{bmatrix} 1 & \sum_{i\in P_j}^{s} \vartheta_j(k) \\ 0_{n_u\times 1} & \mathbb{I}_{n_u\times n_u} \end{bmatrix},$$

$$B_r(\theta(k)) = \begin{bmatrix} 0_{1\times n_u} \\ -\lambda_i(k).\mathbb{I}_{n_u\times n_u} \end{bmatrix}.$$

where $A(\theta(k)) \in \mathbb{R}^{(n_u+1)\times(n_u+1)}$ and $B(\theta(k)) \in \mathbb{R}^{(n_u+1)\times n_u}$ and with states $x_r = [\log(R_s), \log(R_1), \log(R_2)....\log(R_{n_u})] \in \mathbb{R}^{n_u+1}$. Therefore, the reliability model (6.41) is included as additional dynamics in the constraints with a new performance index for network reliability enhancement, $\mathcal{J}_R$. The MPC is robustified by only updating the constraints considering $\mathbb{U} \oplus \delta\mathbb{U} \subseteq \mathcal{U}$ and $\mathbb{X} \oplus \delta\mathbb{X} \subseteq \mathbb{X}$ and robust asymptotic stability with the terminal set $\tilde{\Omega}$. Thus, a similar complexity to the nominal case. The cost function with the additional term of reliability, $\mathcal{L}(k, \hat{u}, x) \in \mathbb{N}_+ \times \mathbb{R}^{n_{\hat{u}}} \times \mathbb{R}^{n_x} \to \mathbb{R}_+$ is given as :

$$\mathcal{L}(k, \hat{u}, x) = \Lambda_1\mathcal{J}_s(k) + \Lambda_2\mathcal{J}_{\triangle\hat{U}}(k) + \Lambda_3\mathcal{J}_E(k) - \Lambda_4\mathcal{J}_R(k)$$

The reliable ReMPC controller is therefore posed as follows:

$$\begin{aligned}
&\min_{\hat{\mathbf{u}}(k),\mathbf{x}(k),x_r(k)} \sum_{i=0}^{N_p-1} \mathcal{L}(k, \hat{u}(k), x(k)) \\
&\text{subject to} \\
&x(i+1|k) = Ax(i|k) + \hat{B}\hat{u}(i|k) + \hat{B}_d d(i|k), \\
&\hat{u}(i|k) \subseteq \mathcal{U}(i|k) \ominus \square\delta\mathbb{U}(i|k), \\
&x(i+1|k) \subseteq \mathbb{X} \ominus \square\delta\mathbb{X}(i|k), \\
&x(i|k) \geq x_s - \varepsilon(i|k), \\
&x(N_p-1|k) \subseteq \tilde{\Omega}, \\
&x_r(i+1|k) = A_r(\theta(k))x_r(i|k) + B_r(\theta(k))u(i|k) \\
&x_r(i|k) \subseteq (0, 1].
\end{aligned} \tag{6.48}$$

where $\ominus$ is a Pontryagin difference of the sets. From the control parameterization, the control

input to the plant at every time instance k is given by

$$u^*(0|k) = \tilde{P}\tilde{M}_1\hat{u}^*(0|k) + \tilde{P}\tilde{M}_2\tilde{d}(k) + K\Delta x(k). \tag{6.49}$$

where $\tilde{d}(k)$ is the forecasted demand.

6.5 Application Example

To demonstrate the capabilities of the proposed controller, first for robustness, an additive demand uncertainty taken as the variation around the demand profile is considered as shown in Figure.6.4. This scenario of actual demand is assumed on the controller to test its level of robustness. With a prediction horizon of 24 hrs (a day of water supply) and a sampling time of 1hr, the robust MPC optimization problem considering reliability (6.48) is solved with CPLEX® QP solver, on Matlab® R2019b (64 bits) using a PC with an Intel core i7 of 8 GB RAM. An aggregate network of the Barcelona water network, Fig. 6.3 composed of 17 tanks, 61 actuators and 25 demand nodes is used as a case study. Tanks store water during off peak hours and supply water when

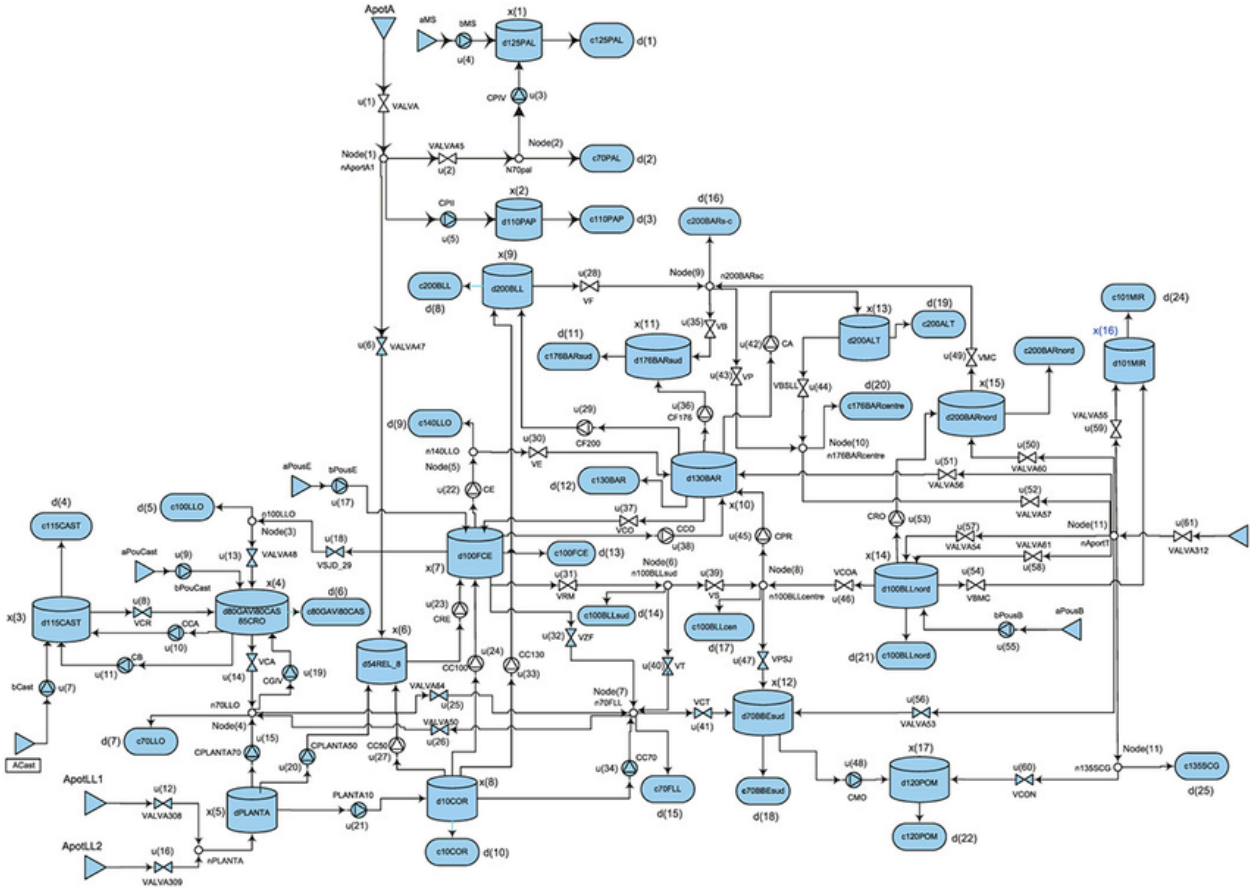

Figure 6.3: Barcelona drinking water network.

demand is at peak or in the occasions of unexpected demand and supply scarcity. This presents a cyclic actuator behaviour in relation to the peak-off peak demand profile. An acyclic graph of the network showing relationships between nodes (actuators) linked by unidirectional pipes (arcs) is used for the network and reliability models. The following assumptions are made (1.) Sources supply required amount of water to demands (2.) The pipes and tanks of the network are always reliable and (3.) The actuators at the start of simulation is perfectly reliable (value of 1).
The minimum paths P_j, which is the set of successful paths from source to demand, through an ensemble of components (pipes, valves and tanks) evaluates the reliability of each path, considering only the actuators. The various paths are then lumped for a network reliability measure, considering their series-parallel arrangement, taking each path as a single entity. Table 6.1 shows some traced minimal paths in the network, there are 607 minimal paths in total. The robustness of

Table 6.1: Examples of Minimum cost paths in the network.

Path	Components sets
1	{aMs, bMs, c125PAL}
2	{AportA, VALVA, VALVA45, c70PAL}
3	{AportA, VALVA, CPII, C110PAP}
4	{AportA, VALVA, VALVA45, CPIV, C125PAL}
.	.
.	.
.	.
607	{AportT, VALVA312, c135SCG}

the designed controller is tested taking Tank 1 (d125PAL) and its associated elements as reference, as shown in the WDN network (Figure 6.3). Tank 1 is directly connected to demand node c125PAL and the nearest supply actuators are CPIV and bMS. These actuators are chosen since they show major changes when there are demand alternations. An eight day demand profile, subdivided into an 80 hour test scenarios is used for the simulations as shown in Figure 6.5. In the first two regions, the extremities of the controller is tested, additive uncertainty is added until the nominal controller ceases to be feasible, thus us labeled as real demand. Thus not shown in the plots, the nominal MPC control is intractable in these regions. The last region is the nominal loading condition. For the actuators' action as shown in Figure 6.7 and 6.6, during the first and second stages of the demand profile, the actuators work to offset the demand variation aided my the tank in Figure 6.8. Since the stored reserve in d125PAL is exhausted in the first region, the actuators function to retain supply to the demand, whilst respecting their own constraints, the feasibility of the control. This is especially evident considering Figure 6.6 (bMS), which shows the controller just maintaining feasibility which was otherwise not the case with the nominal MPC.

In Figure 6.8, the level of water in the tank in the first region is emptied to satisfy the added demand, but the stability and recursive feasibility is preserved due to the RMPC control. The tank starts restocking in the second region and finally converges to the nominal conditions in the third region.

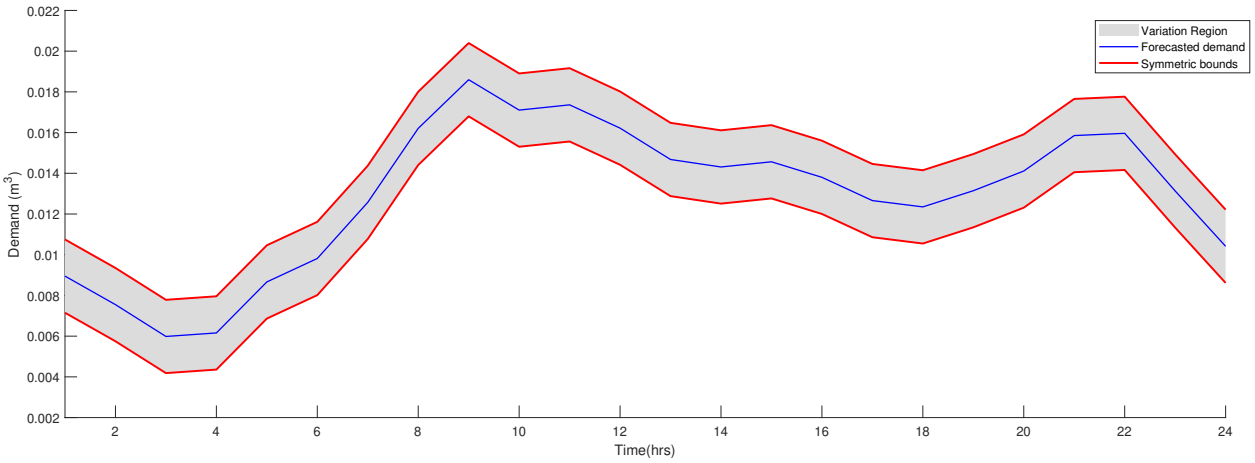

Figure 6.4: A 24 hrs demand profile of node C129PAL with symmetric bounded uncertainty.

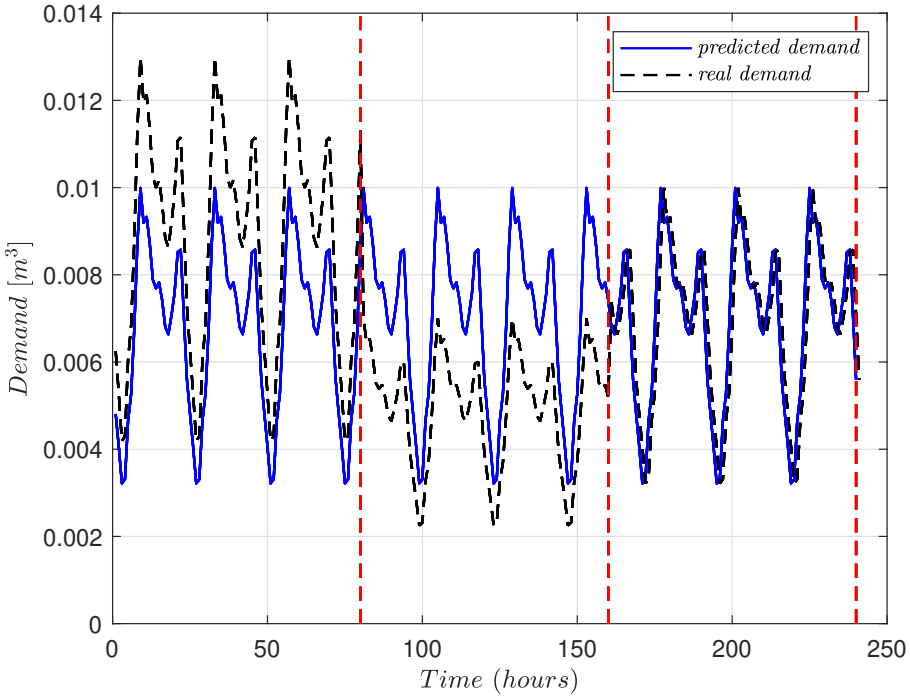

Figure 6.5: 80 hour test scenarios for robust control considering demand node c125PAL.

Figure 6.9 shows that with the inclusion of the reliability cost, not only is there a short term economic gain but also there is a safe operation of the network in the long run. Thus reliable actuators against faults minimizing downtime and maintenance cost. But the improvement of the reliability do not come cheap since the problem presented has two prime conflicting objectives of improving the reliability and minimizing the cost of operations, the short term cost of operation. A set of weights are selected to show the effect of the included reliability index on the cost of oper-

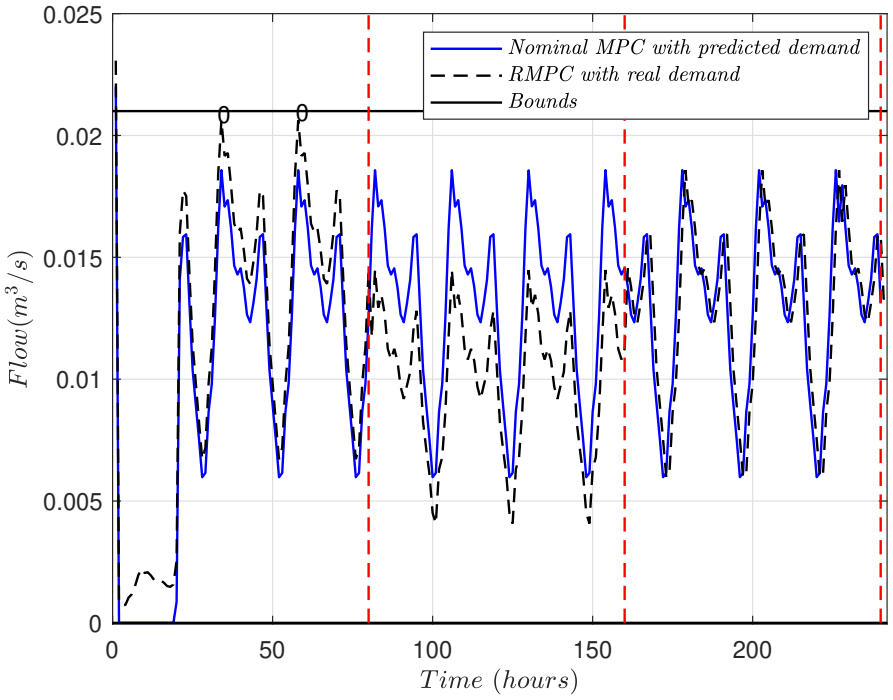

Figure 6.6: Control action of bMS.

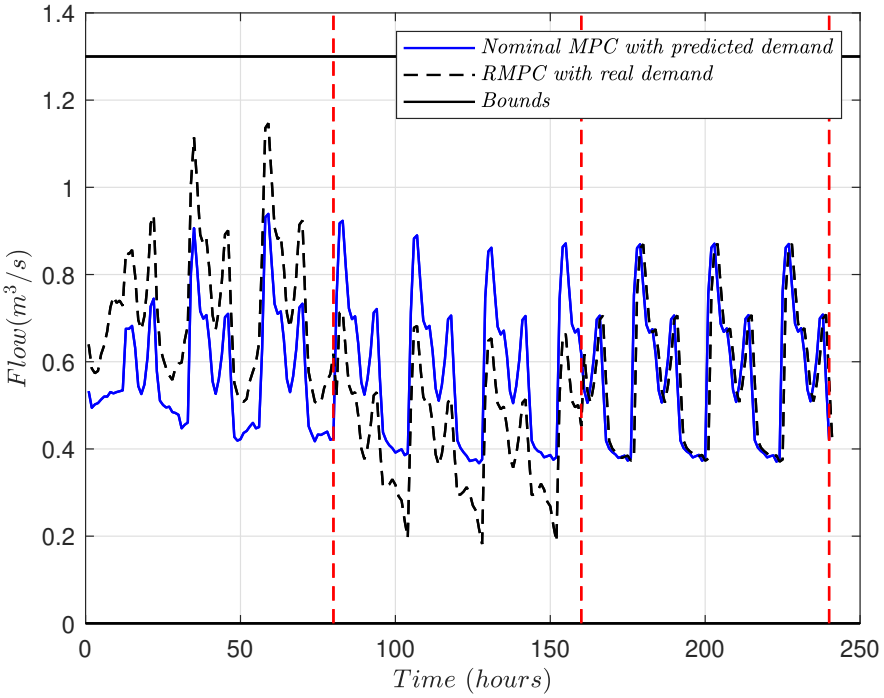

Figure 6.7: Control action of CPIV.

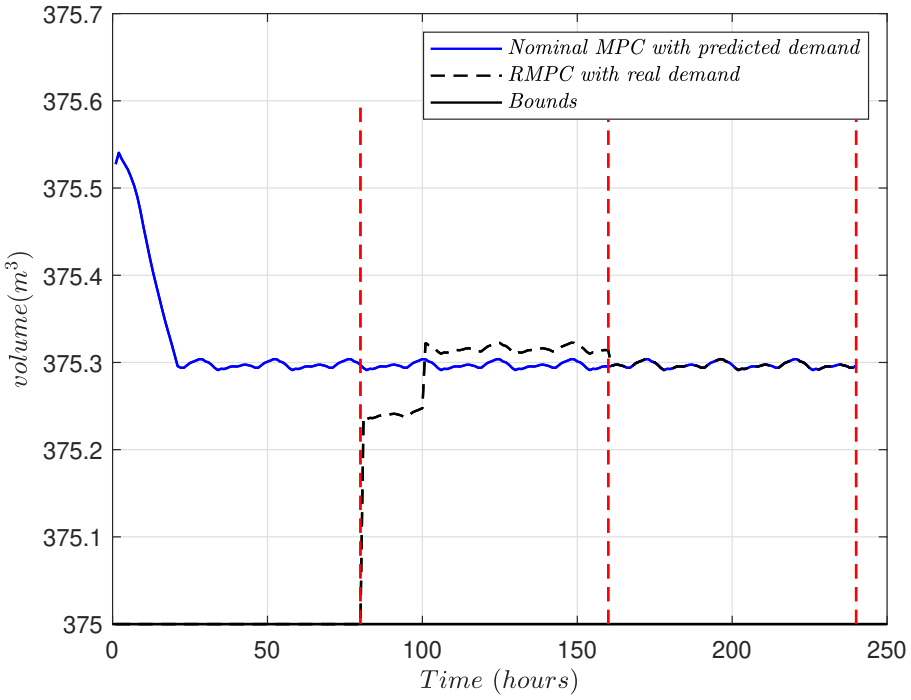

Figure 6.8: Level of Tank d125PAL during robust control test scenarios.

ation presented in a Pareto front presented in Figure 6.11. The selection of appropriate weights is a designer discretion but an optimal solution or point on the front can be sought taking into account the long run economic gain of considering reliability in the control framework. Since the aim of the added reliability index is to achieve long term gain the marginal loss in short term economical gain as shown in Figure 6.10 can be accommodated.

Table 6.2: Cost and reliability after different selection of weights

-	Nominal	Weight 1	Weight 2	Weight 3	Weight 4
Cost	600	587	561	518	400
Reliability	0.965	0.94	0.921	0.9	0.8

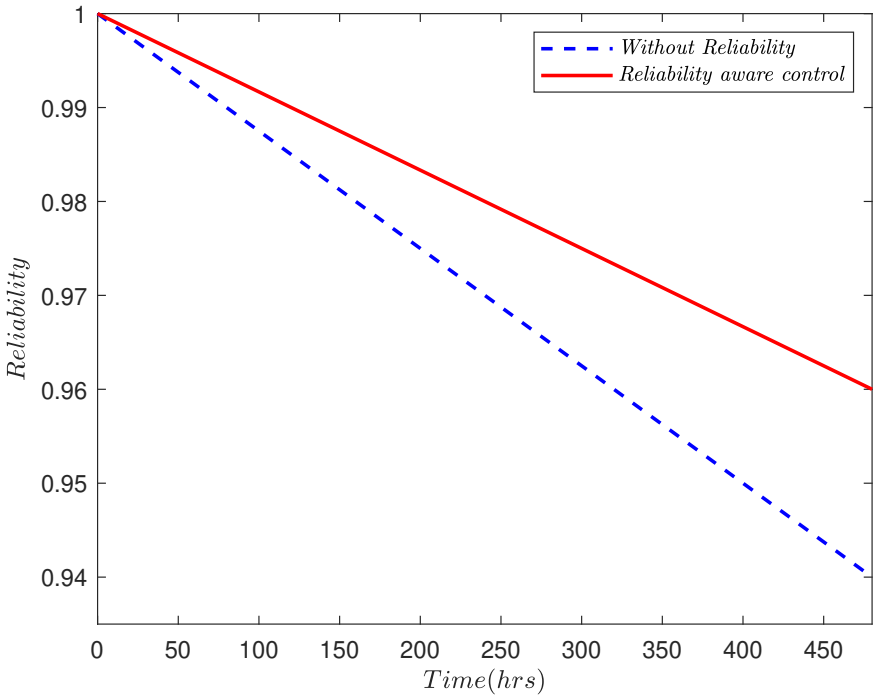

Figure 6.9: Network reliability under different controller configurations.

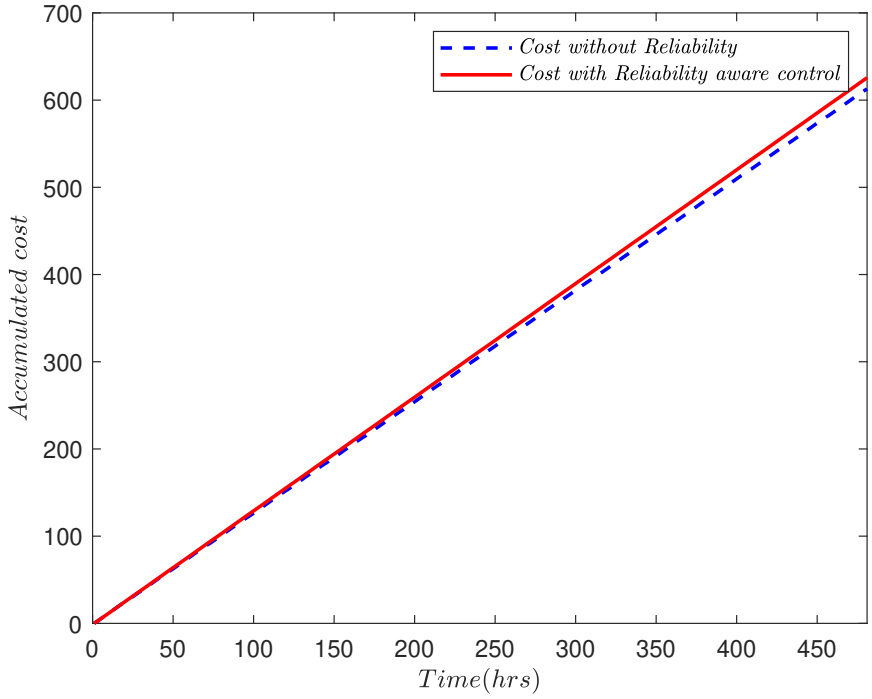

Figure 6.10: Accumulated cost for the 10 day period under different controller configurations.

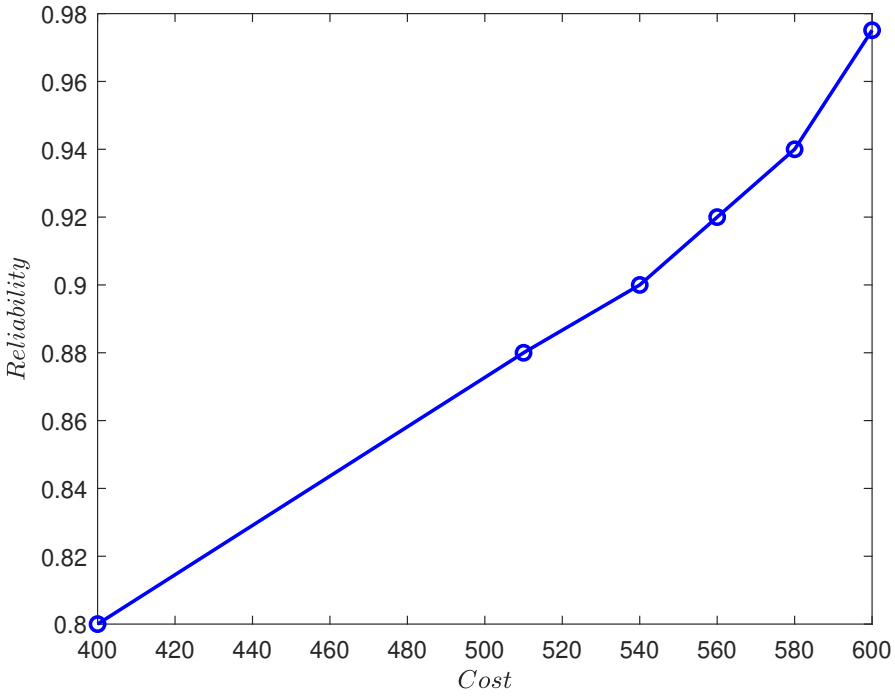

Figure 6.11: Pareto front of Cost vs Reliability.

6.6 Conclusions

In this chapter, the improvement of the reliability of a DWN is considered through appropriate controller design that takes into account a model of the network's reliability, by means of Bayesian network modelling. The resultant nonlinear dynamic Bayesian model is represented in a pseudo-linear form, easing computational cost. Results show an improved reliability of the network when the reliability index is added, at the expense of a marginal cost of operation, which was seen to be minimal, thus offering a long term economic gain. Considering that the forecasted demand is uncertain, that is to present a more realistic control problem for our case, a tube based ReMPC is designed with zonotopic sets to ensure the controller operate close to normal in the presence of unknown but bounded uncertainty. The robustness of the controller is tested with additive loads from a symmetric bounded demand profile on the known forecasted load, results demonstrated the efficacy of desirable controller properties of robust constraint satisfaction, recursive feasibility and robust performance, presenting a more realistic controller suitable for real life deployment that takes into account DWN network reliability.

Chapter 7

Conclusions and Future Work

This chapter summarizes this thesis' contributions to the field of prognostics in general and how prognostics information can be incorporated into control. It also summarizes the proposed set based approaches to prognostics and control; It's merits to both fields and why it should be a considered research interest. Finally the chapter explores the possibilities of future research directions emanating from this thesis.

7.1 Conclusions

The main contributions and conclusions of each chapter are set out as follows:
In Chapter 3, the various sub-models of the wind turbine is mathematically explained by means of a reduced model which is validated with the high fidelity FAST simulator on a 5MW wind turbine reference model which is thus far the most realistic mathematical representation of a wind turbine produced by NREL.
A degradation model via stiffness degradation methodology is explained and mathematically given for the degradation of the composite material of a wind turbine's blade effected by the flapwise root moment. With the intent of appending the nonlinear degradation model to the wind turbine's model, the stiffness degradation which is in cycles is represented in time domain. Therefore with an appended nonlinear degradation model to the nonlinear model of the wind turbine, an approximated LPV is formulated for the degradation dependent model of a wind turbine.
This LPV model is used in the formulation of a zonotopic Kalman filter with appropriate LMIs for an initial zonotopic set formulation that encompasses all considered uncertainty sources; from the stochastic projected wind speed via the LIDAR and sensor noise during estimation stage.
Subsequently the initial uncertain zonotopic set is propagated through reachability set theory into the future to attain the RUL at different instants of the blades lifetime, accompanied with appropriate uncertainty sets. This work presented a novel means of uncertainty quantification and propagation through set-based reachable set theory in prognostics set quantification and propagation, presenting a new paradigm of research.
In Chapter 4, drawing inspiration from **chapter 3**, the prognostic information of a wind turbine's

blade through stiffness degradation is included in an MPC design culminating into a Health-Aware control i.e. a two level MPC control, each control unit for each control stages of the wind turbine.

With the reduced wind turbine explained and validated from the previous chapter, the operational control of a wind turbine is described. Two LPV models are formulated based on the control requirements of each control stage of the wind turbine.

The stiffness degradation is composed of three stages; a 1st stage, where degradation is abrupt, a second stage where it is steady and the longest term and a final stage where deterioration occurs most rapidly. The health-aware control is considered for the 1st and 3rd stages only. The 2nd stage is considered the most active period of the turbine lifetime. Also since degradation is very minimal, it is deemed not economically prudent to employ health-aware control here .

The blade is then run to failure with stress from the flapwise root moment and a plot of the degradation and accumulated stress values given. It is then segmented into various linear and bilinear functions, thus producing a set of piece-wise affine functions which are functions of the accumulated stress. The linear stress model is as given in (Sanchez et al., 2015), which is a function of the model states.

Bearing in mind that the accumulative stress values for the run to failure functions are cyclic, a cycle counting procedure is required. The complex sequential and nonlinear structured rainflow counting methodology is combined with the discontinuous stiffness degradation model for the piece-wise affine functions formulation. To circumvent the discontinuity of the rainflow counting algorithm in the cycle counting, the process of Parametric Online Rainflow- counting (PORFC) is used to allocate cycles in a prediction horizon under the assumption of a preview of wind speed from a LIDAR.

Thus parameters of the piece wise affine functions with pre-allocated weights (in ascending magnitude) for each segment are allocated in the MPC per the accumulated stress value at a particular instant. Cycles are also assigned for each sampling time in the prediction horizon. With these assignments, a two level MPC is formulated where a Health-aware MPC is designed for the control stage where wind speeds is considered most damaging , i.e. wind speed $\leq 12m/s$. The results presents an advantage over other methods by offering a deration scheme of the plant for life extension in a practical ways by derating according to when needed most (according to extent of damage), against other methods like (Sanchez et al., 2015) which offers a kind of constant deration in the plants life which is not economically viable.

In Chapter 5, A data-based prognostics is undertaken in this chapter using an evolving fuzzy degradation models via EFFIG. This was employed on an IGBT. The problem of explainability has been identified as a notorious hindrance to data-based prognostics approaches in their quest for deployment in industry. This chapter sought to produce a simple but yet transparent prognostics procedure for the prediction of the RUL of power semiconductors which not only predicts RULs but ensures explainability.

Thus, with a run-to-failure data on an IGBT which shows a peculiar "stage based" behaviour, two types of features are extracted. One group of features that are very sensitive to the degradation

stages is used as a premise variable of the fuzzy model, and another group that provides good trendability and monotonicity is used for the auto-regressive consequent of the fuzzy model for degradation prediction.
Therefore the product is a prognostics prediction which is not only competitive with other proposed methods but also has the ability to predict the stage of degradation reached, thus enabling explainability.
Considering the importance of uncertainty quantification and propagation to prognostics undertakings, research based on work done in **chapter 3** for set based uncertainty quantification in data-based prognostics proposed via set membership theory and interval analysis is studied.
All uncertainty sources were duly captured in a set form and via set membership theory and interval analysis, the sets were propagated for predictions of bounded RUL. It was tested on two cases, a self-validation and a cross validation case, and as expected the width of the uncertainty set was wider in the cross validation case over the self validation case, since uncertainty is naturally considered more in this scenario.
The results of this work presents a novel data-driven technique which is simple and yet offers advantages over some complex methods such as deep learning which requires a lot of resources in terms of data and computational resource but naturally lacks explainability without external augmentations. Also a novel process of set-based quantification and propagation applied to data-based prognostics technique is proposed. This offers a simple way to represent all uncertainty sources and an easy and computational resourceful path to uncertainty quantification and propagation.
In **Chapter 6**, a characteristic function of degradation, the reliability is included in an MPC control formulating a reliability-aware control which is employed in a DWN.
The reliability of the network is modelled via the Bayesian network theory producing a nonlinear model using the flow path directions of water in the network. Given that MPC requires predicted demand values in its prediction horizon, there is a high possibility of the optimization problem been intractable. Thus, it calls for a robustification of the MPC problem considering uncertain demand. This is done by considering uncertainty to be bounded in zonotopes.
The nonlinear reliability model is appended to the DWN model and the resultant model parametrically approximated via LPV. Hence, with a degradation- dependent reliability DWN LPV model and a zonotopic based robustification, a Reliability-aware Robust MPC is formulated.
First with robustness, it proofs its merit of being robust to such extents of uncertainty which otherwise rendered a nominal case intractable and also increases the reliability of the network but at an expense of increased electricity cost from the network pumps.

7.2 Future Work

This section presents some plausible future research directions that could be an extension of this thesis in the field of prognostics, most especially set-based uncertainty quantification and propagation and the inclusion of prognostic information into control designs.
In the area of set-based uncertainty quantification in physics-based prognostics, a more holistic uncertainty that captures the individual types of uncertainties, such as the propagation uncertainty, parametric uncertainty etc could be applied in **chapter 3** as done in **chapter 5** . For the uncertainty quantification for data-based prognostics it would be interesting to test the method on other complex data based methodologies such as deep learning. The use of less-conservative geometric options such as zonotopes can also be employed and tested with the case in **chapter 3**. It would be of interest to the field to test the efficacy of the methods used here against statistical quantification procedures based on metrics as proposed by (Saxena et al., 2017).
For the direct inclusion of prognostics information via degradation or its characteristic functions, the problem of uncertainty in the degradation functions could be taken into account in future research works. Given that prognostics is a sequence of future state, a research interest could be a robustified control design to prevent the advent of any infeasibility when applied to real life scenarios.
The external allocation of parameters in the MPC might also result in excess use of computational resources in **chapter 4**. Therefore a research direction will be to investigate the use of linearization or constraint relaxation of the nonlinear degradation-stress accumulation model employed in **chapter 4** using a similar technique as done in (Wang et al., 2018b). In terms of circumventing the discontinuous nature of the rainflow counting, utilization of statistical interpretation of degradation data that aid in controller inclusion as proposed by (David et al., 2021) can be considered and compared with the proposed methodology used in **chapter 4** in terms of accuracy and computational cost.
With prognostic information from a data-based prognostics that includes a explainability feature as done in **chapter 5**, a FDI could work in tandem with a prognostic sub level, such that a comprehensive predictive based maintenance regime is acquired. This could then be applied to a control unit for an all-inclusive prescriptive maintenance controller by employing the methods in **chapter 4**. An interest could be in investigating the adoption of variant methods of reachability analysis procedure that have been successfully applied in other fields, like sampling based methods (Thomas et al., 2022) or as done in (Amr et al.) using matrix zonotopes a more suitable geometric representation compared to interval sets

Bibliography

Ahsan, M., Stoyanov, S., and Bailey, C. (2016). Data driven prognostics for predicting remaining useful life of igbt. In *2016 39th International Spring Seminar on Electronics Technology (ISSE)*, 273–278. doi: doi:10.1109/ISSE.2016.7563204.

Ahwiadi, M. and Wang, W. (2022). An adaptive evolving fuzzy technique for prognosis of dynamic systems. *IEEE Transactions on Fuzzy Systems*, 30(3), 841–849. doi: 10.1109/TFUZZ.2021.3049916.

Aisha Sa'ad, Aimé C. Nyoungue, Z.H. (2022). An integrated maintenance and power generation forecast by ann approach based on availability maximization of a wind farm. *Energy Reports*, 8(9), 282–301. doi: https://doi.org/10.1016/j.egyr.2022.06.120.

Al-Mohamad, A., Puig, V., Hoblos, G., and Azzam, J. (2021). Robust zonotopic prognostics approaches for lpv systems based on set-membership and extended kalman filter. In *2021 International Conference on Control, Automation and Diagnosis (ICCAD)*, 1–6. doi: 10.1109/ICCAD52417.2021.9638734.

Alghassi, A., Perinpanayagam, S., and Samie, M. (2016). Stochastic RUL Calculation Enhanced With TDNN-Based IGBT Failure Modeling. *IEEE Transactions on Reliability*, 65(2), 558–573. doi: 10.1109/TR.2015.2499960.

Althoff, M., Frehse, G., and Girard, A. (2021). Set propagation techniques for reachability analysis. *Annual Review of Control, Robotics, and Autonomous Systems*, 4. doi: 10.1146/annurev-control-071420-081941.

Alwi, H. and Edwards, C. (2008). Fault tolerant control using sliding modes with on-line control allocation. *Automatica*, 44, 1859–1866.

Amr, A., Yvonne, S., and Karl, Henrik, J. (????). In *European Journal of Control, title=Hamilton-Jacobi reachability: A brief overview and recent advances, year=2022, volume=, number=, pages=100666, doi=ISSN 0947-3580, https://doi.org/10.1016/j.ejcon.2022.100666.*

Amssaouet, F., Nguyen, T.P.K., Medjaher, K., and Orchard, M.E. (2019). Uncertainty quantification in system-level prognostics: application to tennessee eastman process. *The sixth (6th) edition in the series of the International Conference on Control, Decision and Information Technologies*, 48.

An, D., Choi, J.H., and Kim, N.H. (2013). Options for prognostics methods: A review of data-driven and physics-based prognostics. In *Proceedings of the Annual Conference of the PHM Society 2013*.

Angelov, P. (2012). *Autonomous learning systems: from data streams to knowledge in real-time*. John Wiley & Sons.

A.Vargas-Martínez, V.Puig, E. and R.Morales-Menendez (2010). Mrac + hfault tolerant control for linear parameter varying systems. In *2010 Conference on Control and Fault-Tolerant Systems (SysTol)*, 94–99. doi: 10.1109/SYSTOL.2010.5676069.

Badihi, H., Zhang, Y., and Hong, H. (2015). Wind turbine fault diagnosis and fault-tolerant torque load control against actuator faults. *IEEE Transactions on Control Systems Technology*, 23(4), 1351–1372. doi: 10.1109/TCST.2014.2364956.

Baldi, S., Thuan Le Quang, O.H., and Endel, P. (2017). Real-time monitoring energy efficiency and performance degradation of condensing boilers. *Energy Conversion and Management*, 136, 329–339. doi: https://doi.org/10.1016/j.enconman.2017.01.016.(https://www.sciencedirect.com/science/article/pii/S019689041730016X).

Bansal, S., Bajcsy, A., Ratner, E., Dragan, A.D., and Tomlin, C.J. (2020). A hamilton-jacobi reachability-based framework for predicting and analyzing human motion for safe planning. In *2020 IEEE International Conference on Robotics and Automation (ICRA)*, 7149–7155. doi: 10.1109/ICRA40945.2020.9197257.

Bansal, S., Chen, M., Herbert, S., and Tomlin, C.J. (2017). Hamilton-jacobi reachability: A brief overview and recent advances. In *2017 IEEE 56th Annual Conference on Decision and Control (CDC)*, 2242–2253. doi: 10.1109/CDC.2017.8263977.

Baraldi, Cadini, F., and Mangili, F. (2013). Model-based and data-driven prognostics under different available information. *Mechanical Systems and Signal Processing*, 32, 66–79.

Barradas-Berglind, J., Wisniewski, R., and Soltani, M. (2015). Fatigue damage estimation and data-based control for wind turbines. *IET Control Theory and Applications*, 9(7), 1042–1050.

Baur, M., Albertelli, P., and Monno, M. (2020). A review of prognostics and health management of machine tools. *The International Journal of Advanced Manufacturing Technology*, 107, 1–4. doi: 107.10.1007/s00170-020-05202-3.

Bayington, C., Roemer, M., and Galie, T. (2002). Prognostic enhancements to diagnostic systems for improved condition-based maintenance. In *IEEE Aerospace Conference, Big Sky, MT*, volume 6, 2815–2824.

Beauson, Laurent, A., Rudolph, D., and Jensen, J.P. (2022). The complex end-of-life of wind turbine blades: A review of the european context,. *Renewable and Sustainable Energy Reviews*, 155, 111847. doi: https://doi.org/10.1016/j.rser.2021.111847.

Beganovic, N., Njiri, J.G., and Söffker, D. (2018). Reduction of structural loads in wind turbines based on an adapted control strategy concerning online fatigue damage evaluation models. *Energies*, 11, 15. doi: 10.3390/en11123429.

Behzad, M., Arghan, H.A., Bastami, A.R., and Zuo, M.J. (2017). Prognostics of rolling element bearings with the combination of paris law and reliability method. In *2017 Prognostics and System Health Management Conference (PHM-Harbin)*, 1–6. doi: 10.1109/PHM.2017.8079187.

Bernal-Perez, S., Ano-Villalba, S., Blasco-Gimenez, R., and Rodriguez-D'Derlee, J. (2013). Efficiency and fault ride-through performance of a diode-rectifier- and vsc-inverter-based hvdc link for offshore wind farms. *IEEE Transactions on Industrial Electronics*, 60(6), 2401–2409.

Bianchi, F., De Battista, H., and Mantz, R.J. (2007). *Wind Turbine Control Systems: Principles, Modelling and Gain Scheduling Design*.

Birnbaum, Z. and Saunders, S. (1969). A new family of life distributions. *Journal of Applied Probability*, 6(2), 319–327.

Blanke, M., Kinnaert, M., Lunze, J., and Staroswiecki, M. (2006). *Diagnosis and Fault-Tolerant Control*. Springer-Verlag Berlin Heidelberg.

Blanke, M., Frei, C., Kraus, F., Patton, R., and Staroswiecki, M. (2000). What is fault-tolerant control. *IFAC Proceedings Volumes*, 33. doi: 10.1016/S1474-6670(17)37338-X.

Blesa, J.., Puig, V., and Saludes (2011a). Identification for passive robust fault detection using zonotope-based set-membership approaches. *International journal of adaptive control and signal processing.*, 25(9), 788–812.

Blesa, J., Puig, V., Romera, J., and Saludes, J. (2011b). Fault diagnosis of wind turbines using a set-membership approach. In *18th IFAC World Congress*, 8316–8321. Milan, Italy.

Boutros, K., Puig, V., and Nejjari, F. (2020). Robust economic model predictive control of water transport networks. In *28th Mediterranean Conference on Control and Automation, MED 2020, Saint-Raphaël, France, September 15-18, 2020*, 121–126. IEEE. doi: 10.1109/MED48518.2020.9183029. URL `https://doi.org/10.1109/MED48518.2020.9183029`.

Brown, D., Abbas, M., Ginart, A., Ali, I., Kalgren, P., and Vachtsevanos, G. (2010). Turn-off time as a precursor for gate bipolar transistor latch-up faults in electric motor drives. *2010 Annual Conference of the PHM Society (PHM), Portland.*

Bui, M., Lu, M., Hojabr, R., Chen, M., and Shriraman, A. (2021). Real-time hamilton-jacobi reachability analysis of autonomous system with an fpga. In *2021 IEEE/RSJ International Conference on Intelligent Robots and Systems (IROS)*, 1666–1673. doi: 10.1109/IROS51168.2021.9636410.

C. Ocampo-Martinez, V. Puig, J.Q. and Ingimundarson., A. (2006). Fault-tolerant optimal control of sewer networks: Barcelona case study. *International Journal of Measurement and Control,*, 39(5), 151–156. doi: www.doi.org/10.1177/002029400603900502.

Cadini, F., Sbarufatti, C., Cancelliere, F., and Giglio, M. (2018). State-of-life prognosis and diagnosis of lithium-ion batteries by data-driven particle filters. *Applied Energy*, 235, 661–672. doi: 10.1016/j.apenergy.2018.10.095.

Cai, B., Lui, Y., Lui, K., and Chang, Y. (2020). *Bayesian networks for reliability engineering*. Springer.

Camargos, M., Bessa, I., D'Angelo, M.F.S.V., Cosme, L.B., and Palhares, R.M. (2020). Data-driven prognostics of rolling element bearings using a novel error based evolving takagi–sugeno fuzzy model. *Applied Soft Computing*, 96, 106628. doi: 10.1016/j.asoc.2020.106628.

Camargos, M., Bessa, I., Junior, L.A.Q.C., Coutinho, P., Leite, D.F., and Palhares, R.M. (2021). Evolving fuzzy system applied to battery charge capacity prediction for fault prognostics. In *Atlantis Studies in Uncertainty Modelling*. Atlantis Press. doi: 10.2991/asum.k.210827.010.

Campos-Gaona, D., Moreno-Goytia, E., and Anaya-Lara, O. (2013). Fault ride-through improvement of DFIG-WT by integrating a two-degrees-of-freedom internal model control. *IEEE Transactions on Industrial Electronics*, 60(3), 1133–1145.

Casau, P., Rosa, P., Tabatabaeipour, S., and Silvestre, C. (2012). Fault detection and isolation and fault tolerant control of wind turbines using set-valued observers. In *8th IFAC Symposium on Fault Detection, Supervision and Safety of Technical Processes*, volume 45, 120–125. Mexico City, Mexico.

Casillas, M.V., Garza-Castañón, L.E., and Puig, V. (2015). Sensor placement for leak location in water distribution networks using the leak signature space. In *29th IFAC Symposium on Fault Detection, Supervision andSafety for Technical Processes SAFEPROCESS 2015 Paris*, volume 48, 214–219. doi: https://doi.org/10.1016/j.ifacol.2015.09.530.(https://www.sciencedirect.com/science/article/pii/S2405896315016596.

Celaya, J., Saxena, A., Saha, S., and Goebel, K. (2011). Prognostics of power MOSFETs under thermal stress accelerated aging using data-driven and model-based methodologies. *Annual Conference of the PHM Society (PHM)*, 2.

Cembrano, G., Quevedo, J., Puig, V., Pérez, R., Figueras i Jové, J., Verdejo, J., Escaler, I., Ramón, G., Barnet, G., Rodríguez, P., and Casas, M. (2011a). Plio: A generic tool for real-time operational predictive optimal control of water networks. *Water science and technology : a journal of the International Association on Water Pollution Research*, 64, 448–59. doi: 10.2166/wst.2011.431.

Cembrano, G., Quevedo, J., Puig, V., Pérez, R., Figueras i Jové, J., Verdejo, J., Escaler, I., Ramón, G., Barnet, G., Rodríguez, P., and Casas, M. (2011b). Plio: A generic tool for real-time opera-

tional predictive optimal control of water networks. *Water science and technology : a journal of the International Association on Water Pollution Research*, 64, 448–59. doi: 10.2166/wst.2011.431.

Chamseddine, A., Theilliol, D., Sadeghzadeh, I., Zhang, Y., and Weber, P. (2014). Optimal reliability design for over-actuated systems based on the mit rule: Application to an octocopter helicopter testbed. *Reliability Engineering System Safety*, 132, 196–206. doi: 10.1016/j.ress.2014.07.013.

Chao, M.A., Kulkarni, C., Goebel, K., and Fink., O. (2022). Fusing physics-based and deep learning models for prognostics. *Reliability Engineering System Safety*, 217, 107961. doi: ISSN0951-8320, https://doi.org/10.1016/j.ress.2021.107961.

Chen, W., Ding, S., Sari, A., Naik, A., Khan, A., and Yin, S. (2011a). Observer-based FDI schemes for wind turbine benchmark. In *Proceedings of IFAC World Congress*, volume 44, 7073–7078. Milan, Italy.

Chen, X. and Eder, M. (2020). A critical review of damage and failure of composite wind turbine blade structures. *IOP Conference Series Materials Science and Engineering*, 942. doi: 10.1088/1757-899X/942/1/012001.

Chen, Y., Du, L., Li, Y.F., Huang, H.Z., and Li, X. (2011b). Fmeca for aircraft electric system. In *2011 International Conference on Quality, Reliability, Risk, Maintenance, and Safety Engineering*, 122–125. doi: 10.1109/ICQR2MSE.2011.5976581.

Chen, Z. (2010). Fault diagnosis of gear box based on information entropy. In *Chinese Control and Decision Conference (CCDC)*, 1239–1242. Guilin, China.

Cheng, S. and Pecht, M. (2009). A fusion prognostics method for remaining useful life prediction of electronic products. *IEEE International Conference on Automation Science and Engineering, CASE*, 255(1), 102–107.

Choi, K., Yi, J., Park, C., and Yoon, S. (2021). Deep learning for anomaly detection in time-series data: Review, analysis, and guidelines. *IEEE Access*, 9, 120043–120065. doi: 10.1109/ACCESS.2021.3107975.

Cieslak, J. and Gucik-Derigny, D. (2018). Introduction of a prognostic decision making in a fault tolerant control context. *IFAC-PapersOnLine*, 51, 649–654. doi: 10.1016/j.ifacol.2018.09.644.

Colak, I., Fulli, G., Bayhan, S., Chondrogiannis, S., and Demirbaş, (2015). Critical aspects of wind energy systems in smart grid applications. *Renewable and Sustainable Energy Reviews*, 52, 155–171. doi: 10.1016/j.rser.2015.07.062.

Compare, M., Baraldi, P., and Zio, E. (2020). Challenges to iot-enabled predictive maintenance for industry 4.0. *IEEE Internet of Things Journal*, 7(5), 4585–4597. doi: 10.1109/JIOT.2019.2957029.

Compare, M., Bellani, L., and Zio, E. (2017). Reliability model of a component equipped with phm capabilities. *Reliability Engineering System Safety*, 168, 4–11. doi: ISSN0951-8320,https://doi.org/10.1016/j.ress.2017.05.024.(https://www.sciencedirect.com/science/article/pii/S019689041730016X).

Cordovil, L.A.Q., Coutinho, P.H.S., Bessa, I., D'Angelo, M.F.S.V., and Palhares, R.M. (2020). Uncertain data modeling based on evolving ellipsoidal fuzzy information granules. *IEEE Transactions on Fuzzy Systems*, 28(10), 2427–2436. doi: 10.1109/TFUZZ.2019.2937052.

Cordovil, L.A.Q., Coutinho, P.H.S., Bessa, I., Peixoto, M.L.C., and Palhares, R.M. (2022). Learning event-triggered control based on evolving data-driven fuzzy granular models. *International Journal of Robust and Nonlinear Control*, 32(5), 2805–2827.

Cornelius, J., Brockner, B., Hong, S.H., Wang, Y., Pant, K.m., and Ball, J. (2020). Estimating and leveraging uncertainties in deep learning for remaining useful life prediction in mechanical systems. In *2020 IEEE International Conference on Prognostics and Health Management (ICPHM)*, 1–8. doi: doi:10.1109/ICPHM49022.2020.9187063.

Daigle, M., Saha, B., and Goebel, K. (2012). A comparison of filter-based approaches for model-based prognostics. *2012 IEEE Aerospace Conference*, 1–10.

Daigle, M., Saha, B., and Goebel, K. (2012). A comparison of filter-based approaches for model-based prognostics. In *IEEE Aerospace Conference*. IEEE. doi: 10.1109/aero.2012.6187363.

Daigle, M. and Goebel, K. (2011). A model-based prognostics approach applied to pneumatic valves. *International Journal of Prognostics and Health Management*, 2(2).

Dalal, M., Ma, J., and He, D. (2011). Lithium-ion battery life prognostic health management system using particle filtering framework. *Proceedings of the Institution of Mechanical Engineers, Part O: Journal of Risk and Reliability*, 255(1), 81–90.

Daroogheh, N., Meskin, N., and Khorasani, K. (2014). A novel particle filter parameter prediction scheme for failure prognosis. In *2014 American Control Conference*, 1735–1742. doi: 10.1109/ACC.2014.6859021.

David, C., Mazen, A., Domenico, Di, D., and Guillaume, S. (2021). Data-driven fatigue-oriented mpc applied to wind turbines individual pitch control. *Renewable Energy*, 170, 1008–1019. doi: https://doi.org/10.1016/j.renene.2021.02.052.

Degrenne, N., Kawahara, C., and Mollov, S. (2019). Prognostics framework for power semiconductor igbt modules through monitoring of the on-state voltage. *11th Annual Conference of the PHM Society, Scottsdale, AZ, USA*, 11. doi: 10.36001/phmconf.2019.v11i1.829.

Desimini, R. and Prandini, M. (2019). A novel set-based reachability method for optimal robust control of constrained linear systems. In *2019 18th European Control Conference (ECC)*, 1437–1442. doi: 10.23919/ECC.2019.8796057.

Dewey, H.H., DeVries, D.R., and Hyde, S.R. (2019). Uncertainty quantification in prognostic health management systems. In *2019 IEEE Aerospace Conference*, 1–13. doi: doi:10.1109/AERO.2019.8741821.

Ding, M.S.X. and Li, L. (2021). Control performance monitoring and degradation recovery in automatic control systems: A review, some new results, and future perspectives. *Control Engineering Practice*, 111, 104790. doi: ISSN0967-0661,https://doi.org/10.1016/j.conengprac.2021.104790.

Donders, S. (2002). *Fault Detection and Identification for Wind Turbine Systems, a closed-loop analysis.* Master's thesis, University of Twente, Faculty of Applied Physics Systems and Control Engineering.

Dong, H. and Jin, X., W.C. (2014). Lithium-ion battery state of health monitoring and remaining useful life prediction based on support vector regression-particle filter. *Mechanical Systems and Signal Processing*, 271, 114–123.

Downing, S.D. and Socie, D.F. (1982). Simple rainflow counting algorithms. *International Journal of Fatigue*, 4, 31–40.

Duda, Richard O, P.E.H. and Stork., D.G. (2012). *Pattern classification*. John Wiley Sons, New Jersey USA.

Duong, P.L.T. and Raghavan, N. (2017). Uncertainty quantification in prognostics: A data driven polynomial chaos approach. In *2017 IEEE International Conference on Prognostics and Health Management (ICPHM)*, 135–142. doi: doi:10.1109/ICPHM.2017.7998318.

Elattar, H., Elminir, H., and Riad, A.e.d.. (2016a). Prognostics: a literature review. *Complex Intelligent Systems,*, 2(2), 125–154. doi: 10.1007/s40747-016-0019-3.

Elattar, H.M., Elminir, H.K., and Riad, A.M. (2016b). Prognostics: a literature review. *Complex Intelligent Systems*, 2(2), 125–154.

Elattar, H., Elminir, H., and Riad, A. (2018). Towards online data-driven prognostics system. *Complex Intell. Syst*, 4, 271–282. doi: https://doi.org/10.1007/s40747-018-0082-z.

Eleffendi, M.A. and Johnson, C.M. (2016). Application of kalman filter to estimate junction temperature in igbt power modules. *IEEE Transactions on Power Electronics*, 31(2), 1576–1587. doi: 10.1109/TPEL.2015.2418711.

Endo, T., Mitsunaga, K., and Nakagawa, H. (1967). Fatigue of metals subjected to varying stress-prediction of fatigue lives. In *Preliminary Proceedings of the Chugoku-Shikoku District Meeting. Japan Society of Mechanical Engineers*, 41–44. Tokyo, Japan.

Evans, M., Cannon, M., and Kouvaritakis, B. (2015). Robust mpc tower damping for variable speed wind turbines. *IEEE Transactions on Control Systems Technology*, 23, 290–296. doi: 10.1109/TCST.2014.2310513.

Fan, H., Yan, Y., and Yang, F. (2012). Research of dynamic linked lists for the fault tree analysis process. In *2012 International Conference on Quality, Reliability, Risk, Maintenance, and Safety Engineering*, 93–96. doi: 10.1109/ICQR2MSE.2012.6246194.

Frank, P.M., Garcia, E.A., and Koppen-Seliger, B. (2000). Modelling for fault detection and isolation versus modelling for control. mathematics and computers in simulation. *Mathematics and Computers in Simulation*, 53(4-6), 259–271. doi: https://doi.org/10.1076/mcmd.7.1.1.3633.

Freire, N., Estima, J., and Marques Cardoso, A. (2013). Open-circuit fault diagnosis in pmsg drives for wind turbine applications. *IEEE Transactions on Industrial Electronics*, 60(9), 3957–3967.

Futter, D. (1995). Vibration monitoring of industrial gearboxes using time domain averaging. In *IMechE 2nd International conference on gearbox noise, vibration and diagnostics*, volume 5, 35–46. London, United Kingdom.

Georg, S. (2015). *Fault Diagnosis and Fault-Tolerant Control of ind Turbines*. Ph.D. thesis, Universitt Rostock.

Gertler, J., Romera, J., Puig, V., and Quevedo, J. (2010). Leak detection and isolation in water distribution networks using principal component analysis and structured residuals,(2010). 191 – 196. doi: 10.1109/SYSTOL.2010.5676043.

Gertler, J. (1998). *Fault Detection and Diagnosis in Engineering Systems*. Marcel Dekker Inc., New York.

Gong, M., Tang, D., Yu, J., and Tian, L. (2021). A physics-informed transfer learning approach for anomaly detection of aerospace cmg with limited telemetry data. In *2021 Global Reliability and Prognostics and Health Management (PHM-Nanjing)*, 1–5. doi: 10.1109/PHM-Nanjing52125.2021.9612988.

Gong, X., Qiao, W., and Zhou, W. (2010). Incipient bearing fault detection via wind generator stator current and wavelet filter. In *IEEE 36th Annual Conference on Industrial Electronics Society IECON*, 2615–2620. Glendale, USA.

Gong, X. and Qiao, W. (2015). Current-based mechanical fault detection for direct-drive wind turbines via synchronous sampling and impulse detection. *IEEE Transactions on Industrial Electronics*, 62(3), 1693–1702. doi: 10.1109/TIE.2014.2363440.

Gono, R., Kratky, M., and Rusek, S. (2012). Modeling and analysis of performance degradation data for reliability assessment: A review. *AASRI Procedia*, 2, 75–80. doi: https://doi.org/10.1016/j.aasri.2012.09.017.

Gorjian, N., Ma, L., Mittinty, M., Yarlagadda, P., and Sun, Y. (2010a). A review on degradation models in reliability analysis.. *Engineering Asset Lifecycle Management.*, 20(7), 369–384,. doi: https://doi.org/10.1007/978-0-85729-320-6_42.

Gorjian, N., Ma, L., Mittinty, M.N., Yarlagadda, P.K., and Sun, Y. (2010b). A review on degradation models in reliability analysis. In *WCE 2010, London.*

Gouriveau, R., Medjaher, K., and Zerhouni, N. (2016a). *From Prognostics and Health Systems Management to Predictive Maintenance 1: Monitoring and Prognostics*. John Wiley Sons, New Jersey USA.

Gouriveau, R., Medjaher, K., and Zerhouni, N. (2016b). *From Prognostics and Health Systems Management to Predictive Maintenance 1: Monitoring and Prognostics*. doi: 10.1002/9781119371052.

Gray, C. and Watson, S. (2010). Physics of failure approach to wind turbine condition based maintenance. *Wind Energy*, 13(5), 395–405.

Grosso, J., Ocampo-Martinez, C., Puig, V., Limon, D., and Pereira, M. (2014). In *Economic MPC for the management of drinking water networks*. doi: 10.1109/ECC.2014.6862384.

Gu, J., Barker, D., and Pecht, M. (2007). Uncertainty assessment of prognostics of electronics subject to random vibration. *AAAI Fall Symposium - Technical Report*.

Haghifam, M.R. (2015). Application of bayesian networks in composite power system reliability assessment and reliability-based analysis. *IET Generation, Transmission Distribution*, 9. doi: 10.1049/iet-gtd.2014.0660.

Hanif, A., Yu, Y., DeVoto, D., and Khan, F. (2019). A comprehensive review toward the state-of-the-art in failure and lifetime predictions of power electronic devices. *IEEE Transactions on Power Electronics*, 34(5), 4729–4746. doi: 10.1109/TPEL.2018.2860587.

Haque, M.S., Choi, S., and Baek, J. (2018). Auxiliary particle filtering-based estimation of remaining useful life of igbt. *IEEE Transactions on Industrial Electronics*, 65(3), 2693–2703. doi: doi:10.1109/TIE.2017.2740856.

Harno, H.G. and Kim, Y. (2019). Zonotopic reachability analysis for an unmanned helicopter. In *2019 19th International Conference on Control, Automation and Systems (ICCAS)*, 646–648. doi: 10.23919/ICCAS47443.2019.8971606.

Heng, A., Zhang, S., and Tan, A. (2009). Rotating machinery prognostics: State of the art, challenges and opportunities. *Mechanical Systems and Signal Processing*, 23(3), 724–739.

Hong, C., Lee, C., Lee, K., Ko, M., Kim, D., and Hur, K. (2020). Remaining useful life prognosis for turbofan engine using explainable deep neural networks with dimensionality reduction. *Sensors*, 20, 6626.

Hong L., D.J. (2014). A time domain approach to diagnose gearbox fault based on measured vibration signals. *Journal of Sound and Vibration*, 333(7), 2164–2180.

Horn, J.T. and Leira, B.J. (2019). Fatigue reliability assessment of offshore wind turbines with stochastic availability,. *Reliability Engineering System Safety*, 191, 106550.

Hua, C. (2021). *Reinforcement Learning Aided Performance Optimization of Feedback Control Systems*. Springer Fachmedien Wiesbaden.

Huang, D., Bai, R., Zhao, S., Wen, P., He, J., Wang, S., and Chen, S. (2021). A hybrid bayesian deep learning model for remaining useful life prognostics and uncertainty quantification. In *2021 IEEE International Conference on Prognostics and Health Management (ICPHM)*, 1–8. doi: 10.1109/ICPHM51084.2021.9486527.

IEA (2020). Iea (2020), renewables 2020, iea, paris. URL `https://www.iea.org/reports/renewables-2020`.

Inthamoussou, F.A., Bianchi, F.D., De Battista, H., and Mantz, R.J. (2014). Lpv wind turbine control with anti-windup features covering the complete wind speed range. *IEEE Transactions on Energy Conversion*, 29(1), 259–266.

Isermann, R. (2011). *Fault-Diagnosis Applications, Model-based condition monitoring: actuators, drives, machinery, planst, sensors and fault-tolerant systems*. Springer-Verlag Berlin Heidelberg.

Ismail, A., Saidi, L., Sayadi, M., and Benbouzid, M. (2019). Gaussian Process Regression Remaining Useful Lifetime Prediction of Thermally Aged Power IGBT. In *45th Conference of the IEEE Industrial Electronics Society (IECON)*, volume 1, 6004–6009. doi: 10.1109/IECON.2019.8926710.

Ismail, A., Saidi, L., Sayadi, M., and Benbouzid, M. (2020). Remaining useful life estimation for thermally aged power insulated gate bipolar transistors based on a modified maximum likelihood estimator. *International Transactions on Electrical Energy Systems*, 30(6), 1–18.

ISO-13381-1 (2004). Condition monitoring and diagnostics of machines prognostics part1: General guidelines, international standard, iso.

Jardine, A.K.S., Lin, D., and Banjevic, D. (2006). A review on machinery diagnostics and prognostics implementing condition-based maintenance. *Mechanical Systems and Signal Processing.*, 20(7), 1483–1510,. doi: https://doi.org/10.1016/j.ymssp.2005.09.012.

Javed, K., Gouriveau, R., Zerhouni, N., and Nectoux, P. (2015). Enabling health monitoring approach based on vibration data for accurate prognostics. *IEEE Transactions on Industrial Electronics*, 62(1), 647–656. doi: doi:10.1109/TIE.2014.2327917.

Javidsharifi, M., Pourroshanfekr Arabani, H., Kerekes, T., Sera, D., and Spataru, S. (2022). Effect of battery degradation on the probabilistic optimal operation of renewable-based microgrids. *Electricity*, 3, 53–74,. doi: https://doi.org/10.3390/electricity3010005.

Jensen, W.R. and Foster, S.N. (2019). Remaining useful life estimation of stator insulation using particle filter. In *2019 IEEE Energy Conversion Congress and Exposition (ECCE)*, 7004–7011. doi: 10.1109/ECCE.2019.8912598.

Jiang, R. and Murthy, D. (1999). Exponentiated weibull family for analyzing bathtub failure-rate data. *Reliability, IEEE Transactions on*, 48(1), 68–72.

Johnston, D.R., LaForte, J. T., P.P.E., and Galpern, H.N. (1979). Frequency acceleration of voltage endurance. *IEEE Transactions on Electrical Insulation*, 142, 121–126.

Jonkman, J. and Buhl, M. (2005). *FAST user's guide*. National Renewable Energy Laboratory, Colorado, USA. Technical Report NREL/EL-500-38230.

Jonkman, J., Butterfield, S., Musial, W., and Scott, G. (2009). *Definition of a 5-MW Reference Wind Turbine for Offshore System Development*.

Kabir, A., Bailey, C., Lu, H., and Stoyanov, S. (2012). A review of data-driven prognostics in power electronics. In *Proceedings of the International Spring Seminar on Electronics Technology*, volume 6273136, 189–192. doi: 10.1109/ISSE.2012.6273136.

Kallesøe, C., Izaili-Zamanabadi, R., Rasmussen, H., and Cocquempot, V. (2004). Model based fault diagnosis in a centrifugal pump application using structural analysis, (2004). In *Proceedings of the IEEE International Conference on Control Applications*, volume 2, 1229 – 1235 Vol.2. doi: 10.1109/CCA.2004.1387541.

Kang, R., GONG, W., and CHEN, Y. (2020). Model-driven degradation modeling approaches: Investigation and review. *Chinese Journal of Aeronautics*, 33-4, 1137–1153. doi: https://doi.org/10.1016/j.cja.2019.12.006.

Karami, F., Poshtan, J., and Poshtan, M. (2010). Model-based fault detection in induction motors. In *IEEE International Conference on Control Applications*, 1957–1962. Yokohama, Japan.

Karimi, S., Gaillard, A., Poure, P., and Saadate, S. (2008). FPGA-based real-time power converter failure diagnosis for wind energy conversion systems. *IEEE Transactions on Industrial Electronics*, 55(12), 4299 – 4308.

Karimi Pour, F., Puig, V., and Cembrano, G. (2019). Economic health-aware lpv-mpc based on system reliability assessment for water transport network. *Energies*, 12, 3015. doi: 10.3390/en12153015.

Karimi Pour, F., Theilliol, D., Puig, V., and Cembrano, G. (2021). Health-aware control design based on remaining useful life estimation for autonomous racing vehicle. *ISA Transactions*, 113, 196–209. doi: 10.1016/j.isatra.2020.03.032. URL `https://hal.archives-ouvertes.fr/hal-02560292`.

Kharait, R.A., Stiles, P., Carriere, J., and McClung, L. (2017). Impact of degradation rates on solar pv financing for projects located in the united states. In *2017 IEEE 44th Photovoltaic Specialist Conference (PVSC)*, 2833–2835. doi: 10.1109/PVSC.2017.8366032.

Khelassi, A., Jiang, J., Theilliol, D., Weber, P., and Zhang, Y.M. (2011). Reconfiguration of control inputs for overactuated systems based on actuators health. *IFAC Proceedings Volumes*, 44(1), 13729–13734. doi: https://doi.org/10.3182/20110828-6-IT-1002.02174.

Khoury, B., Bessa, I., Nejjari, F., and Puig, V. (2022a). A set-based uncertainty quantification of evolving fuzzy models for data-driven prognostics. In *15th International Conference on Diagnostics of Processes and Systems*.

Khoury, B., Bessa, I., Puig, V., Nejjari, F., and Palhares, R.M. (2022b). Data-driven prognostics based on evolving fuzzy degradation models for power semiconductor devices. In *Proceedings of the 7th European Conference of the Prognostics and Health Management Society 2022.* PHM Society, 241 Woodland Drive, State College, PA 16803.

Khoury, B., Nejjari, F., and Puig, V. (2020a). Health-aware lpv model predictive control of wind turbines. *IFAC-PapersOnLine*, 53(2), 826–831. doi: https://doi.org/10.1016/j.ifacol.2020.12.838.

Khoury, B., Nejjari, F., and Puig, V. (2022c). Health-aware linear parameter varying model predictive control of wind turbines. *IEEE Transactions on Control Systems Technology (submitted)*.

Khoury, B., Nejjari, F., and Puig, V. (2022d). Reliability–aware zonotopic tube–based model predictive control of a drinking water network. *Int. J. Appl. Math. Comput. Sci.*, 32(2), 197–211. doi: 10.34768/amcs-2022-0015. URL `https://doi.org/10.34768/amcs-2022-0015`.

Khoury, B., Puig, V., and Nejjari, F. (2020b). Model-based prognosis approach using a zonotopic kalman filter with application to a wind turbine. In *Proceedings of the 5th European Conference of the Prognostics and Health Management Society (PHME 2020))*, volume 5, 9. doi: p.1258:1-1258: 9.ISBN978-1-936263-32-5.

Khoury, B., Puig, V., and Nejjari, F. (2022e). A set-based prognostics approach for wind turbine blade health monitoring. *IFAC-PapersOnLine*, 55, 402–407. doi: 10.1016/j.ifacol.2022.07.162.

Kia, S., Henao, H., and Capolino, G. (2009). Torsional vibration effects on induction machine current and torque signatures in gearbox-based electromechanical system. *IEEE Transactions on Industrial Electronics*, 56(11), 4689–4699.

Kim, N., An, D., and Choi, J.H. (2017). *Prognostics and Health Management of Engineering Systems*. Springer, Switzerland.

Krasnosel'skiĭ, M.A. and Pokrovskiĭ, A.V. (1989). *Systems with hysteresis*. Springer Verlag.

Kraus, M. and Feuerriegel, S. (2019). Forecasting remaining useful life: Interpretable deep learning approach via variational bayesian inferences. *Decis. Support Syst*, 125, 113100.

Körber, A. and King, R. (2010). Model predictive control for wind turbines. *European Wind Energy Conference and Exhibition 2010, EWEC 2010*, 2.

Lakehal, A. and Laouacheria, F. (2017). Reliability based rehabilitation of water distribution networks by means of bayesian networks. *Journal of Water and Land Development*, 34. doi: 10.1515/jwld-2017-0050.

Lampman, S. (2009). *ASM Metals Handbook - Fatigue and Fracture*, volume 19. ASM International, Novelty.

Le V., Stoica Maniu, A.T. and Camacho (2013). *Zonotopes: From Guaranteed State Estimation to Control.* Wiley, NJ.

Lee, J., Wu, F., Zhao, W., Ghaffari, M., Liao, L., and Siegel, D. (2014). Prognostics and health management design for rotary machinery systems—reviews, methodology and applications. *Mechanical systems and signal processing*, 42(1-2), 314–334. doi: https://doi.org/10.1016/j.ymssp.2013.06.004.

Leon, M.J., Kim, B., Helga, N.p., Justine, B., Malcom, M., and Bent, S. (2017). Materials for wind turbine blades: An overview. *materials*, 10, 1–24. doi: 10.3390/ma10111285.

Li, R. and Frogley, M. (2013). On-line fault detection in wind turbine transmission system using adaptive filter and robust statistical features. *International Journal of Prognostics and Health Management. Special Issue on Wind Turbine PHM*, 4, 115–123.

Li, S., Chen, Z., Liu, Q., Shi, W., and Li, K. (2020). Modeling and analysis of performance degradation data for reliability assessment: A review. *IEEE Access*, 8, 74648–74678. doi: 10.1109/ACCESS.2020.2987332.

Liang, D., Qin, C., Wang, S., and Guo, H. (2018). Reliability evaluation of dc distribution power network. In *2018 China International Conference on Electricity Distribution (CICED)*, 654–658. doi: 10.1109/CICED.2018.8592284.

Liao, L. and Kóttig, F. (2004). Review of hybrid prognostics approaches for remaining useful life prediction of engineered systems, and an application to battery life prediction. *IEEE Transactions on Reliability*, 63(1), 191–207,. doi: https://doi.org/10.1109/tr.2014.2299152.

Liu, W., Zhang, W., Han, J., and Wang, G. (2012). A new wind turbine fault diagnosis method based on the local mean decomposition. *Renewable Energy*, 48, 411–415.

Liu, Y., Zhao, Y., and Wu, F. (2016). Ellipsoidal state-bounding-based set-membership estimation for linear system with unknown-but-bounded disturbances. *IET Control Theory Applications*, 10(4), 431–442.

Loesch Vianna, W.O., de Souza Ribeiro, L.G., and Yoneyama, T. (2015). Electro hydraulic servovalve health monitoring using fading extended kalman filter. In *2015 IEEE Conference on Prognostics and Health Management (PHM)*, 1–6. doi: 10.1109/ICPHM.2015.7245033.

Lu, B. and Sharma, S.K. (2009). A literature review of igbt fault diagnostic and protection methods for power inverters. *IEEE Transactions on Industry Applications*, 45, 1770–1777.

Luo, J., Namburu, M., Pattipati, K., Qiao, L., Kawamoto, M., and Chigusa, S. (2003). Model-based prognostic techniques. In *2003 AUTOTESTCON, Charlotte, NC (Proceedings)*. doi: 10.1109/AUTEST.2003.

Löfberg, J. (2003). *Min-Max Approaches to Robust Model Predictive Control*. Ph.D. thesis, Linköping Studies in Science and Technology, Linköping.

Löw, S., Obradovic, D., and Bottasso, C. (2020). Model predictive control of wind turbine fatigue via online rainflow-counting on stress history and prediction. *Journal of Physics Conference Series*, 1618. doi: 10.1088/1742-6596/1618/2/022041.

Madhav, M. (2016). *Model based prognostics for prediction of remaining useful life*. Ph.D. thesis, Lulea University of Technology.

Mangili, F. (2013). *Development of advanced computational methods for prognostics and health management in energy components and systems*. Ph.D. thesis, Politecnico di Milano (Milan).

Manzinger, S., Pek, C., and Althoff, M. (2021). Using reachable sets for trajectory planning of automated vehicles. *IEEE Transactions on Intelligent Vehicles*, 6(2), 232–248. doi: 10.1109/TIV.2020.3017342.

Marvin Rausand, A.H. (2004). *System Reliability Theory: Models and Statistical Method 2ed.* John Wiley Sons. Inc, New Jersey.

Mayne, D., Seron, M., and Raković, S.V. (2005). Robust model predictive control of constrained linear system with bounded disturbances. *Automatica*, 41, 219–224. doi: 10.1016/j.automatica.2004.08.019.

Medjaher, K. and Zerhouni, N. (2013). Framework for a hybrid prognostics. *Chemical Engineering Transactions*, 33, 91–96. doi: 10.3303/CET1333016.

Meeker, W.Q., Escobar, L.A., and Zayac, S. (2003). *Use of sensitivity analysis to assess the effect of model uncertainty in analyzing accelerated life test data. In Case Studies in Reliability and Maintenance.(W. R. Blischke and D. N. Prabhakar Murthy, eds.)*. Wiley., New York, NY, USA, 1st edition.

Meslem, N. and Martinez Molina, J.J. (2019). Reachability-Based Method for Control Performance Analysis. In *CCTA 2019 - 3rd IEEE Conference on Control Technology and Applications*, 805–810. Hong Kong, China. doi: 10.1109/CCTA.2019.8920594. URL `https://hal.archives-ouvertes.fr/hal-02267149`.

Miller, A. (1999). *A New wavelet basis for the decomposition of gear motion error signals and its application to gearbox diagnostics*. Master Thesis, Pennsylvania State University, United States of America.

Milosavljevic, P., Cortinovis, A., Marchetti, A.G., Faulwasser, T., Mercangöz, M., and Bonvin, D. (2016). Optimal load sharing of parallel compressors via modifier adaptation. In *2016 IEEE Conference on Control Applications (CCA)*, 1488–1493. doi: 10.1109/CCA.2016.7588011.

Miner, M. (1945). Cumulative damage in fatigue. *Journal of Applied Mechanics*, 12(3), 159–164.

Moshtaghi, M., Leckie, C., and Bezdek, J.C. (2016). Online clustering of multivariate time-series. In *Proceedings of the SIAM International Conference on Data Mining*. doi: 10.1137/1.9781611974348.41.

Mudholkar, G. and Srivastava, D. (1993). he exponentiated weibull family: a graphical approach. *Reliability, IEEE Transactions on*, 42(2), 299–302.

Müller, M., Angeli, D., and Allgöwer, F. (2013). Economic model predictive control with self-tuning terminal cost. *European Journal of Control*, 19, 408–416. doi: 10.1016/j.ejcon.2013.05.019.

Nagy-Kiss, A.M., Ichalal, D., Schutz, G., and Ragot, J. (2015). Fault tolerant control for uncertain descriptor multi-models with application to wastewater treatment plant. In *2015 American Control Conference (ACC)*, 5718–5725. doi: 10.1109/ACC.2015.7172235.

Nejjari, F., Sarrate, R., and Blesa, J. (2015). Optimal pressure sensor placement in water distribution networks minimizing leak location uncertainty. *Procedia Engineering*, 119, 953–962,. doi: https://doi.org/10.1016/j.proeng.2015.08.979.

Nelson, W. (1982). *Applied Life Data Analysis.* Wiley-Interscience, New Jersey.

Nguyen, H. and Kwak, S. (2020). Enhance reliability of semiconductor devices in power converters. *Electronics*, 9, 2068. doi: 10.3390/electronics9122068.

Niknam, S., Thomas, T., Hines, J., and Sawhney, R. (2013). Analysis of acoustic emission data for bearings subject to unbalance. *International Journal of Prognostics and Health Management. Special Issue on Wind Turbine PHM*, 4, 80–89.

Nikulin, M., Limnios, N., Balakrishnan, N., Kahle, W., and Huber-Carol, C. (2010). *Advances in Degradation Modeling: Applications to Reliability, Survival Analysis, and Finance.* Springer., New York, NY, USA, 1st edition.

Ocampo-Martinez, C. and Puig, V. (2009). Fault-tolerant model predictive control within the hybrid systems framework: Application to sewer networks. *International Journal of Adaptive Control and Signal Processing*, 23. doi: 10.1002/acs.1099.

Odgaard, P., Knudsen, T., Overgaard, A., Steffensen, H., and Jørgensen, M. (2015a). Importance of dynamic inflow in model predictive control of wind turbines. In *9th IFAC Symposium on Control of Power and Energy Systems CPES*, volume 48, 90–95. New Delhi, India.

Odgaard, P., Sanchez, H., Escobet, T., and Puig, V. (2015b). Fault diagnosis and fault tolerant control with application on a wind turbine low speed shaft encoder. In *9th IFAC Symposium on Fault Detection, Supervision and Safety for Technical Processes*, volume 48, 1357–1362. Paris, France.

Odgaard, P., Stoustrup, J., Nielsen, R., and Damgaard, C. (2009). Observer based detection of sensor faults in wind turbines. In *European Wind Energy Conference*, 4421–4430. Marseille, France.

Ofsthun, S. (2002). Integrated vehicle health management for aerospace platforms. *IEEE Instrumentation and Measurement Magazine*, 5(3), 21–24.

Ompusunggu, A.P., Papy, J.M., and Vandenplas, S. (2016). Kalman-filtering-based prognostics for automatic transmission clutches. *IEEE/ASME Transactions on Mechatronics*, 21(1), 419–430. doi: 10.1109/TMECH.2015.2440331.

Onori, S., Rizzoni, G., and Cordoba-Arenas, A. (2012). A prognostic methodology for interconnected systems: preliminary results. *IFAC Proceedings Volumes*, 45, 1125–1130.

Orchard, M., Kacprzynski, G., K. Goebel, B.S., and Vachtsevanos., G. (2008). Advances in uncertainty representation and management for particle filtering applied to prognostics. In *2008 International Conference on Prognostics and Health Management*, 1–6. doi: doi:10.1109/PHM.2008.4711433.

Ozdemir, A., Seiler, P., and Balas, G. (2011). Wind turbine fault detection using counter-based residual thresholding. In *Proceedings of 18th IFAC World Congress*, 8289–8294. Milan, Italy.

P. Weber, C. Simon, D.T.V.P. (2012). Fault-tolerant control design for over-actuated system conditioned by reliability: a drinking water network application. In *IFAC Proceedings Volumes.*, volume 45, 558–563. doi: https://doi.org/10.3182/20120829-3-MX-2028.00147.

Paris, P. and Erdogan, F. (1963). A critical analysis of crack propagation laws. *Journal of Basic Engineering.*, 85D, 528–534. doi: 07.07.2020.2020.url:http://phmeurope.org/2020/data-challenge-2020.

Parker, M.A., Ran, L., and Finney, S.J. (2013). Distributed control of a fault-tolerant modular multilevel inverter for direct-drive wind turbine grid interfacing. *IEEE Transactions on Industrial Electronics*, 60(2), 509–522.

Patil, N., Das, D., Yin, C., Lu, H., Bailey, C., and Pecht, M. (2009). A fusion approach to igbt power module prognostics. In *EuroSimE 2009 - 10th International Conference on Thermal, Mechanical and Multi-Physics Simulation and Experiments in Microelectronics and Microsystems*, 1–5. doi: 10.1109/ESIME.2009.4938491.

Patton, R., Frank, P., and Clark, R. (1989). *Fault Diagnosis in Dynamic Systems: Theory and Application*. NY,Prentice-Hall, Inc.

Pech, M., Vrchota, J., and J., B. (2021). Predictive maintenance and intelligent sensors in smart factory: Review. *Sensors*, 21(4), 1470. doi: https://doi.org/10.3390/s21041470.

Pedersen, M.M. (2018). Introduction to metal fatigue. Technical report ME-TR11. Technical report, Aarhus University, Mechanical engineering.

Pedrycz, W. and Wang, X. (2016). Designing fuzzy sets with the use of the parametric principle of justifiable granularity. *IEEE Transactions on Fuzzy Systems*, 24(2), 489–496.

Peng, W., Li, Y.F., Yang, Y.J., Mi, J., and Huang, H.Z. (2017). Bayesian degradation analysis with inverse gaussian process models under time-varying degradation rates. *IEEE Transactions on Reliability*, 66(1), 84–96. doi: 10.1109/TR.2016.2635149.

Peng, Y., Dong, M., and Zuo, M.J. (2010). Current status of machine prognostics in condition-based maintenance: a review. *International Journal of Advanced Manufacturing Technology*, 50(1-4), 297–313,. doi: https://doi.org/10.1007/s00170-009-2482-0.

Pfaendtner, J. and Broadbelt, L.J. (2008). Mechanistic modeling of lubricant degradation. 1. structurereactivity relationships for free-radical oxidation. *Industrial Engineering Chemistry Research*, 47(9), 2886–2896. doi: https://doi.org/10.1021/ie0714807.

Philippe, W. and Lionel, J. (2006). Complex system reliabiity modelling with dynamic object oriented bayesian networks. *IET Generation, Transmission and distribution*, 91(2), 149–162.

Pour, F.K., Puig, V., and Cembrano, G. (2018). Health-aware lpv-mpc based on system reliability assessment for drinking water networks. In *2018 IEEE Conference on Control Technology and Applications (CCTA)*, 187–192. doi: 10.1109/CCTA.2018.8511348.

Pour, F.K., Theilliol, D., Puig, V., and Cembrano, G. (2021). Health-aware control design based on remaining useful life estimation for autonomous racing vehicle. *ISA Transactions*, 132, 196–209. doi: ISSN0019-0578,https://doi.org/10.1016/j.isatra.2020.03.032.(https://www.sciencedirect.com/science/article/pii/S0019057820301403).

Pugno, M.C., Cornetti, P., and Carpinteri, A. (2006). A generalized paris' law for fatigue crack growth. *Journal of the Mechanics and Physics of Solids*, 54(7), 1333–1349. doi: https://doi.org/10.1016/j.jmps.2006.01.007.

Puig, V. and Ocampo-Martínez., C. (2015). Decentralised fault diagnosis of large-scale systems: Application to water transport networks. In *6th International Workshop on Principles of Diagnosis, 2015, Paris.*, volume 2, 99–104.

Puig, V., Escobet, T., Sarrate, R., and Quevedo, J. (2015). Fault diagnosis and fault tolerant control in critical infrastructure systems. *Studies in Computational Intelligence*, 565, 263–299. doi: 10.1007/978-3-662-44160-2_10.

Quintana-Rojo, C., Callejas, F., Tarancón Morán, M., and Martínez-Rodríguez, I. (2020). Econometric studies on the development of renewable energy sources to support the european union 2020–2030 climate and energy framework: A critical appraisal. *Sustainability*, 12, 4828. doi: 10.3390/su12124828.

Rakovic, S.V., Kouvaritakis, B., Cannon, M., Panos, C., and Findeisen, R. (2012). Parameterized tube model predictive control. *IEEE Transactions on Automatic Control*, 57(11), 2746–2761. doi: 10.1109/TAC.2012.2191174.

Raković, S.V., Kerrigan, E., Kouramas, K., and Mayne, D. (2005). Invariant approximations of the minimal robust positively invariant set. *Automatic Control, IEEE Transactions on*, 50, 406 – 410. doi: 10.1109/TAC.2005.843854.

Rausand, M. and Hoyland, A. (2004). *System Reliability Theory (second edition)*, chapter 2, 17–22. Wiley series in probability and statistics.

Ray, A. and Caplin, J. (2000). Life extending control of aircraft: trade-off between flight performance and structural durability. *Aeronautical Journal*, 104(1039), 397–408. doi: https://doi.org/10.1017/S0001924000091843.

Ray, A., Caplin, J., and Joshi, S. (2000). Robust damage-mitigating control of aircraft structures. *AIAA guidance, navigation, and control conference and exhibit*, 4568. doi: https://doi.org/10.2514/6.2000-4568.

Ren, Y., Wang, X., and Zhang, C. (2019). Bearing fault detection and separation of wind turbine based on artificial immune system. In *2019 CAA Symposium on Fault Detection, Supervision and Safety for Technical Processes (SAFEPROCESS)*, 443–448. doi: 10.1109/SAFEPROCESS45799.2019.9213421.

Rezamand, M., Kordestani, M., Carriveau, R., Ting, D.S.K., Orchard, M.E., and Saif, M. (2020). Critical wind turbine components prognostics: A comprehensive review. *IEEE Transactions on Instrumentation and Measurement*, 69(12), 9306–9328. doi: 10.1109/TIM.2020.3030165.

Robinson, E., Marzat, J., and Raissi, T. (2017). Model-based prognosis using an explicit degradation model and inverse form for uncertainty propagation. *IFAC-PapersOnLine*, 50, 14242–14247. doi: 10.1016/j.ifacol.2017.08.1815.

Robinson, E.I. (2018). *Filtering and uncertainty propagation methods for model-based prognosis*. Ph.D. thesis, École doctorale Informatique, Télécommunications et Électronique (Paris).

Rugh, W. and Shamma, J. (2000). Research on gain scheduling. *Automatica*, 36, 1401–1425. doi: 10.1016/S0005-1098(00)00058-3.

Saha, B., Celaya, J.R., Wysocki, P.F., and Goebel, K.F. (2009). Towards prognostics for electronics components. In *2009 IEEE Aerospace conference*, 1–7. doi: 10.1109/AERO.2009.4839676.

Salazar, J., Weber, P., Nejjari, F., Sarrate, R., and Theilliol, D. (2017). System reliability aware model predictive control framework. *Reliability Engineering System Safety*, 167, 663–672. doi: 10.1016/j.ress.2017.04.012.

Samie, M., Alghassi, A., and Perinpanayagam, S. (2015). Unified igbt prognostic using natural computation. In *2015 IEEE International Conference on Digital Signal Processing (DSP)*, 698–702. doi: 10.1109/ICDSP.2015.7251965.

Sanchez, H., Escobet, T., Puig, V., and Odgaard, P. (2015). Fault diagnosis of advanced wind turbine benchmark using interval-based ARRs and observers. *IEEE Transactions on Industrial Electronics*, 62(6), 3783–3793.

Sangwan, V., Kumar, R., and Rathore, A.K. (2018). An empirical capacity degradation modeling and prognostics of remaining useful life of li-ion battery using unscented kalman filter. In *2018 8th IEEE India International Conference on Power Electronics (IICPE)*, 1–6. doi: 10.1109/IICPE.2018.8709470.

Sankararaman, S. and Goebel, K. (2014). Uncertainty in prognostics: Computational methods and practical challenges. In *2014 IEEE Aerospace Conference*, 1–9. doi: doi:10.1109/AERO.2014.6836342.

Sankararaman, S. and Goebel, K. (2013). Why is the remaining useful life prediction uncertain?. In *PHM 2013 - Proceedings of the Annual Conference of the Prognostics and Health Management Society 2013*, 337–349.

Sara, K., Xu, Y., Zheng, Z., and Wang., P. (2022). Physics-informed machine learning model for battery state of health prognostics using partial charging segments. *Mechanical Systems and Signal Processing*, 172. doi: ISSN0888-3270,https://doi.org/10.1016/j.ymssp.2022.109002.

Saxena, A., Celaya, J., Saha, B., Saha, S., and Goebel., K. (2017). Evaluating prognostics performance for algorithms incorporating uncertainty estimates. In *IEEE Aerospace Conference, 2010*, 1–11. doi: doi:10.1109/AERO.2010.5446828.

Schulte, H., Zajac, M., and Gerland, P. (2012). Takagi-sugeno sliding mode observer design for fault diagnosis in pitch control systems of wind turbines. In *8th IFAC Symposium on Fault Detection, Supervision and Safety of Technical Processes*, 546–551. Mexico City, Mexico.

Schwabacher, M. and Goebel, K. (2007). A survey of artificial intelligence for prognostics. In *AAAI Fall Symposium: Artificial Intelligence for Prognostics*.

Sheibat-Othman, N., Othman, S., Benlahrache, M., and Odgaard, P. (2013). Fault detection and isolation in wind turbines using support vector machines and observers. In *American Control Conference (ACC)*, 4459–4464. Washington DC, USA.

Shirazi, F.A., Grigoriadis, K.M., and Viassolo, D. (2012). Wind turbine integrated structural and lpv control design for improved closed-loop performance. *International Journal of Control*, 85(8), 1178–1196.

Shuting, W., Yonggang, L., Herming, L., and Guiji, T. (2006). A compositive diagnosis method on turbine-generator rotor winding inter-turn short circuit fault. In *IEEE International Symposium on Industrial Electronics (ISIE)*, 1662–1666. Montreal, Canada.

Shyama, M. and Pillai, A. (2019). *Fault-Tolerant Techniques for Wireless Sensor Network—A Comprehensive Survey*, 261–269. doi: 10.1007/978-981-13-3765-9_27.

Sikorska, J., Hodkiewicz, M., and Ma, L. (2011). Prognostic modeling options for remaining useful life estimation by industry. *Mechanical Systems and Signal Processing*, 25, 1803–1836. doi: 10.1016/j.ymssp.2010.11.018.

Sonnenfeld, G., Goebel, K., and Celaya, J. (2008). An agile accelerated aging, characterization and scenario simulation system for gate controlled power transistors. In *2008 IEEE AUTOTESTCON*, 208–215. doi: doi:10.1109/AUTEST.2008.4662613.

Sun, B., Zeng, S., Kang, R., and Pecht, M.G. (2012). Benefits and challenges of system prognostics. *IEEE Transactions on Reliability*, 61(2), 323–335. doi: 10.1109/TR.2012.2194173.

Theilliol, D., Weber, P., Chamseddine, A., and Zhang, Y. (2015). Optimization-based reliable control allocation/reallocation design for over-actuated systems. In *IEEE International Conference on Unmanned Aircraft Systems, (ICUAS 2015).* doi: https://doi.org/10.1109/ICUAS.2015.7152415.

Thomas, L., Lucas, J., Riccardo, B., and Marco, P. (2022). A simple and efficient sampling-based algorithm for general reachability analysis . In *4th Annual Conference on Learning for Dynamics and Control*, volume 168, 1–14. Hong Kong, China. URL `https://hal.archives-ouvertes.fr/hal-02267149`.

Toosi, H.E., Merabet, A., and Swingler, A. (2022). Impact of battery degradation on energy cost and carbon footprint of smart homes. *Electric Power Systems Research*, 209, 107955,. doi: https://doi.org/10.1016/j.epsr.2022.107955.

Toro, R., Ocampo-Martinez, C., Logist, F., Van Impe, J., and Puig, V. (2011). Tuning of predictive controllers for drinking water networked systems. In *Proc. 18th IFAC World Congress*, 14507–14512. Milano, Italy.

Urbano, E., Gonzalez-Abreu, A.D., Kampouropoulos, K., and Romeral, L. (2021). Uncertainty analysis for industries investing in energy equipment and renewable energy sources. *Renewable Energy and Power Quality Journal,*, 19, 126–130. doi: 10.24084/repqj19.234.

Vachtsevanos, G.and Lewis, F. and Roemer, M. (2016). *Intelligent Fault Diagnosis and Prognosis for Engineering Systems*. John Wiley Sons, New Jersey USA.

Van Paepegem, W. and Degrieck, J. (2002). A new coupled approach of residual stiffness and strength for fatigue of fibre-reinforced composites. *INTERNATIONAL JOURNAL OF FATIGUE*, 24(7), 747–762.

Vapnik, V. (2012). *The nature of statistical learning theory.* Springer science busi- ness media, 2013, Geneva, Switzerland.

Vassilopoulos, A., Brøndsted, P., and Nijssen, R. (eds.) (2010). *Advances in Wind Turbine Blade Design and Materials*. Woodhead Publishing Limited, Cambridge.

Vedreño Santos, F., Riera-Guasp, M., Henao, H., and Pineda-Sanchez, M. (2014). Diagnosis of rotor and stator asymmetries in wound-rotor induction machines under nonstationary operation through the instantaneous frequency. *IEEE Transactions on Industrial Electronics*, 61(9), 4947–4959.

Velarde, P., Maestre, J.M., Ocampo-Martinez, C., and Bordons, C. (2016). Application of robust model predictive control to a renewable hydrogen-based microgrid. In *2016 European Control Conference (ECC)*, 1209–1214. doi: 10.1109/ECC.2016.7810454.

Veldman - de Roo, F., Tejada, A., van Waarde, H., and Trentelman, H.L. (2015). Towards observer-based fault detection and isolation for branched water distribution networks without cycles. In *2015 European Control Conference (ECC)*, 3280–3285. doi: 10.1109/ECC.2015.7331040.

Wang, G., Shi, P., Wang, B., and Zhang, J. (2014). Fuzzy n-ellipsoid numbers and representations of uncertain multichannel digital information. *IEEE Transactions on Fuzzy Systems*, 22(5), 1113–1126.

Wang, Y., Alamo, T., Puig, V., and Cembrano, G. (2018). A distributed set-membership approach based on zonotopes for interconnected systems. *2018 IEEE Conference on Decision and Control (CDC)*, 668–673.

Wang, Y., Alamo, T., Puig, V., and Cembrano, G. (2018a). Economic model predictive control with nonlinear constraint relaxation for the operational management of water distribution networks. *Energies*, 11. doi: 10.3390/en11040991.

Wang, Y., Puig, V., and Cembrano, G. (2017a). Non-linear economic model predictive control of water distribution networks. *Journal of Process Control*, 56, 23–34. doi: 10.1016/j.jprocont.2017.05.004.

Wang, Y., Puig, V., and Cembrano, G. (2017b). Non-linear economic model predictive control of water distribution networks. *Journal of Process Control*, 56, 23–34. doi: 10.1016/j.jprocont.2017.05.004.

Wang, Y., Teodoro, A., Vicenç, P., and Gabriela, C. (2018b). Economic model predictive control with nonlinear constraint relaxation for the operational management of water distribution networks. *Energies*, 11(4), 991. doi: https://doi.org/10.3390/en11040991.

Wang, Y., Peng, Y., and Chow, T.W.S. (2021). Adaptive particle filter-based approach for rul prediction under uncertain varying stresses with application to hdd. *IEEE Transactions on Industrial Informatics*, 17(9), 6272–6281. doi: 10.1109/TII.2021.3051285.

Weber, P., Medina-Oliva, G., Simon, C., and Iung., B. (2012). Overview on bayesian networks applications for dependability, risk analysis and maintenance areas. *Engineering Applications of Artificial Intelligence.*, 25(4), 671–682,. doi: https://doi.org/10.1016/j.engappai.2010.06.002.(https://www.sciencedirect.com/science/article/pii/S095219761000117X.

Wu, W.and Hu, J. and J., Z. (2007). Prognostics of machine health condition using an improved arima-based prediction method. In *2nd IEEE Conference on Industrial Electronics and Applications, ICIEA*, 1062–1067.

Wu, R. and Ma, J. (2019). An improved lstm neural network with uncertainty to predict remaining useful life. In *2019 CAA Symposium on Fault Detection, Supervision and Safety for Technical Processes (SAFEPROCESS)*, 274–279. doi: doi:10.1109/SAFEPROCESS45799.2019.9213408.

Xiang, W., Tran, H.D., and Johnson, T.T. (2018). Output reachable set estimation and verification for multilayer neural networks. *IEEE Transactions on Neural Networks and Learning Systems*, 29(11), 5777–5783. doi: 10.1109/TNNLS.2018.2808470.

Xiong, J., Jauberthie, C., Travé-Massuyès, L., and Le Gall, F. (2013). Fault detection using interval kalman filtering enhanced by constraint propagation. *Proceedings of the IEEE Conference on Decision and Control*, 490–405. doi: 10.1109/CDC.2013.6759929.

Xiong, Z., Qiu, Y., Feng, Y., and Chen, L. (2018). Fatigue damage of wind turbine gearbox under extreme wind conditions. In *2018 Prognostics and System Health Management Conference (PHM-Chongqing)*, 1208–1214. doi: 10.1109/PHM-Chongqing.2018.00212.

Yan, R., Shi, Z., and Zhong, Y. (2020). Task assignment for multiplayer reach–avoid games in convex domains via analytical barriers. *IEEE Transactions on Robotics*, 36(1), 107–124. doi: 10.1109/TRO.2019.2935345.

Yang, K., e.a. (2004). *Multivariate Statistical Methods in Quality Management 1st ed.* McGraw-Hill Professional.

Yang, J., Peng, C., Jiayu, X., Zeng, J., Xing, S., Jin, J., and Deng, H. (2013). Structural investigation of composite wind turbine blade considering structural collapse in full-scale static tests. *Composite Structures*, 97, 15–29. doi: 10.1016/j.compstruct.2012.10.055.

Yang, S., Bryant, A., Mawby, P., Xiang, D., Ran, L., and Tavner, P. (2011). An industry-based survey of reliability in power electronic converters. *IEEE Transactions on Industry Applications*, 47(3), 1441–1451. doi: 10.1109/TIA.2011.2124436.

Yassine, M., Shojafar, M., Haqiq, A., and Darwish, A. (2019). *Cybersecurity and Privacy in Cyber Physical Systems*. CRC press, NY.

Yuan, M., Zhao, H., Xie, Y., Ren, H., Tian, L., Wang, Z., Zhang, B., and Chen, J. (2022). Prediction of stiffness degradation based on machine learning: Axial elastic modulus of [0m /90n]s composite laminates. *Composites Science and Technology.*, 218(7), 109–186. doi: https://doi.org/10.1016/j.compscitech.2021.109186.

Zaccaria, V., Ferrari, M., and Kyprianidis, K. (2019). Adaptive control of micro gas turbine for engine degradation compensation. In *Proceedings of the ASME Turbo Expo 2019: Turbomachinery Technical Conference and Exposition. Volume 3: Coal, Biomass, Hydrogen, and Alternative Fuels; Cycle Innovations; Electric Power; Industrial and Cogeneration; Organic Rankine Cycle Power Systems. Phoenix, Arizona, USA.* doi: V003T06A004.ASME.https://doi.org/10.1115/GT2019-90894.

Zagórowska, M., Wu, O., Ottewill, J., Reble, M., and Thornhill, N.. (2020). A survey of models of degradation for control applications. *Annual Reviews in Control*, 50, 150–173.

Zeller, M. and Montrone, F. (2018). Combination of component fault trees and markov chains to analyze complex, software-controlled systems. In *2018 3rd International Conference on System Reliability and Safety (ICSRS)*, 13–20. doi: 10.1109/ICSRS.2018.8688854.

Zhang, S., Zhang, S., Wang, B., and Habetler, T.G. (2019). Deep learning algorithms for bearing fault diagnostics - a review. In *2019 IEEE 12th International Symposium on Diagnostics for Electrical Machines, Power Electronics and Drives (SDEMPED)*, 257–263. doi: 10.1109/DEMPED.2019.8864915.

Zhang, Y. and Jiang, J. (2008). Bibliographical review on reconfigurable fault-tolerant control system. *Annual Reviews in Control*, 32, 229–252. doi: 10.1016/j.arcontrol.2008.03.008.

Zheng, F., Jiang, J., Zaidan, M.A., He, W., and Pecht, M. (2015). Prognostics of lithium-ion batteries using a deterministic bayesian approach. In *2015 IEEE Conference on Prognostics and Health Management (PHM)*, 1–4. doi: 10.1109/ICPHM.2015.7245037.

Zhou, T., Droguett, E.L., and Ali Mosleh, . (2022). Physics-informed deep learning: A promising technique for system reliability assessment. *Applied Soft Computing*, 126, 109217. doi: ISSN1568-4946,https://doi.org/10.1016/j.asoc.2022.109217.

Zimroz, R., Bartelmus, W., Barszcz, T., and Urbanek, J. (2012). *Statistical Data Processing for Wind Turbine Generator Bearing Diagnostics*, 509–518. Springer Berlin Heidelberg.

Zio, E. and Di Maio, F. (2010). A data-driven fuzzy approach for predicting the remaining useful life in dynamic failure scenarios of a nuclear system. *Reliability Engineering System Safety*, 955(1), 49–57. doi: https://doi.org/10.1016/j.ress.2009.08.001.